

DOKUZ EYLÜL UNIVERSITY
GRADUATE SCHOOL OF NATURAL AND APPLIED SCIENCES

DESIGNING TRANSITION METAL COMPLEXES
WITH N,S-DONOR LIGANDS

by

Ece Su ÇAKMAKÇI

February, 2023

İZMİR

**DESIGNING TRANSITION METAL COMPLEXES
WITH N,S-DONOR LIGANDS**

A Thesis Submitted to the

Graduate School of Natural and Applied Sciences of Dokuz Eylül University

In Partial Fulfillment of the Requirements for the Degree of Master of Science

in Chemistry

by

Ece Su ÇAKMAKÇI

February, 2023

İZMİR

M.Sc THESIS EXAMINATION RESULT FORM

We have read the thesis entitled “**DESIGNING TRANSITION METAL COMPLEXES WITH N,S-DONOR LIGANDS**” completed by **ECE SU ÇAKMAKÇI** under supervision of **PROF.DR. ELİF SUBAŞI** and we certify that in our opinion it is fully adequate, in scope and in quality, as a thesis for the degree of Master of Science.

.....
Prof.Dr. Elif SUBAŞI

Supervisor

.....
Prof. Dr. Funda DEMİRHAN

(Jury Member)

.....
Prof. Dr. Hülya AYAR KAYALI

(Jury Member)

.....
Prof. Dr. Okan FISTIKOĞLU

Director

Graduate School of Natural and Applied Sciences

ACKNOWLEDGMENT

All research and studies on the thesis were done in Dokuz Eylul University, Faculty of Science, Department of Chemistry. There are a few people I would like to thank for their trust in me and for their unwavering support in all circumstances.

First of all, I would like to thank my supervisor Prof. Dr. Elif Subaşı who has stood by me since the first day we met, throughout my working period and in any situation. She never spare her support and trust in me. The beginning of a study is first to establish a bond and trust and then to convince the student that she can do it. I offer my most sincere thanks to her for making me trust myself. I am very grateful for her guidance.

My feere and colleague Emine ÖZTÜRK. I would like to thank her for keeping my faith high throughout my thesis and the process and for dedicating the time and care she devoted to her studies to mine as well. We are a good team.

My undergraduate friends Bilge PAKYAPAN and Fatmanur DİLERBAY were my biggest supporters throughout the process. Thank you too for getting your valuable time for me.

My superhero, my friend, my little girl Angel... The friend I grew up with. I am glad you were with me on this long journey. My best part is my other half. You've always been by my side. I love you and thank you first and then life for helping us find each other.

Lastly, my father Erdal ÇAKMAKÇI and my mother Fatma ÇAKMAKÇI, who have provided financial and moral support throughout my life. I know you are as happy as I am, even more so than I am. This work is primarily for you. Thank you both very much.

Ece Su ÇAKMAKÇI

DESIGNING TRANSITION METAL COMPLEXES WITH N,S-DONOR LIGANDS

ABSTRACT

Transition metal(II) complexes were synthesized from the reaction of ligand with metal(II) chlorides. All complexes have been characterised by spectroscopic methods. In the bis[chloro(2-Acetyl-5-Bromo-Thiophen-N-Methyl-Thiosemicarbazone)] cobalt (II) complex, the cobalt atom adopts a distorted tetrahedral geometry around the cobalt(II) ion, with two neutral S-thiosemicarbazone monodentate ligands coordinated through one of the thiocarbonyl sulfur atoms and two chlorides. In the bis[2-Acetyl-5-Bromo-Thiophen-N-Methyl-Thiosemicarbazone]nickel(II) and bis[2-Acetyl-5-Bromo-Thiophen-N-Methyl-Thiosemicarbazone] palladium(II) complexes, ligand is coordinated with the metal center, as a mono anionic bidentate *N,S* donors which are in *trans* position and that metal(II) ions adopt square planar coordination. Bis[2-Acetyl-5-Bromo-Thiophen-N-Methyl-Thiosemicarbazone] zinc(II) indicates that the anionic thiosemicarbazone ligands bind to the metal in a distorted tetrahedral arrangement with *N,S* donor atoms. The antimicrobial activity of compounds was investigated against bacterial and fungal stains. Ligand activity was observed to be lower than metal compounds. The Zinc(II) complex had the best antibacterial activity against *E. faecalis*, while the Cobalt(II) complex showed the best activity against *S. aureus* bacteria. Cobalt(II) and Palladium(II) complexes were relatively more effective against Gram-negative bacteria. It was determined that metal complexes were more effective against gram positive bacteria. A little antifungal activity was observed in Zinc(II) and Cobalt(II) complexes.

Keywords: Metal(II) complexes, thiosemicarbazone, crystal structure, antimicrobial activity

N,S-DONOR LİGANDLI GEÇİŞ METAL KOMPLEKSLERİNİN TASARIMI

ÖZ

Geçiş metal(II) kompleksleri tiyosemikarbazon ligandının metal(II) klorürlerle reaksiyonundan sentezlenmiştir. Sentezlenen bileşikler, element analiz, FT-IR, ¹H NMR ve tek kristal X-ışını kırınım yöntemleri ile karakterize edilmiştir. Analitik ve spektral veriler, tüm bu komplekslerin tek çekirdekli türler olduğunu göstermektedir. bis[kloro(2-Asetil-5-Bromo-Tiyofen-N-Metil-Tiyosemikarbazon)] kobalt(II) kompleksinde, kobalt atomu, iki nötr tek dişli S-tiyosemikarbazon ligandının tiyokarbonil kükürt atomunun biri ve iki klor atomu aracılığıyla ile kobalt(II) iyonu etrafında bozulmuş bir tetrahedral geometri benimsemektedir. Bis[2-Asetil-5-Bromo-Tiyofen-N-Metil-Tiyosemikarbazon]nikel(II) ve bis[2-Asetil-5-Bromo-Tiyofen-N-Metil-Tiyosemikarbazon]paladyum(II) komplekslerinde ise ligand, bir asidik protonun ayrışması yoluyla, trans pozisyonunda olan monoanyonik iki dişli N,S donörleri aracılığıyla metal merkeze koordine olmuştur. Bu metal (II) iyonlarının kare düzlemsel koordinasyonu benimsedikleri görülmektedir. Bis[2-Asetil-5-Bromo-Tiyofen-N-Metil-Tiyosemikarbazon]çinko(II) kompleksinde, anyonik tiyosemikarbazon ligandlarının metale N,S şelatlama sistemi aracılığıyla bozulmuş bir tetrahedral yapıda bağlandığını görülmektedir. Ligand ve metal(II) komplekslerinin antimikrobiyal ve antifungal aktivitesi bakteri ve mantar suşlarına karşı incelenmiştir. Ligandın metal komplekslerine kıyasla daha zayıf aktivite gösterdiği gözlenmiştir. Çinko(II) kompleksi *E. faecalis*'e karşı en iyi antibakteriyel aktiviteye sahipken, Kobalt(II) kompleksi *S. aureus* bakterisine karşı en iyi aktiviteyi göstermiştir. Kobalt(II) ve Paladyum(II) komplekslerinin, *Gram-negatif* bakterilere karşı nispeten daha etkili oldukları görülmektedir. Metal komplekslerinin *Gram-negatif* bakterilere karşı *Gram-pozitif* bakterilere göre daha az etkili olduğu belirlenmiştir. Çinko(II) ve Kobalt(II) komplekslerinde bir miktar antifungal aktivite gözlenmiştir.

Anahtar kelimeler: Metal(II) kompleksleri, tiyosemikarbazon, kristal yapı, antimikrobiyal aktivite

CONTENTS

	Page
M.Sc THESIS EXAMINATION RESULT FORM.....	ii
ACKNOWLEDGMENT.....	iii
ABSTRACT.....	iv
ÖZ.....	v
LIST OF FIGURES.....	ix
LIST OF TABLES.....	xii
CHAPTER ONE - INTRODUCTION.....	1
1.1. Schiff Bases.....	1
1.2 Thiosemicarbazide.....	2
1.2.1 General Properties of Thiosemicarbazide.....	2
1.2.1.1 Physical Properties of Thiosemicarbazide.....	2
1.2.1.2 Chemical Properties of Thiosemicarbazide.....	3
1.2.2 Synthesis of Thiosemicarbazide.....	4
1.2.3 Metal Complexes of Thiosemicarbazide.....	5
1.2.4 Biological Activities of Thiosemicarbazides.....	6
1.3 Thiosemicarbazones.....	7
1.3.1 General Properties of Thiosemicarbazones.....	9
1.3.2 Geometric Isomer of Thiosemicarbazones.....	10
1.3.3 Types of Ligands.....	11
1.3.3.1 Bis-Thiosemicarbazones.....	11
1.3.3.2 Bonding Modes of Ligands.....	12
1.3.3.3 Bonding Modes in Neutral Form.....	13

1.3.3.4 Bonding Modes in Anionic Form	13
1.3.3.5 Bonding Modes of Bis-Thiosemicarbazones	14
1.3.4 Coordination of Thiosemicarbazones to Metal Atom	14
1.3.4.1 Monodentate Thiosemicarbazone Complexes	15
1.3.4.2 Bidentat Thiosemicarbazone Complexes	17
1.3.4.3 Tridentate Thiosemicarbazone Complexes	18
1.3.5 Geometry of Thiosemicarbazone Complexes	20
1.3.6 Biological Activities of Thiosemicarbazones	21
1.4 Studies in the Literature on Thiosemicarbazone and Metal Complexes	22
1.4.1 Co(II) and Co(III) complexes.....	23
1.4.2 Ni(II) complexes	24
1.4.3 Zn(II) complexes	30
1.4.4 Palladium(II) Thiosemicarbazone Complexes	32
CHAPTER TWO – MATERIAL AND METHODS	36
2.1. Instruments	36
2.2. Chemicals	36
2.2.1. Purification of Solvents	36
2.3. Synthesis of the HL ligand	37
2.4. Preparation of the Starting Complex, [Pd(COD)Cl ₂].....	37
2.5. Synthesis of the Complexes (1-4)	37
2.5.1. Bis[chloro (2-Acetyl-5-Bromo-Thiophen-N-Methyl-Thiosemicarbazone)] cobalt (II), [CoCl ₂ (S-HL) ₂]	38
2.5.2. Bis[chloro(2-Acetyl-5-Bromo-Thiophen-N-Methyl-Thiosemicarbazone)] nickel(II), [Ni(N,S-HL) ₂]	38

2.5.3. Bis[chloro(2-Acetyl-5-Bromo-Thiophen-N-Methyl-Thiosemicarbazone)] palladium(II), [Pd(N,S-HL) ₂]	39
2.5.4. Bis[chloro(2-Acetyl-5-Bromo-Thiophen-N-Methyl-Thiosemicarbazone)] zinc(II), [Zn(N,S-HL) ₂]	39
2.6. Determination and Refinement of The Crystal Structure	39
2.7. Antimicrobial activity	40
2.8. Agar Well Diffusion Method	41
2.9. Determination of MIC and MBC	41
CHAPTER THREE – RESULTS AND DISCUSSIONS	42
3.1 Synthesis and Characterization of the Complexes	42
3.2 Physical Properties	43
3.3 Infrared Spectra	44
3.4 ¹ H NMR Spectra	53
3.5 Structural Description of Compounds	62
3.6 Antibacterial Studies	70
CHAPTER FOUR – CONCLUSIONS	73
REFERENCES	74

LIST OF FIGURES

	Page
Figure 1.1 Synthesis reaction of schiff bases	2
Figure 1.2 Thiosemicarbazide	2
Figure 1.3 trans(N1-S)- and cis(N1-S) thiosemicarbazide (a and b)	3
Figure 1.4 Crystal structure of the cis-thiosemicarbazide cation	4
Figure 1.5 Isomers of protonated thiosemicarbazide	4
Figure 1.6 General synthesis mechanism of thiosemicarbazides	5
Figure 1.7 Binding of thiosemicarbazide in metal complexes	5
Figure 1.8 Coordination sites of substituted thiosemicarbazide	6
Figure 1.9 Obtaining thiosemicarbazone compounds	7
Figure 1.10 Mechanism of formation of thiosemicarbazones	8
Figure 1.11 Numbering of thiosemicarbazone	9
Figure 1.12 Bis-thiosemicarbazones	9
Figure 1.13 Thione and thiol tautomers of thiosemicarbazones	10
Figure 1.14 Isomer structures of thiosemicarbazones	10
Figure 1.15 Structure of mono-thiosemicarbazones	11
Figure 1.16 Structure of bis-thiosemicarbazones	12
Figure 1.17 Thione and thiol forms of thiosemicarbazones	12
Figure 1.18 Bonding modes in neutral form	13
Figure 1.19 Bonding modes in anionic form	14
Figure 1.20 Bonding modes of bis-thiosemicarbazones	14
Figure 1.21 Coordination types of thiosemicarbazones with metal ions	15
Figure 1.22 N donor thiosemicarbazone	16
Figure 1.23 S donor thiosemicarbazone	16
Figure 1.24 NS donor thiosemicarbazone	17
Figure 1.25 NN donor thiosemicarbazone	18
Figure 1.26 Synthesis procedure of compounds	19
Figure 1.27 Synthesis of Ni(II) complex of ONS donor thiosemicarbazone	20
Figure 1.28 Co complex structure of 3-thiophenylaldehyde thiosemicarbazone	23
Figure 1.29 Cobalt-nickel complex structure of coumarin-3-yl thiosemicarbazone ..	23
Figure 1.30 Synthesis of ligand and metal(II) complexes	24

Figure 1.31 Structure of nickel(II) complex	24
Figure 1.32 Synthesis of Ni(II) thiosemicarbazonato complex	25
Figure 1.33 Crystal structure of the Ni(II) complex	26
Figure 1.34 Schematic representations of compounds 1–4.....	27
Figure 1.35 Structure of complex 4.....	27
Figure 1.36 Synthetic scheme of Ni(II) complexes	28
Figure 1.37 Crystal structures of Haribabu's nickel complexes	28
Figure 1.38 ORTEP diagram of the complex 1a.....	29
Figure 1.39 ORTEP diagram of the complex 5.....	29
Figure 1.40 ORTEP diagram of the complex 7a.....	30
Figure 1.41 Zinc chloride complex structures of thiosemicarbazone	30
Figure 1.42 Synthesis of Al-Riyahee's zinc complex.....	31
Figure 1.43 Crystal structure of 2a complex.....	31
Figure 1.44 Chemical structures of the ligand and metal complexes	32
Figure 1.45 Synthesis reaction of ONS coordinated Pd(II) complex.....	33
Figure 1.46 NNS donor Pd(II) complex.....	33
Figure 1.47 NNN donor Pd(II) complex	34
Figure 1.48 NS donor Pd(II) complex	34
Figure 1.49 Molecular structures of ligands	35
Figure 1.50 Molecular structures of Pd(II) complexes	35
Figure 2.1 Synthesis of HL ligand	37
Figure 2.2 Synthesis of Pd(COD)Cl ₂	37
Figure 2.3 Synthesis of complexes.....	38
Figure 3.1 HL ligand.....	42
Figure 3.2 HL ligand and their metal complexes.....	43
Figure 3.3 C=N bonds of complexes	46
Figure 3.4 The FT-IR spectrum of HL.....	48
Figure 3.5 The FT-IR spectrum [CoCl ₂ (S-HL) ₂].....	49
Figure 3.6 The FT-IR spectrum of [Ni(N,S-L) ₂]	50
Figure 3.7 The FT-IR spectrum of [Pd(N,S-L) ₂]	51
Figure 3.8 The FT-IR spectrum of [Zn(N,S-L) ₂].....	52
Figure 3.9 N(1)H and N(2)H protons of HL and Co complex.....	54

Figure 3.10 N(1)H protons of HL and complexes	55
Figure 3.11 CH ₃ protons of HL and complexes	56
Figure 3.12 The ¹ H-NMR spectrum of HL	57
Figure 3.13 The ¹ H-NMR spectrum of [CoCl ₂ (S-HL) ₂]	58
Figure 3.14 The ¹ H-NMR spectrum of [Ni(N,S-L) ₂]	59
Figure 3.15 The ¹ H-NMR spectrum of [Pd(N,S-L) ₂]	60
Figure 3.16 The ¹ H-NMR spectrum of [Zn(N,S-L) ₂]	61
Figure 3.17 The molecular structures of the complexes (a) Co(II), (b) Ni(II)	63
Figure 3.18 The molecular structures of the complexes (c) Pd(II) and (d) Zn(II)	64
Figure 3.19 C–H···π interactions of Co(II) complex	65
Figure 3.20 The crystal packing view of complex Ni(II)	66
Figure 3.21 Intermolecular N3–H3···S3 and N6–H6···S2 hydrogen bonds of Pd(II) complex	67
Figure 3.22 The intermolecular N12–H12···O1 hydrogen bonds	68
Figure 3.23 Inhibition zone diameter	72

LIST OF TABLES

	Page
Table 2-1 Crystal data and structure refinement parameters for complexes Co(II), Pd(II), Ni(II), and Zn(II)	40
Table 3-1 Physical properties and elemental analysis data for the thiosemicarbazone ligand and the complexes	44
Table 3-2 Characteristic FT-IR bands (cm^{-1}) of compounds	45
Table 3-3 $^1\text{H-NMR}$ data for compounds	53
Table 3-4 Selected bond lengths (\AA) and angles ($^\circ$) for the complexes Ni(II), Pd(II), Zn(II) and Co(II)	68
Table 3-5 Hydrogen bonds and other weak interactions for complexes Co(II), Ni(II), Pd(II), and Zn(II). (\AA , $^\circ$).....	69
Table 3-6 Comparison of antimicrobial activities of different metal ligands with agar diffusion method	70
Table 3-7 Minimum inhibition concentrations of different metal ligands.....	70

CHAPTER ONE

INTRODUCTION

Thiosemicarbazide yields thiosemicarbazone compounds with a wide spectrum of biological activity with high coordination ability as a result of condensation reaction with compounds containing carbonyl groups. Biological activity of thiosemicarbazone derivatives varies depending on the carbonyl group.

The investigation of thiosemicarbazide-derived compounds, which started with the Ni(II) complex of the thiosemicarbazide compound in 1934, became more important with the identification of the biological activities of thiosemicarbazones in 1946.

The complex compounds it gives with thiosemicarbazones and transition metals are the subject of many researches due to their pharmacological properties. Thiosemicarbazones are also of interest in coordination chemistry due to their polydentate binding in addition to their biological activity.

TSCs and transition metal complexes have a broad spectrum of biological activity, some of which are anti-viral, antifungal, anti-tumour and antioxidant effects. As a general rule, the N(1)-N(2)H-C(3)(=S)-N(4)H₂ thiosemicarbazide group coordinates with N(1) and S atoms in the coordination compounds that thiosemicarbazones make with transition metals. However, there are other attachment models as well. Thioalkylation of thiosemicarbazide derivatives is characterized by the ability to coordinate these complexes.

1.1 Schiff Bases

Compounds formed as a result of condensation reaction of primary amines with aldehydes or ketones and defined by carbon-nitrogen double bond (imine bond) are called Schiff bases (Figure 1.1).

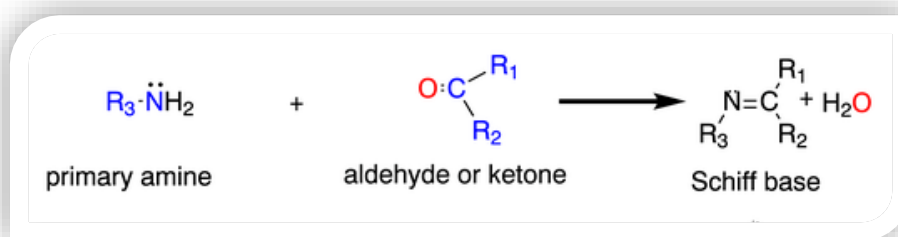


Figure 1.1 Synthesis reaction of schiff bases

Schiff bases can be named aldimine or ketimine depending on whether the reacting carbonyl compounds are aldehydes or ketones. However, it is possible to obtain a wide variety of Schiff bases with different structures depending on the structures and molar ratios of the amine and carbonyl compounds.

1.2 Thiosemicarbazide

1.2.1 General Properties of Thiosemicarbazide

1.2.1.1 Physical Properties of Thiosemicarbazide

Thiosemicarbazide (Figure 1.2), which is a primary hydrazide, is a compound that can be dissolved in water and ethyl alcohol, can be crystallized as elongated or plates, and its melting point can vary between 170°C and 181°C depending on its crystal structure (Gatterman & Wieland, 1932; Bailor, 1953).

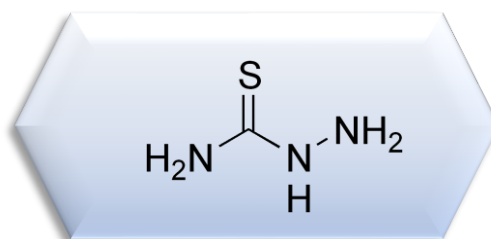


Figure 1.2 Thiosemicarbazide

As it is known, due to the tautomerity caused by the (NH–C(S)–NH₂) system in thiosemicarbazide systems, firstly (N=C(S-)–NH₂), then (N=C(S-)–NH) using appropriate reagents systems can be created. The N=C(S-)–NH₂ system is encountered in the literature as isothiosemicarbazide (Yamazaki, 1975).

1.2.1.2 Chemical Properties of Thiosemicarbazide

The three-dimensional crystal structure of the thiosemicarbazide molecule was investigated for the first time in 1969 and it was determined that it was in the trans configuration in the free state. In chelate compounds where thiosemicarbazide acts as a bidentate ligand and where the terminal hydrazine amino group is protonated, the molecular structure prefers the cis configuration (Figure 1.3) (Campbell, 1975; Coghi, Lanfredi & Tiripicchio, 1976).

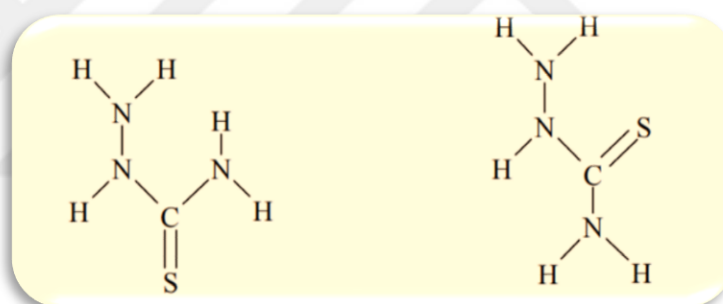


Figure 1.3 trans(N1-S)- and cis(N1-S) thiosemicarbazide (a and b)

While thiosemicarbazide is in the trans form in its normal state, in the protonated state of the hydrazine nitrogen atom, the hydrazine part of the molecule rotates 180° around the C-N imine bond and switches to the cis form. Protonation of the terminal nitrogen atom prevents the interaction of intramolecular and intermolecular hydrogen bonds compared to free thiosemicarbazide. Therefore, a larger area is provided for the NH₃⁺ group (Figure 1.4).

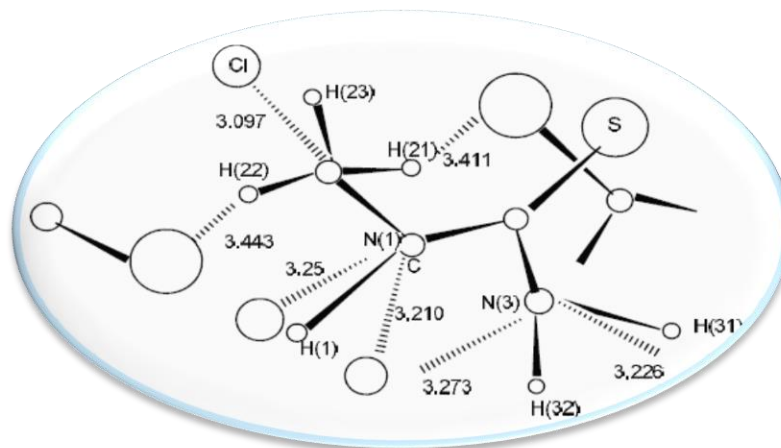


Figure 1.4 Crystal structure of the cis-thiosemicarbazide cation

Protonation of the hydrazine nitrogen atom may mean that it contributes more to the A structure (Figure 1.5). However, when we look at the protonated molecules from different atoms, the fact that the sulfur atom does not make hydrogen bonds and creates an effective negative charge indicates that the B and C structures are suitable (Figure 1.5). In addition, an important effect of the protonation of the NH_2 group causes a shortening of the C–N bond and an elongation of the N–N bond (Bailor, 1953).

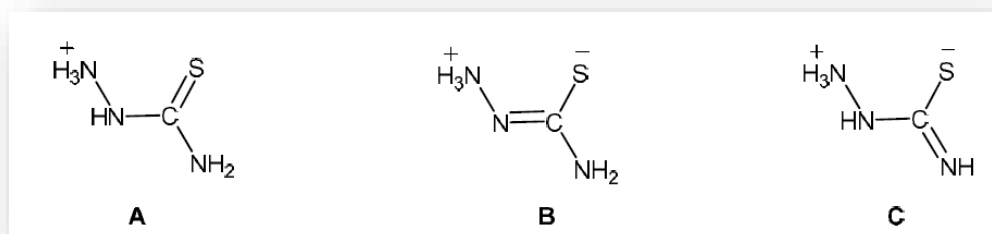


Figure 1.5 Isomers of protonated thiosemicarbazide

1.2.2 Synthesis of Thiosemicarbazide

Thiosemicarbazide is obtained by refluxing hydrazine sulfate ($\text{H}_2\text{N-NH}_2 \cdot \text{H}_2\text{SO}_4$) and potassium rodanide (KSCN) in anhydrous alcohol at $104\text{--}110^\circ\text{C}$ at pH 5.5–6.6 (Gospodinov, Stanev & Dorev, 1962). The same compound is achieved when other compounds (thiocyanate and isothiocyanate) are used. However, depending on the pH

value of the environment, anionic structures (usually for sulfur) can also be obtained (Figure 1.6).

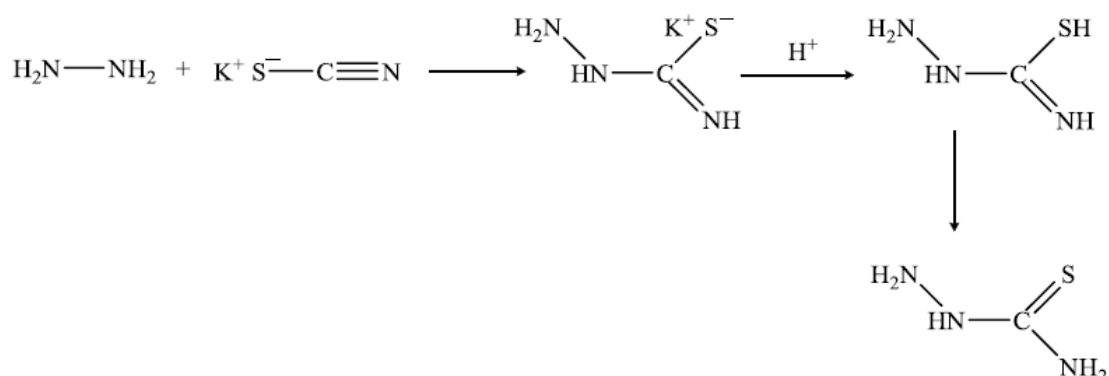


Figure 1.6 General synthesis mechanism of thiosemicarbazides

1.2.3 Metal Complexes of Thiosemicarbazide

When the metal complexes of thiosemicarbazide are examined, it is seen that it coordinates with the metal across the *N* and *S* atoms, in many complexes it acts as a monodentate ligand with only *S*, and in some it acts as a bidentate ligand with *S* and *N*¹. When a substitute is attached to the *S* atom, the thiosemicarbazide coordinates to the metal with the hydrazine and thioamide nitrogen atoms (Figure 1.7) (Campbell, 1975).

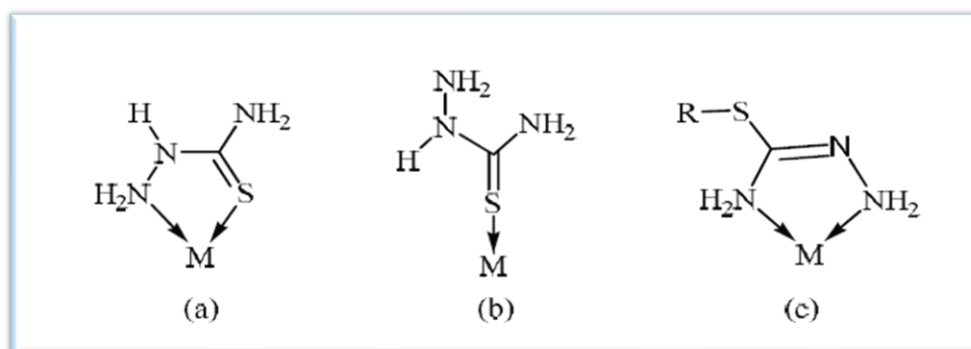


Figure 1.7 Binding of thiosemicarbazide in metal complexes

Thiosemicarbazide ligands can participate in coordination in metal complexes as neutral bidentate, as well as as mononegative bidentate or as a binegative tetradentate

(Angelusiu et al., 2009; Emara, Seleem, & Madyan, 2009; Mostafa, Bekheit, El-Agez, Thompson, & Efvenson, 2000).

In complexes where thiosemicarbazides, in which a carbonyl group is substituted at the N¹ position, act as a bidentate ligand; Although coordination occurs through the S atom and the N¹H, N atom (Emara et al., 2009), it also occurs through the O atom of the carbonyl group and the N²H, N atom of the hydrazide group (Angelusiu et al., 2009; Shashidhar, Shivakumar, & Halli, 2006).

Emara et al. showed the ways of bonding to the metal atom of thiosemicarbazides in which a carbonyl group is substituted at the N¹ position as follows in Figure 1.8.

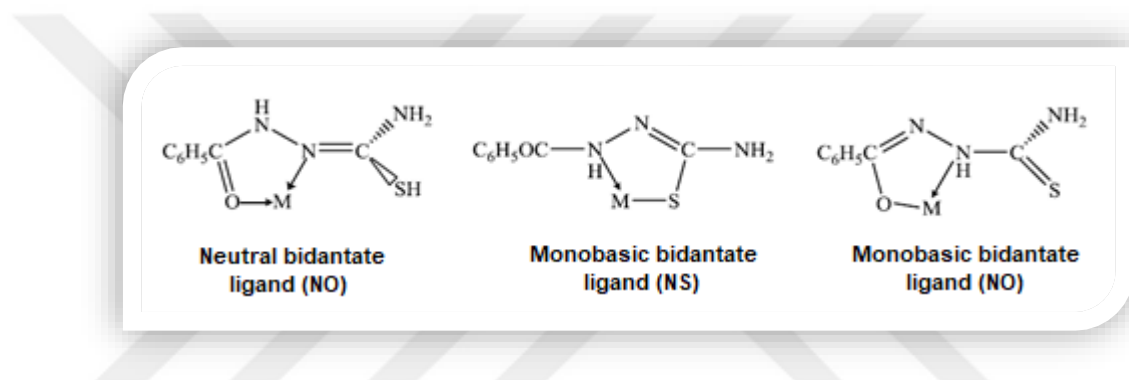


Figure 1.8 Coordination sites of substituted thiosemicarbazide

1.2.4 Biological Activities of Thiosemicarbazides

Thiosemicarbazides contain sulfur and nitrogen donor atoms. Because of these multifunctional forms of coordination, they are involved in medicine and pharmaceuticals. These compounds exhibit biological activities including antibacterial, antifungal and anticancer activities (Youssef, El-Zahany, El-Seidy, Caselli, & Cenini, 2009).

Thiosemicarbazide compounds are highly studied compounds due to their biological properties such as potential antibacterial (Hassanien, Gabr, Abdel-Rhman, & El-Asmy, 2008; Keshk, El-Desoky, Hammouda, Abdel-Rahman, & Hegazi, 2008), antifungal (Emara et al., 2009), antitumor (Angelusiu et al., 2009) properties. In the studies, it is known that thiosemicarbazides are effective against bacteria, and it is known that these activities increase more in their compounds or metal complexes. On

the other hand, there are also studies in which thiosemicarbazide ligands exhibit better antibacterial activity than their complexes (Shashidhar et al., 2006)

1.3 Thiosemicarbazones

Thiosemicarbazone compounds; It is prepared by the condensation of thiosemicarbazide compounds with aliphatic, aromatic or heterocyclic aldehydes or ketones (Figure 1.9). The method of obtaining is generally carried out by boiling the carbonyl compound and thiosemicarbazide in a 1:1 mole ratio in $\text{CH}_2\text{H}_5\text{OH}$ under reflux.

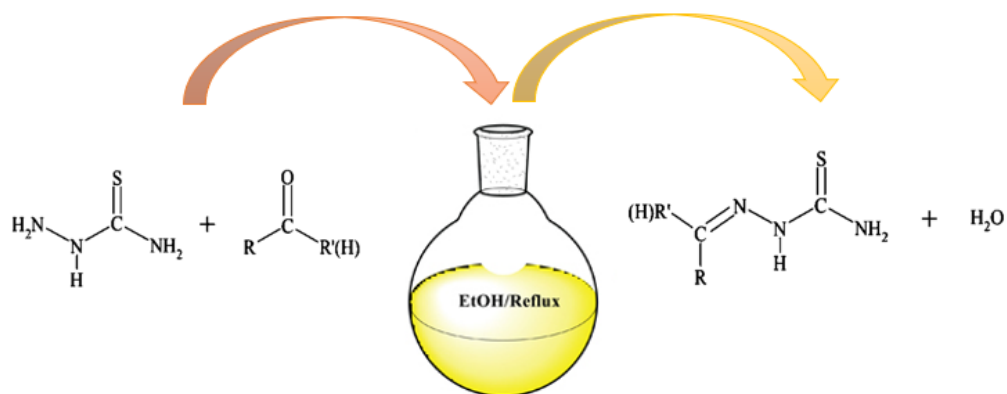


Figure 1.9 Obtaining thiosemicarbazone compounds

The reaction takes place more easily in the environment where some of the carbonyl compound is in salt form and the H^+ ion concentration is high. This is a condensation reaction. By reason of the high electronegativity of the oxygen atom, the $\text{C}=\text{O}$ bond is polar, which makes the carbon atom a positive center open to nucleophilic attacks and also causes the activation of hydrogen atoms. Due to its planar structure, Lewis bases easily attack the carbon atom from above and below. The compound, which has a trigonal structure at the beginning of the addition reaction, starts to become tetragonal at the transition stage and the oxygen atom becomes negative. The formation of the transition state and product is caused by the negative oxygen atom (Figure 1.10). However, inductive and electronic effects also play a role in these formations (Padhye, & Kauffman, 1985).

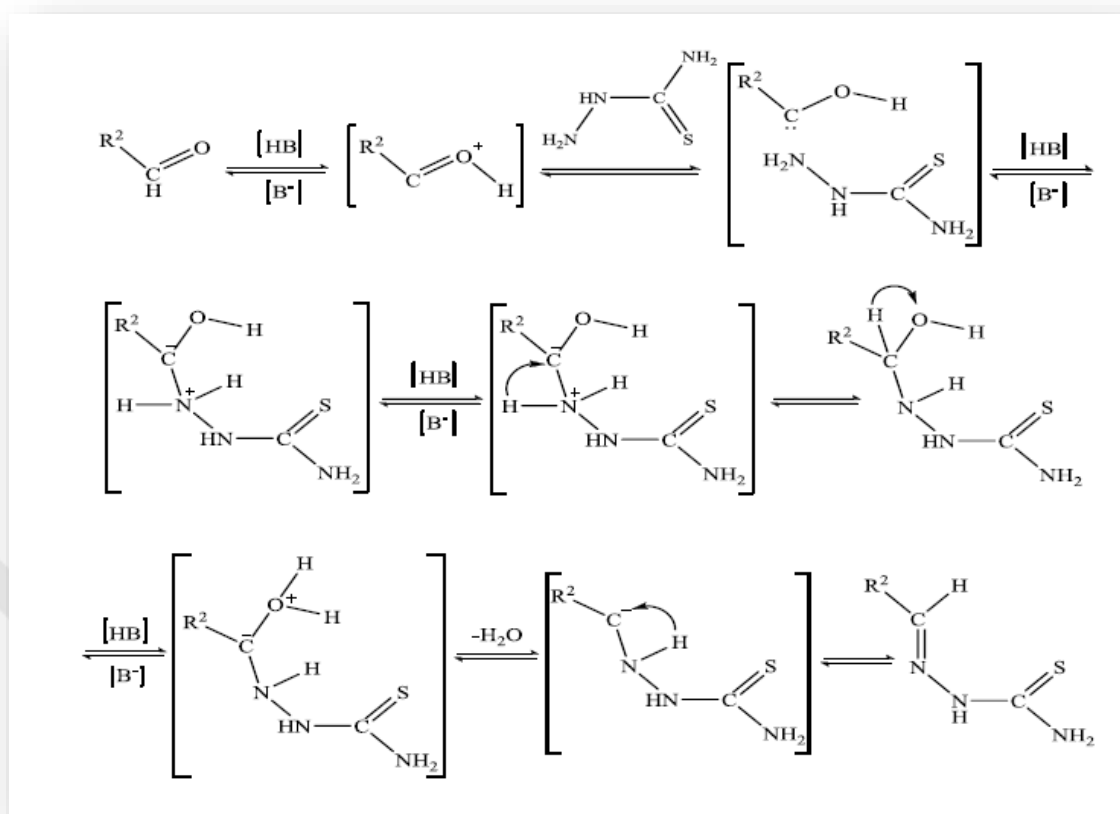


Figure 1.10 Mechanism of formation of thiosemicarbazones

There are three separate nitrogen atoms on the thiosemicarbazide. Although there are unshared electron pairs on each nitrogen atom, a lone nitrogen atom attacks the carbonyl group. Since the electrons on the N² and N⁴ nitrogen atoms are delocalized with the carbonyl group, these atoms partially lose their nucleophilic properties. Since there is no such delocalization at the N¹ nitrogen atom, thiosemicarbazide attacks the carbonyl groups with this nitrogen atom.

While thiosemicarbazone compounds are named according to the IUPAC system, the numbering starts from the hydrazine group of the molecule (Figure 1.11).

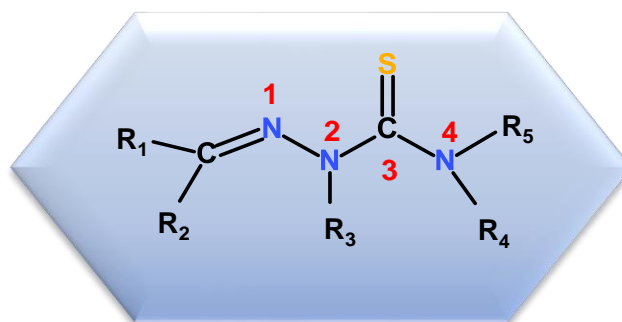


Figure 1.11 Numbering of thiosemicarbazone

Thiosemicarbazones are generally classified as mono-thiosemicarbazones and bis-thiosemicarbazones:

- a) Mono-thiosemicarbazones
- b) Bis-thiosemicarbazones: Bis-thiosemicarbazones (Figure 1.12) have either a ring or two segments joined by a C-C bond and are shown in the examples below (Lobana, Sharma Bawa, & Khanna, 2009).

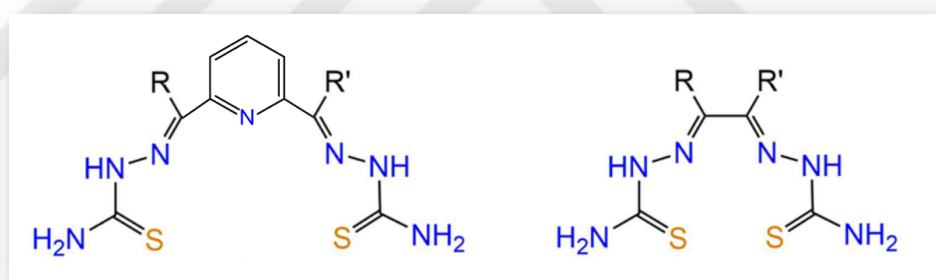


Figure 1.12 Bis-thiosemicarbazones

1.3.1 General Properties of Thiosemicarbazones

According to the kind of aldehyde or ketone used for condensation, thiosemicarbazone compounds can form monodentate, bidentate or polydentate chelates with metal ions. The resulting complexes are colored and are used for the selective and sensitive determination of metal ions due to these properties (Prathapachandra Kurup, & Joseph, 2003).

Thiosemicarbazones exist in solution as an equilibrium mixture of thion (thio keto A) and thiol (thio enol B) tautomers (Figure 1.13) (Pal, Basuli, & Bhattacharya, 2002).

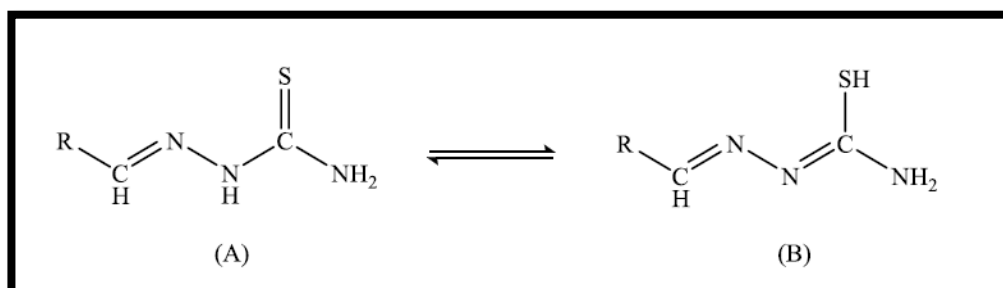


Figure 1.13 Thione and thiol tautomers of thiosemicarbazones

1.3.2 Geometric Isomer of Thiosemicarbazones

Semicarbazone-based compound derivatives exist as geometric isomer structures that can be easily converted to each other. Isomerism is usually due to C=N double bonds. According to the literature, compounds with this structure containing imine bonds are found in high proportion of E isomer in dimethyl sulfoxide solution and as Z isomer in less polar solvents (Khalilian, Mirzaei, & Taherpour, 2015).

Studies have shown that unsubstituted thiosemicarbazones are generally planar in the solid phase C=N–NH–CX–NH₂ skeleton and the S atom is trans with respect to the N atom of azomethine (Figure 1.14 A). Also, in thiosemicarbazones where the amine group is completely substituted, the S atom is cis relative to the N atom of azomethine (Figure 1.14 B). On the other hand, S-substituted thiosemicarbazones conform to the Z-form (Fig. 1.14 C) (Casas, Garcia-Tasende, & Sordo, 2000).

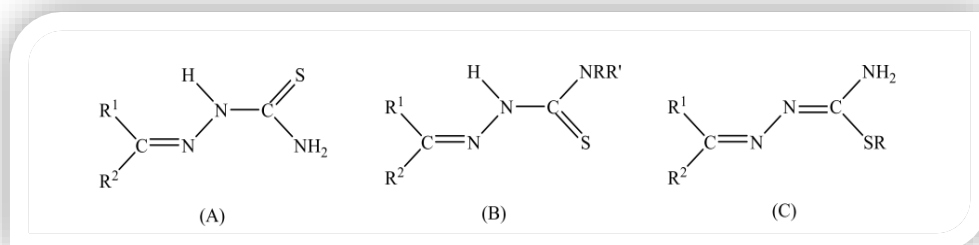


Figure 1.14 Isomer structures of thiosemicarbazones

1.3.3 Types of Ligands

Thiosemicarbazone ligands are divided into various subclasses by the differentiation of the functional groups (R1, R2, R3 and R4) in their structures. In the structure of aldehyde-based thiosemicarbazones, there is a hydrogen atom as a functional group (R2). As the R1 functional group, it can be various alkyl, aryl or heterocyclic groups. The (N1) functional groups attached to the nitrogen atom can contain two separate hydrogen atoms, as well as a hydrogen atom and various functional groups similar to the R1 functional group (Figure 1.15).

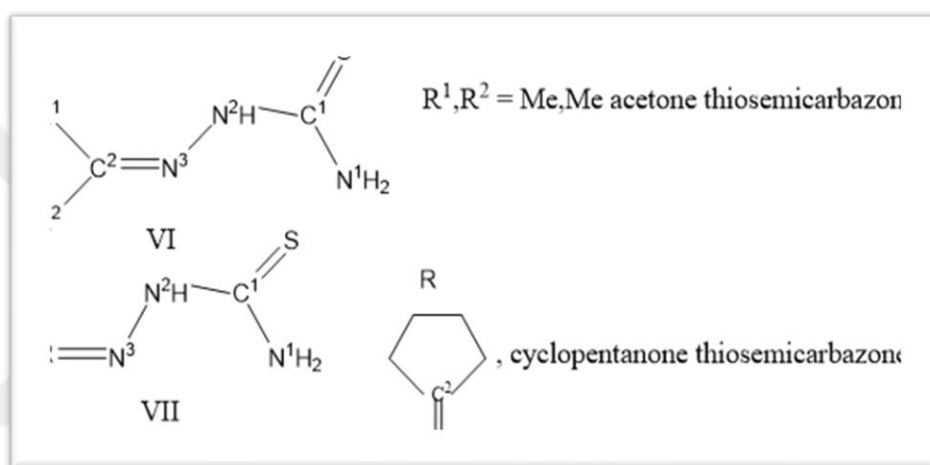


Figure 1.15 Structure of mono-thiosemicarbazones

1.3.3.1 Bis-Thiosemicarbazones

Bis-thiosemicarbazones can be linked to each other via C-C bond or ring. Structures VIII and IX can be cited as examples in Figure 1.16.

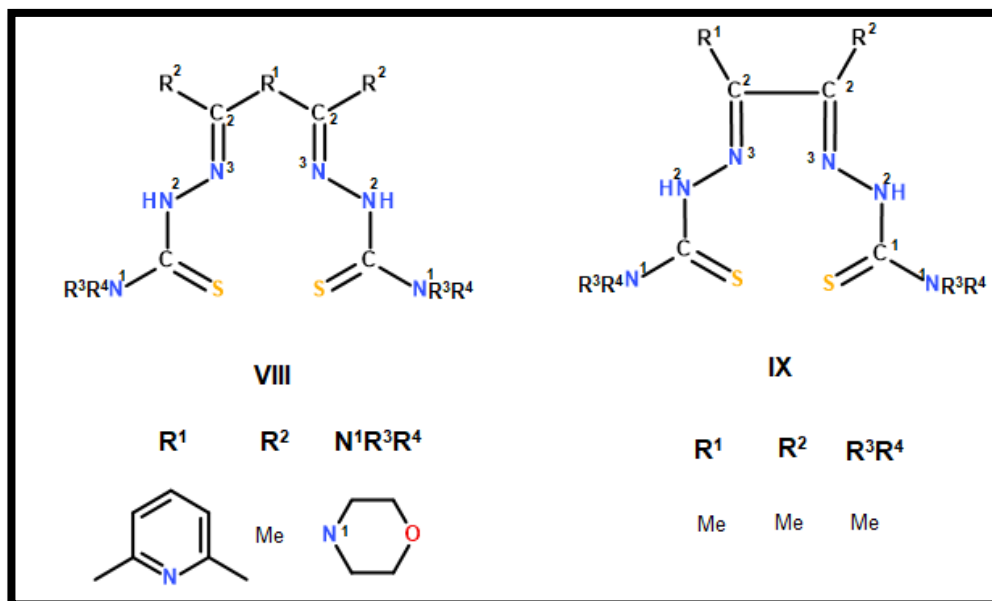


Figure 1.16 Structure of bis-thiosemicarbazones

1.3.3.2 Bonding Modes of Ligands

Thiosemicarbazones are present in the ligand structure in the form of thion-thiol (Xa-Xb). While coordinating to the metal, they can bind in neutral (Xa) or anionic form (Xc). Thiosemicarbazones can be coordinated by varying the metal depending on the ligand structure (Figure 1.17).

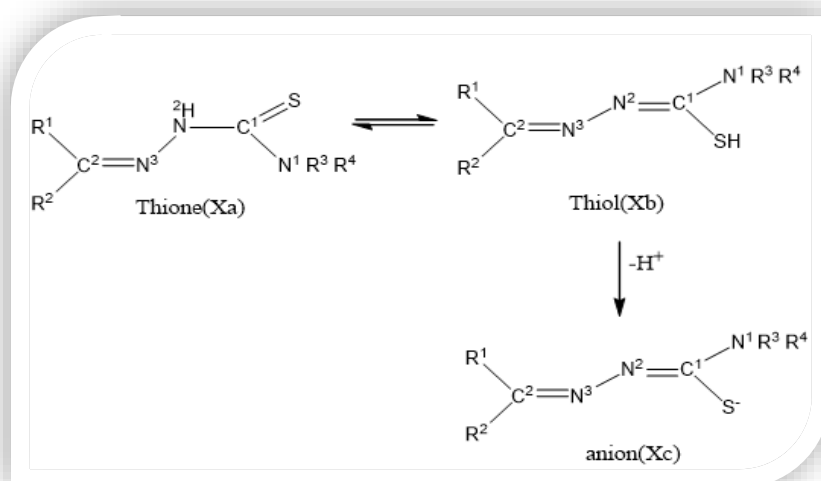


Figure 1.17 Thione and thiol forms of thiosemicarbazones

1.3.3.3 Bonding Modes in Neutral Form

Monodentate bonding (Figure 1.18) can be seen over the neutral form S atom during coordination to the metal. In addition, bidentate bonding is also observed over the S and N3 atoms. However, if the ligand has a suitable donor atom in its structure, this donor atom can also participate in the bonding. The most common neutral bonding patterns are observed in the figure below. (Bermejo et al., 1999; Gomez-Saiz et al., 2003; Jouad, Riou, Allain, Khan, & Bouet, 2001; Labisbal et al., 2003; Lhuachan, Siripaisarnpipat, & Chaichit, 2003; Lobana, Rekha, & Butcher, 2004; Lobana et al., 2006; Lobana, Khanna, Butcher, Hunter, & Zeller, 2007; Lobana, Kumari, & Butcher, 2008).

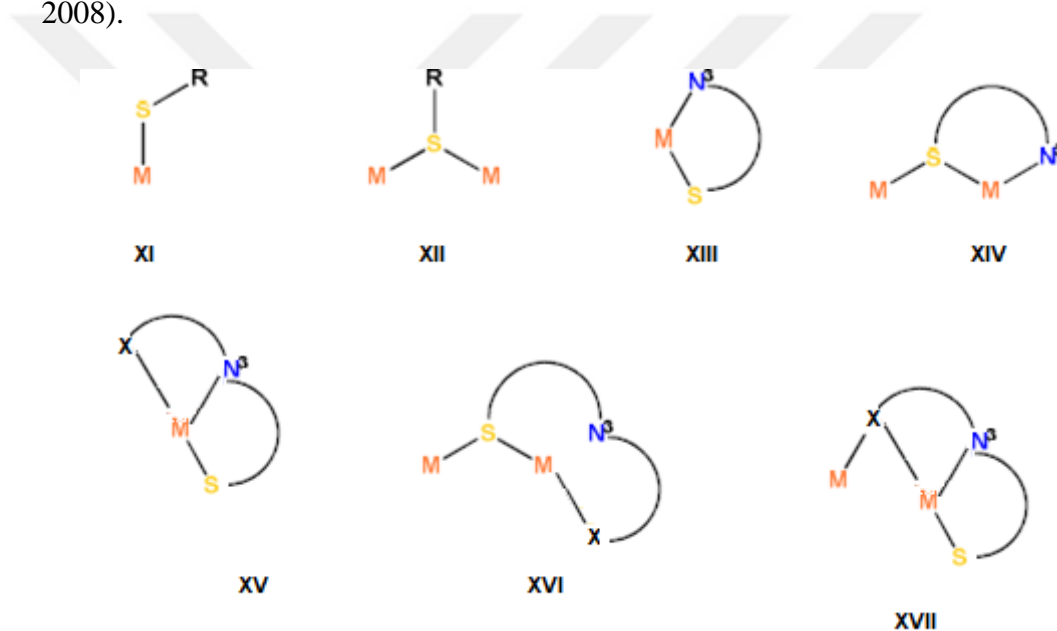


Figure 1.18 Bonding modes in neutral form

1.3.3.4 Bonding Modes in Anionic Form

In anionic form, the ligands show similar binding patterns to the neutral form. They also accommodate different binding modes as illustrated in the Figure 1.19 (Lobana et al., 2009).

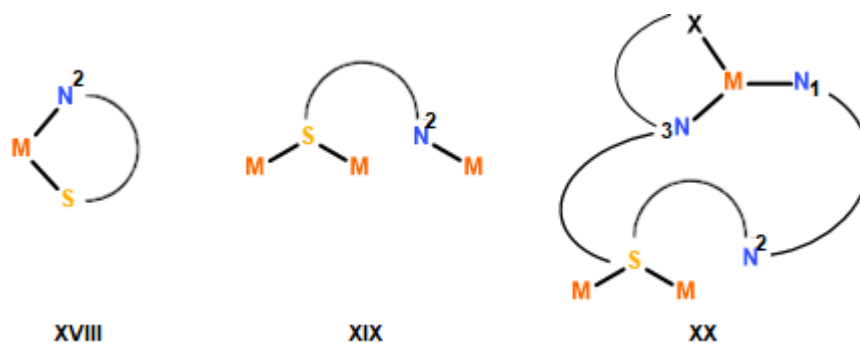


Figure 1.19 Bonding modes in anionic form

1.3.3.5 Bonding Modes of Bis-Thiosemicarbazones

Bis-thiosemicarbazones may bind in neutral, anionic, monothiosemicarbazone-like forms (Figure 1.20). (Casas et al., 2003; Gil, Bermejo, Castineiras, Beraldo, & West, 2000; Pedrido et al., 2005).

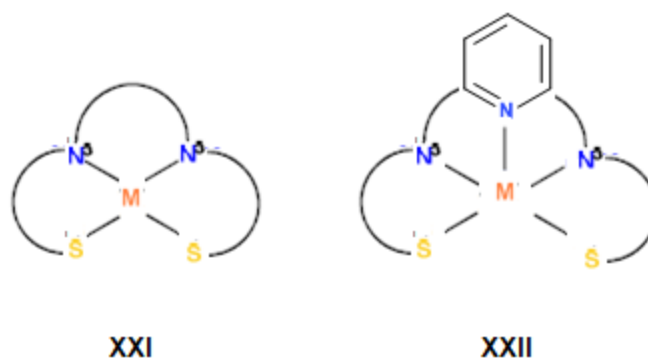


Figure 1.20 Bonding modes of bis-thiosemicarbazones

1.3.4 Coordination of Thiosemicarbazones to Metal Atom

Thiosemicarbazones, which are in the balance of thione/thiol in solution, act as a neutral bidentate ligand in the metal complex mechanism, while the thiol molecular structure acts as a single-charged bidentate ligand by losing a proton (Wilson, Venkatraman, Whitaker, & Tillison, 2005). For these reasons, it can be in complex cationic, neutral, or anionic forms with the effect of pH, according to the preparation procedures. While the metal complexes in the thiol structure of thiosemicarbazones

have not been sufficiently defined, many thione group metal complexes have been described (Figure 1.21). (Padhye, & Kauffman, 1985). In thiosemicarbazone complexes, the ligand is usually monodentate, It has been observed that it is coordinated to metal as a bidentate or tridentate.

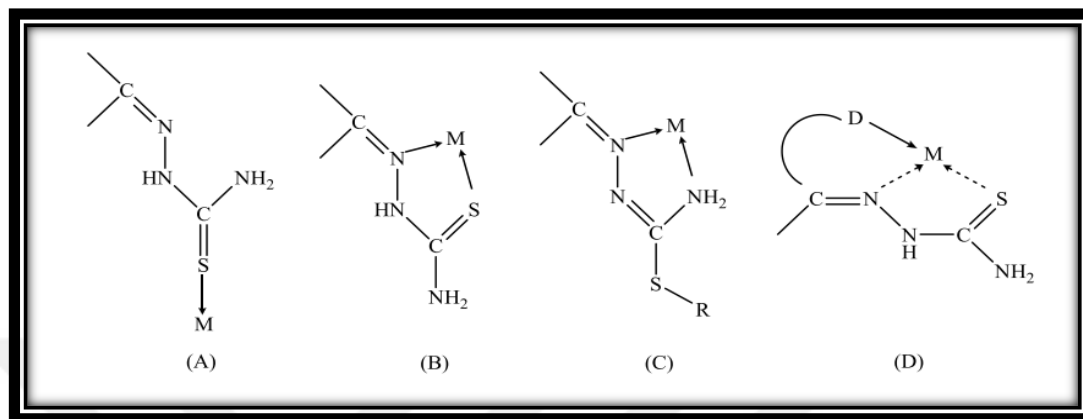


Figure 1.21 Coordination types of thiosemicarbazones with metal ions

1.3.4.1 Monodentate Thiosemicarbazone Complexes

It is known that participation in coordination in thiosemicarbazone and its derivatives is with sulfur atom and hydrazine atom N^I . However, there are compounds in which it is monodentate (monodentate) (Casas et al., 2000). Thiosemicarbazone acts as either an N donor or an S donor in such compounds.

Figure 1.22 shows an example of compounds in which thiosemicarbazone acts as an N donor. In this study conducted in 2003, the complex $[L_2PtCl_2]$, in which the TSC ligand is coordinated in a monodentate manner, was synthesized. With the complexation, the $\nu(CN)+\nu(NH)$ vibration of the ligand observed at $1515-1535\text{ cm}^{-1}$ shifted to $10-15\text{ cm}^{-1}$ higher area. While $\nu(CN)+\nu(N-N)$ vibration in the ligand was $1159-1284\text{ cm}^{-1}$, it shifted to the low area as 1220 cm^{-1} in the metal complex. This information maintains that the ligand is coordinated with the metal ion through the N atom of group $C=N$ (Bakkar, Siddiqi, & Monshi, 2003).

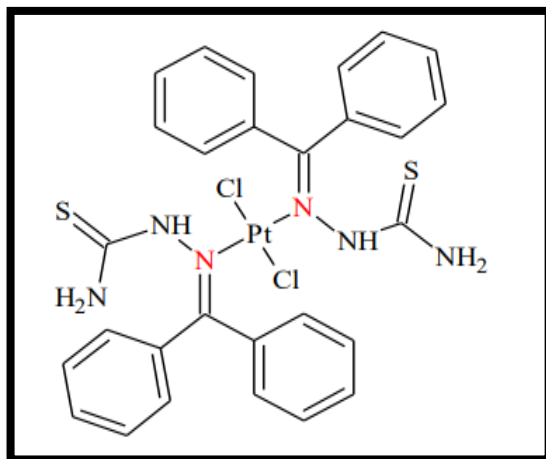


Figure 1.22 N donor thiosemicarbazone

The compound $[\text{ZnCl}_2(\text{HAPhTSC})_2]$ (Figure 1.23) is obtained as a result of the reaction of acetone- N^1 -phenylthiosemicarbazone with zinc chloride in a ratio of 1:2. In this reaction, the thiosemicarbazone was coordinated to the metal only with S atom and retained its free configuration. The metal in the center is surrounded by sulfur atoms and chloride atoms of both thiosemicarbazones (Bel'skii, Prisyazhnyuk, Kolchinskii, & Koksharova, 1987).

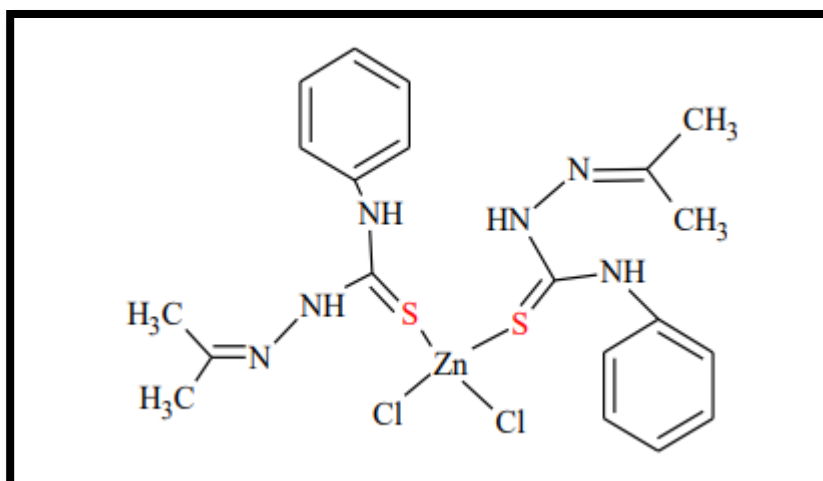


Figure 1.23 S donor thiosemicarbazone

1.3.4.2 Bidentate Thiosemicarbazone Complexes

Thiosemicarbazone ligands act as NS or NN donors in bidentate complexes. Examples exist of both forms of coordination.

In a study by Prabhu and Ramesh (2013), naphthaldehyde thiosemicarbazone ligand(L) and $[\text{Pd}(\text{Br})_2(\text{PPh}_3)_2]$ compound dichloromethane/ethanol (1:1) $[\text{Pd}(\text{L})\text{Br}(\text{PPh}_3)_2]$ closed at room temperature mononuclear palladium(II) thiosemicarbazone complex represented by the formula synthesized. When the X-ray diffraction studies of the complex are examined (Figure 1.24); It has been observed that the ligand is bound as a bidentate from *N* and *S* atoms and the periphery of the Pd(II) ion is in a disturbed square plane geometry.

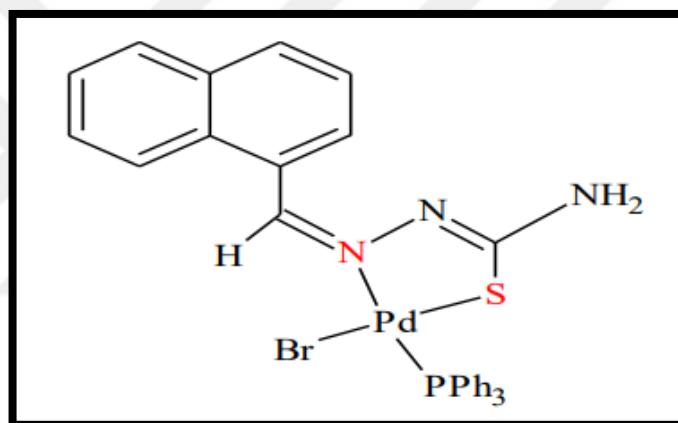


Figure 1.24 NS donor thiosemicarbazone

In a study carried out in 2006; Three new Co(II) complexes were synthesized using acetone *S*-methylthiosemicarbazone (H_2L). Whereas the complexes were characterised by infrared spectroscopy and magnetic measurements, the crystalline structures of the compounds $[\text{CoL}_2\text{Cl}]\text{I}$ and $[\text{CoLBr}_2]$ were determined by X-ray diffraction. In both complexes, acetone *S*-methylisothiosemicarbazone ligand bidentate NN acts as a donor. Looking at the structural analysis; It was observed that $[\text{CoL}_2\text{Cl}]\text{I}$ complex (Figure 1.25 A) preferred triangular bipyramid geometry as a result of steric interactions of ligands. The absence of steric hindrance in the $[\text{CoLBr}_2]$ compound resulted in the formation of distorted tetrahedral geometry (Figure 1.25 B) (Novakovic, Bogdanovic, & Leovac, 2006).

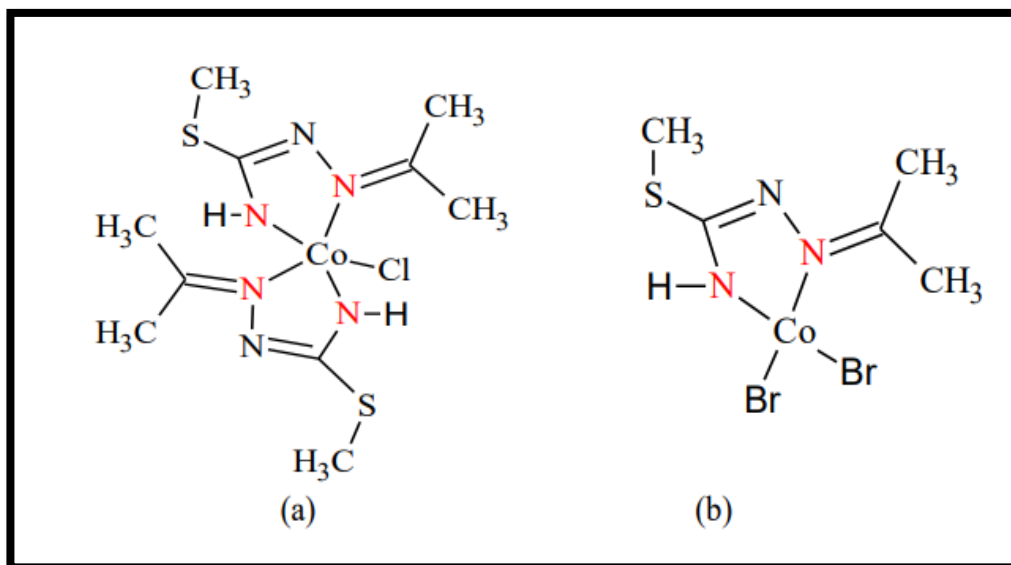


Figure 1.25 NN donor thiosemicarbazone

1.3.4.3 Tridentate Thiosemicarbazone Complexes

When the studies on tridentate thiosemicarbazone ligands are examined in the literature, it is seen that the ligands are mostly in coordination with ONS and ONN donor atoms. There are also studies where it coordinates with NNS and NSP donor atoms.

In a study published by Hussein et al. in 2015, four new dioxomolybdenum (VI) complexes were synthesized. In all synthesized complexes (Figure 1.26) ligands were coordinated with the ONS donor atoms to the molybdenum cation. The results of X-ray crystallography analysis illustrate that the complexes show a distorted octahedral structure and the coordination formed is completed with a solvent molecule such as methanol or H₂O (Hussein, Guan, Haque, Ahamed, & Majid, 2015).

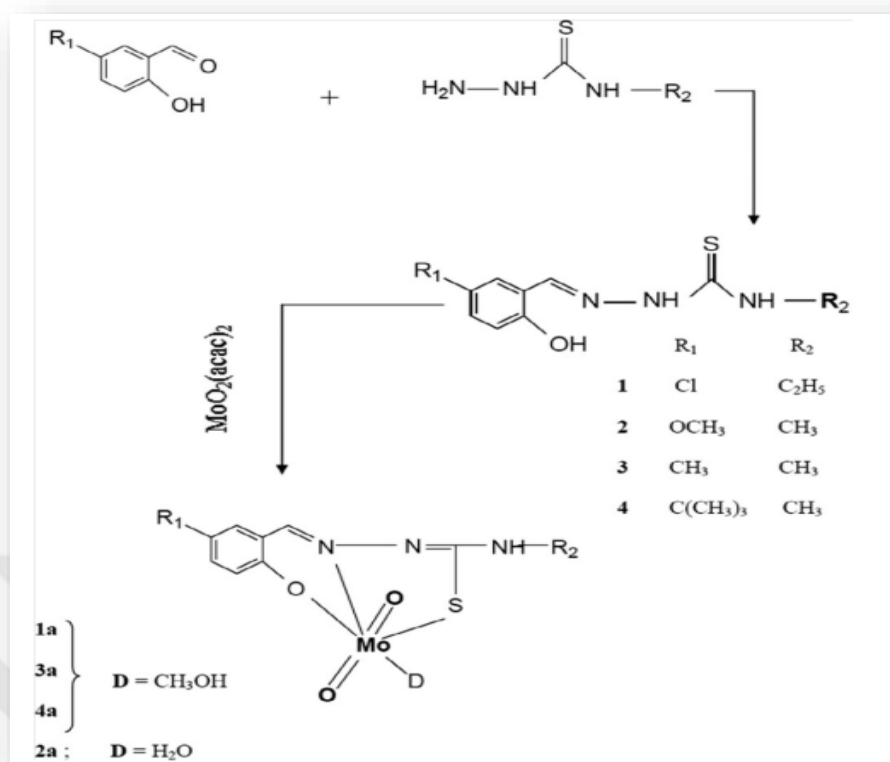


Figure 1.26 Synthesis procedure of compounds

[NiL(PPh₃)₂]₂.PPh₃ synthesis scheme (Figure 1.27), which contains a triphenylphosphine molecule in its structure between the crystal cavities. IR, ¹H, ¹³C and ³¹P NMR spectra were used for ligand and complex characterizations. The complex's molecular structure has been identified by X-ray diffraction. In the nickel(II) complex, the thiosemicarbazone ligand coordinates to the metal in tridentate form with the ONS donor structure. The complex in which the other coordination is completed with triphenylphosphine is in square planar geometry (Guveli et al., 2010).

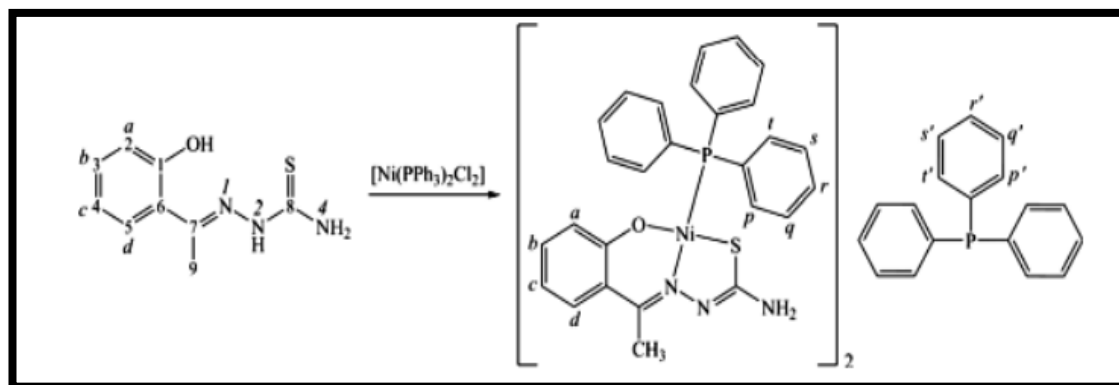


Figure 1.27 Synthesis of Ni(II) complex of ONS donor thiosemicarbazone

1.3.5 Geometry of Thiosemicarbazone Complexes

The most common geometry types in thiosemicarbazone complexes are; Squareplane (Sen, Shit, Mitra, & Batten, 2008) and octahedral (Kannan, Sivagamasundari, Ramesh, & Liu, 2008; Zidan & El-Said, 2004) geometry types, while tetrahedral complexes of thiosemicarbazone complexes (Chandra, Raizada, Tyagi, & Gautam, 2007) were also synthesized. Chandra et al. proposed an octahedral geometry for Ni(II) complexes of benzyl bistiosemicarbazone, and a tetrahedral geometry for Cu(II) complexes.

Rarely, five-coordinate complexes have also been encountered. 6-methyl-2-formylpyridine N⁴ synthesized by Akbar Ali et al. the monoligand Cu(II) complex of dimethylthiosemicarbazone is five coordinated (Ali, Mirza, Monsur, Hossain, & Nazimuddin, 2001).

Seven-coordinated complexes of thiosemicarbazones have also been rarely encountered (Rai, Sengupta, & Pandey, 2005). Bermejo et al. proposed the geometry of the Sn(II) complex of the bis(4-N methylthiosemicarbazone)-2,6-diacetylpyridine ligand as a pentagonal bipyramid (Bermejo et al., 2004).

1.3.6 Biological Activities of Thiosemicarbazones

Thiosemicarbazone compounds are of interest due to their various biological activities. These compounds and their derivatives are involved in a great variety of biological activities like antitumor, antibacterial and antiviral. It is known that when some drugs are administered in metal complexes, their efficacy increases and many metal chelates inhibit tumor growth. Chemically, however, heterocyclic thiosemicarbazones are of interest. They are versatile ligands because of their ability to have donor atoms and coordinate in both neutral and deprotonated form (Zidan & El-Said, 2004). Heterocyclic thiosemicarbazones and their metal complexes are preferred for study due to their diverse biological activity (Jouad et al., 2001)

It is known that various biological activities of thiosemicarbazones are due to their capacity to chelate heavy metals. The biological activities of metal complexes differ according to either metal ions or free ligands (Husain, Abid, & Azam, 2007; Kasuga et al., 2001).

Recently, the use of chelating properties in therapy has attracted attention because they are therapy chelates of Fe(III) complexes of α (N) heterocyclic TSC. As a result of research, 2-pyrazine carboxyaldehyde thiosemicarbazone class ligands remove excess Fe in iron-loaded mice; ligands have also been found to be effective in removing excess stored Fe in patients with Cooley's anemia (Spingarn, & Sartorelli, 1979).

Inhibitory activities of 2-acetylpyridinethiosemicarbazone derivatives against RNA polymerases of influenza virus were found. Recently, the increase in antileukemic properties of these ligands with iron(III), copper (II) and nickel(II) complexes with 1:1 mole ratio has proven that the activity increases with chelate formation (Scovill, Klayman, & Franchino, 1982).

Thiophene-2-carboxaldehyde N4-substituted thiosemicarbazone and Cu(II) complexes have been figured out to be biologically active. The compounds were tested against *Entamoeba histolytica* in vitro. Studies have proven that the compounds are more effective than the drug (metronidazole) in commercial use (Sharma, Athar, Maurya, & Azam, 2005).

In conclusion, studies have shown that thiosemicarbazone and thiosemicarbazone metal complexes have been figured out to be antifungal, antibacterial, antiviral, antimicrobial, antimalarial, antitumor, antiamoebic, anti-HIV, antileukemic, antioxidant, and anticancer.

1.4 Studies in the Literature on Thiosemicarbazone and Metal Complexes

Depending on the diversity of aldehyde and ketone groups in the structures of thiosemicarbazone derivatives, these compounds and their derivatives have been interesting because they exhibit different behaviors in compounds with transition metals and other metal groups (Kovala Demertezi et al., 2004). On the other hand, it has been proven by studies that metal complexes show more effective biological activity than ligands (Kasuga et al. 2003).

In studies carried out to examine the structure-activity relationship during the exchange of thiosemicarbazone derivative compounds with metal ions, it is detected that *in vivo* activity of metal complexes is higher than thiosemicarbazone compounds. Cardia et al. (2000) listed the factors affecting the biological activities of metal complexes as follows:

- Substitution of hydrogen from aryl with an alkyl group
- The introduction of different substituents into the aromatic ring
- The length of the chain attached to the S atom.
- Substitution of the primary amine group with the secondary amine

In the studies, metal thiosemicarbazone complexes were examined by classification depending on the metal configuration d.

1.4.1 Co(II) and Co(III) complexes

Alomar et al. (2009) synthesized cobalt(II) complexes (Figure 1.28) in disordered tetrahedral structure by heating 3-thiophenylthiosemicarbazone in ethanolic medium by adding $\text{CoCl}_2 \cdot 6\text{H}_2\text{O}$ or CoBr_2 to thiosemicarbazone under reflux for 24 hours. They reported that in this complexation, the ligand is coordinated with metals through the *N* and *S* atoms of azomethine.

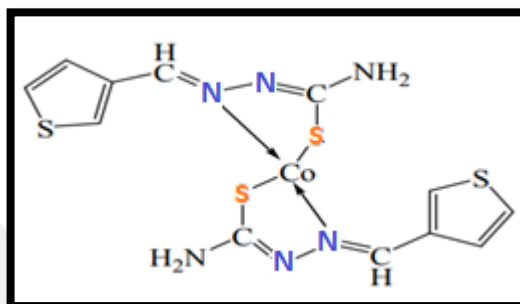


Figure 1.28 Co complex structure of 3-thiophenylthiosemicarbazone

When the complex was examined in terms of structure, it was observed that ligand was in thiol form and the distorted tetrahedral structure was close to the square plane.

Refat et al. (2009) synthesized metal complexes (Figure 1.29) by heating coumarin-3-yl thiosemicarbazones with $\text{CoCl}_2 \cdot 6\text{H}_2\text{O}$ and $\text{NiCl}_2 \cdot 6\text{H}_2\text{O}$ in an ethanolic environment for 1 hour under reflux. It has been stated that coumarin-3-yl thiosemicarbazones are coordinated as bidentate ligands in their metal complexes due to the thiol sulfur and azomethine nitrogen groups in their structures.

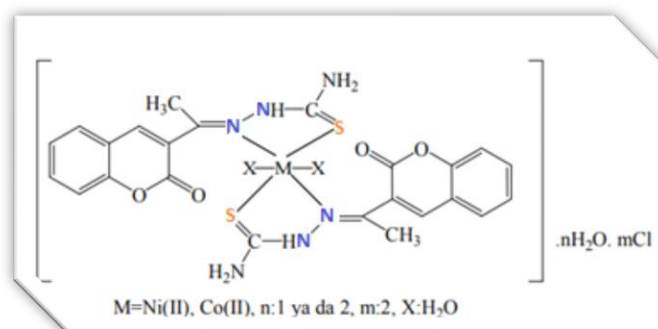


Figure 1.29 Cobalt-nickel complex structure of coumarin-3-yl thiosemicarbazone

In this study, thiosemicarbazone based Co(II), Ni(II), Cu(II) and Zn(II) metal complexes (Figure 1.30) have been synthesised. It was determined by the analyzes that all the compounds were in octahedral geometry. When the activities of the synthesized complexes were examined, the Co(II) complex was the most active. (Gokulnath, Mnikandan, Anitha, & Umarani, 2021).

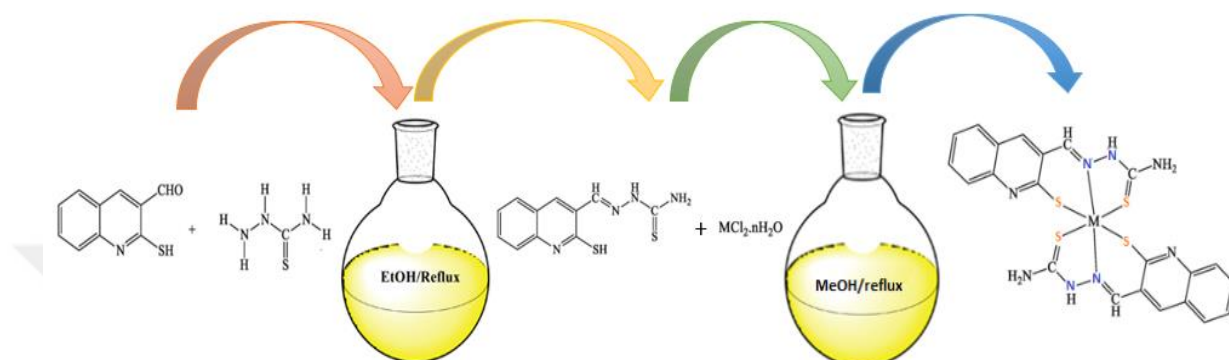


Figure 1.30 Synthesis of ligand and metal(II) complexes

1.4.2 Ni(II) complexes

In the study performed with thiosemicarbazone ligands and Ni(II) nickel salts, variability is observed according to the structure of the reacting ligand. Guveli et al. (2011) synthesized nickel(II) complexes (Figure 1.31) with the ONS and ONN donor groups TSC.

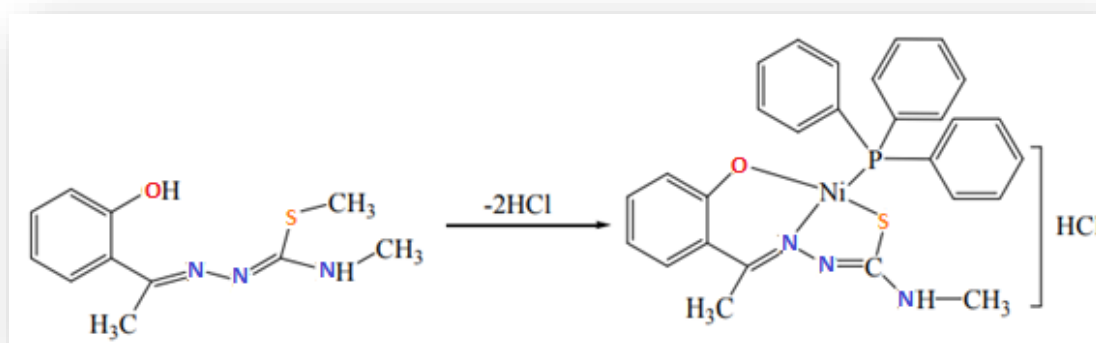


Figure 1.31 Structure of nickel(II) complex

They reported that the complexation reaction occurs when azomethine forms a ligand with triphenylphosphine over nitrogen, phenolate oxygen and sulfur atoms.

Wang et al. (2009) synthesized complexes of 6-hydroxy chromene-3-carbaldehyde thiosemicarbazone with nickel(II) nitrate (Figure 1.32). They reported that the thiosemicarbazone ligand coordinates with metals in a tridentate structure and forms five-membered chelates.

Nickel(II) complex was synthesized. It was clarified by the analyzes that the complex has a square plane structure (Figure 1.33) (Prabhu, & Ramesh, 2016).



Figure 1.32 Synthesis of Ni(II) thiosemicarbazonato complex

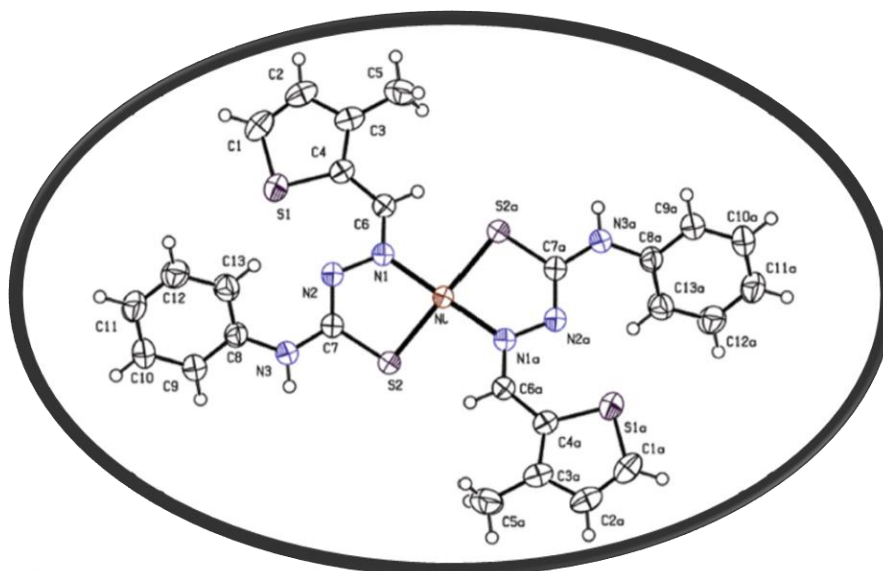


Figure 1.33 Crystal structure of the Ni(II) complex

In this study, the crystal structures of two new coordination compounds synthesized (Figure 1.34) with thio-ligands were investigated. In complex 4 (Figure 1.35), the ligand is coordinated to the metal in anionic form, the bidentate with the *N*- and *S*-donor atoms. It has been clarified that the structure of the complex is a square plane. In Complex 3, however, the ligand is neutrally bound only on the *S* donor atom. Considering the bond angles in the complex, it was observed that the angle of the P-Cu-P bond was the largest and the geometry was observed to be distorted tetrahedral (Lobana et al., 2022).

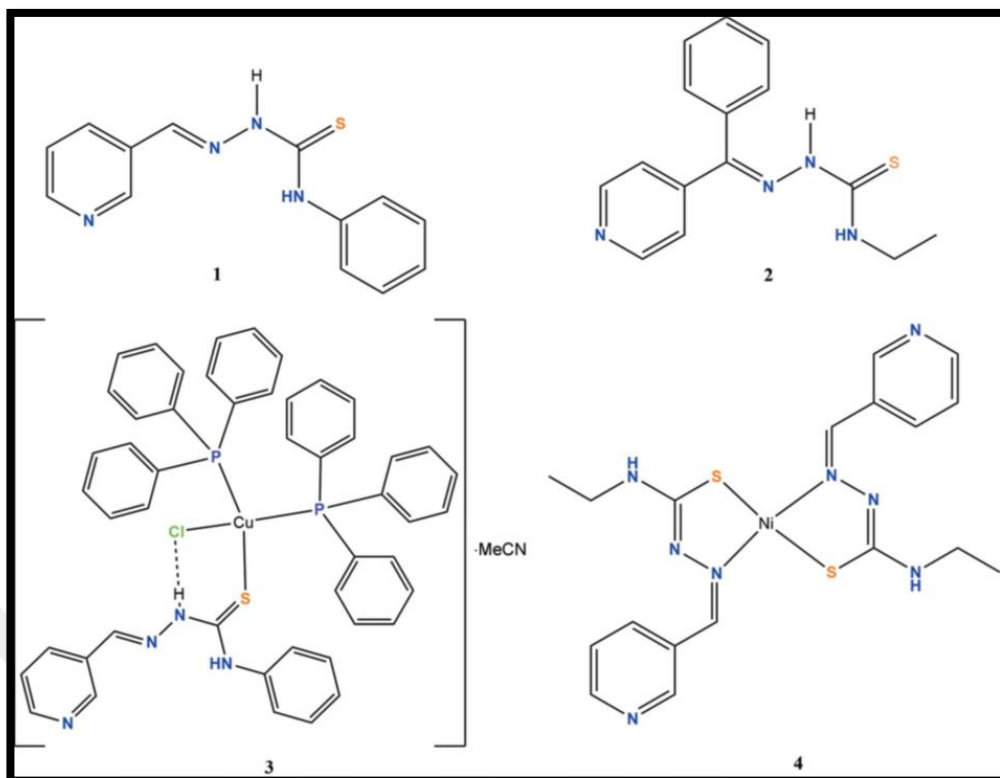


Figure 1.34 Schematic representations of compounds 1–4

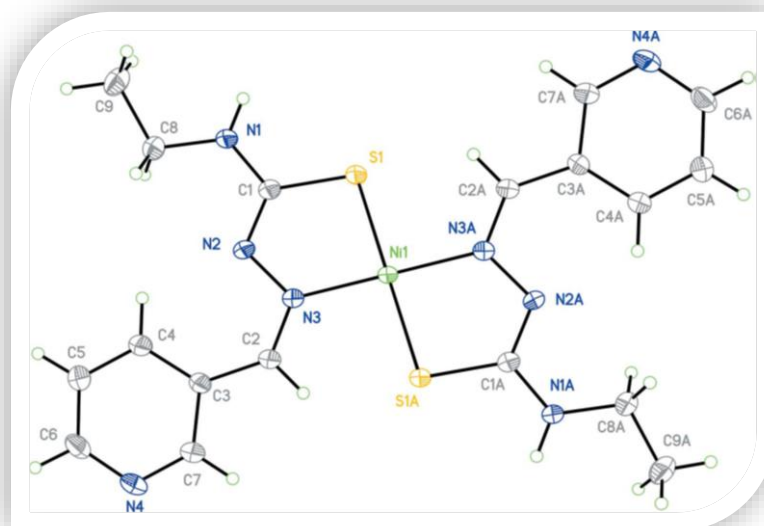


Figure 1.35 Structure of complex 4

New Ni(II) complexes (Figure 1.36) containing TSC ligands which are indole-based were synthesized and their structures were elucidated by various spectroscopic methods. The square planarity of the synthesized Ni(II) complexes was illuminated by single-crystal X-ray crystallography (Figure 1.37) (Haribabu et al., 2017).

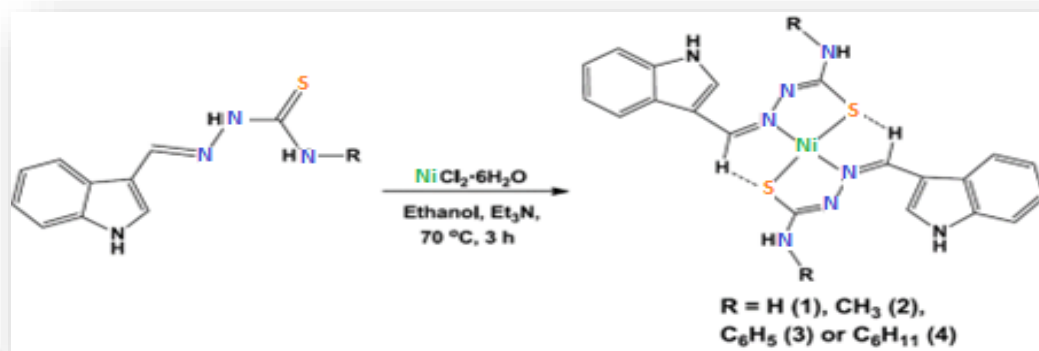


Figure 1.36 Synthetic scheme of Ni(II) complexes

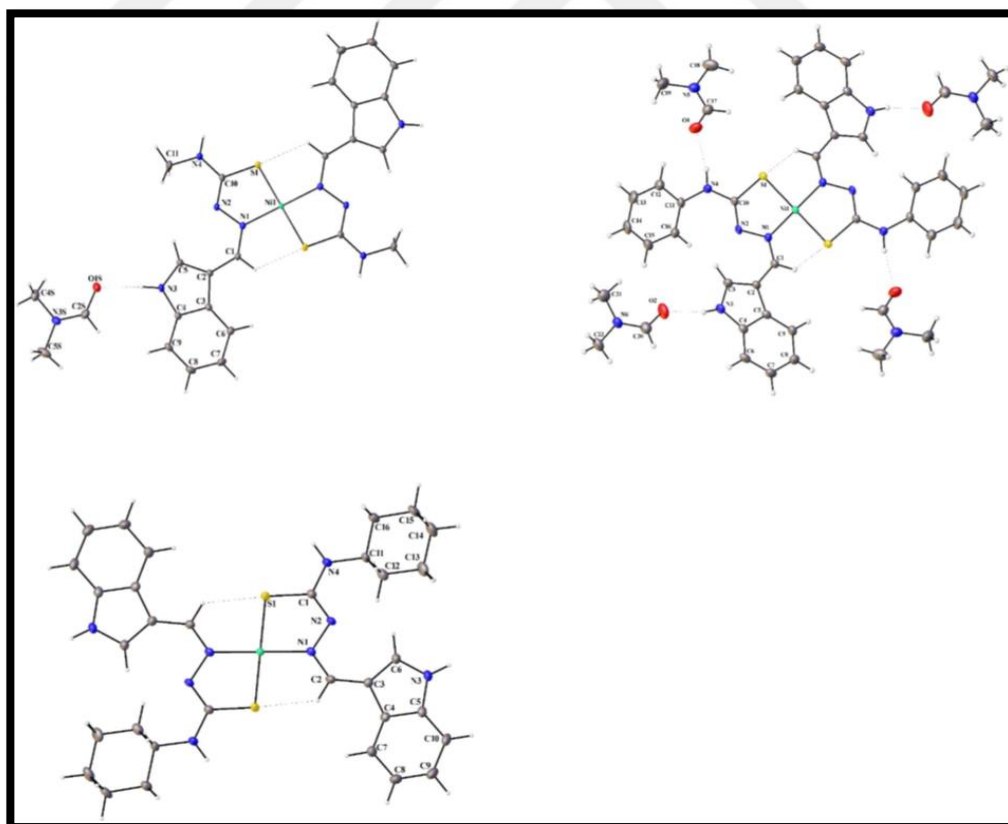


Figure 1.37 Crystal structures of Haribabu's nickel complexes

Seven Ni(II) complexes (Figure 1.38; Figure 1.39; Figure 1.40) were synthesized and their structures were characterized physico-chemically. It has been observed that thiosemicarbazones are coordinated in the forms of structures formed in the complexes, both in the thion and thiole form. In the complexes, the ligands are tridentate coordinated to the metal. It is supported by the spectral characterization data that the Ni(II) complex, one of the synthesized compounds, shows octahedral coordination (Rapheal, Manoj, Kurup, & Fun, 2021).

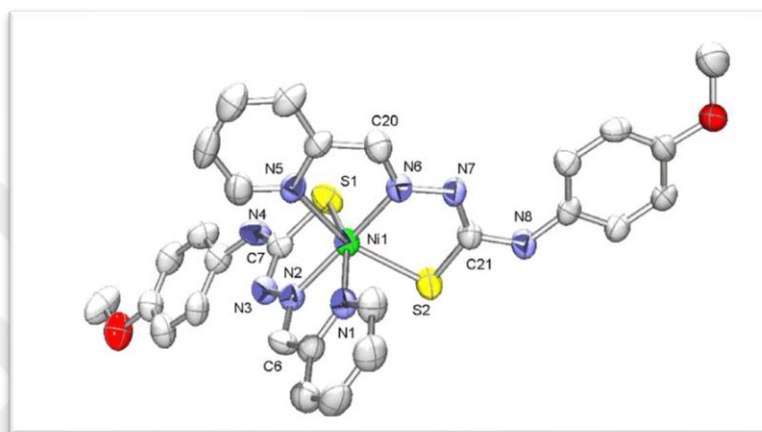


Figure 1.38 ORTEP diagram of the complex 1a

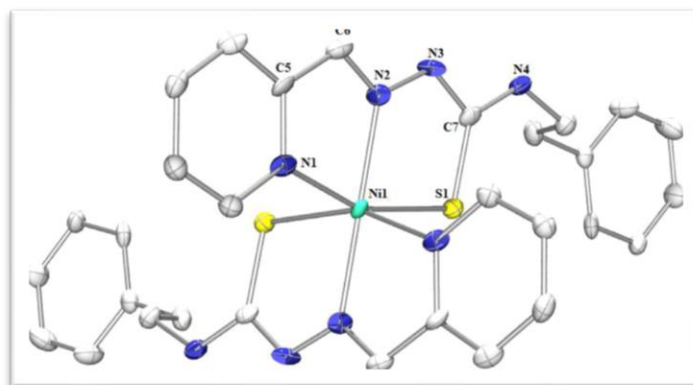


Figure 1.39 ORTEP diagram of the complex 5

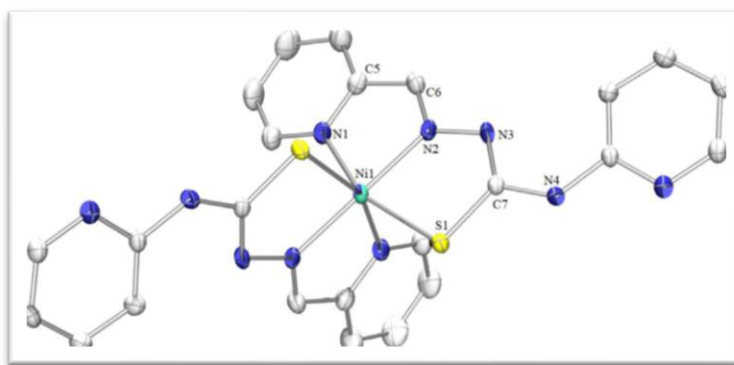


Figure 1.40 ORTEP diagram of the complex 7a

1.4.3 Zn(II) complexes

Zinc plays an important role in a variety of biological systems. As an important cofactor, it can act as a regulatory ion in cell metabolism. The complexes of thiosemicarbazones with Zn(II) (Figure 1.41) especially show antimicrobial activity. The ability to make hydrogen bonds in metal complexes determines the antimicrobial activity of ligands (Kovala-Demertzi et al. 2006).

Kovala-Demertzi et al. (2006) synthesized metal complexes with square pyramidal and octahedral geometry by heating thiosemicarbazone with zinc chloride under reflux in ethanolic environment.

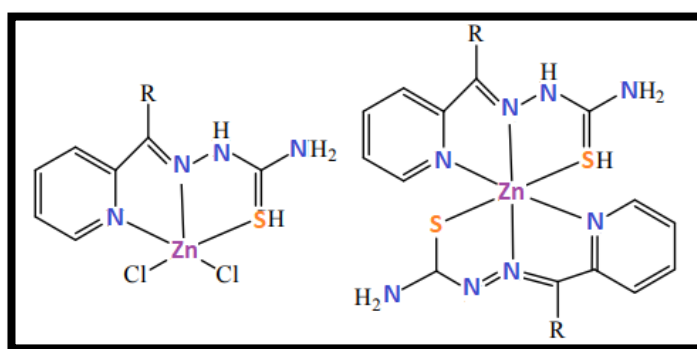


Figure 1.41 Zinc chloride complex structures of thiosemicarbazone

Al-Riyahee et al., (2022) synthesized the Zn(II) complex (Figure 1.42) by heating it under reflux in study. It has been observed that the geometry of the complex is spherical square pyramidal (Al-Riyahee, Horton, Coles, Amoroso, & Pope, 2022).

that the Mn(II) complex exhibit higher activity against human liver (Hep G2) than Zn(II) (Abdalla, Hassan, Elganzory, Aly, & Alshater, 2021).

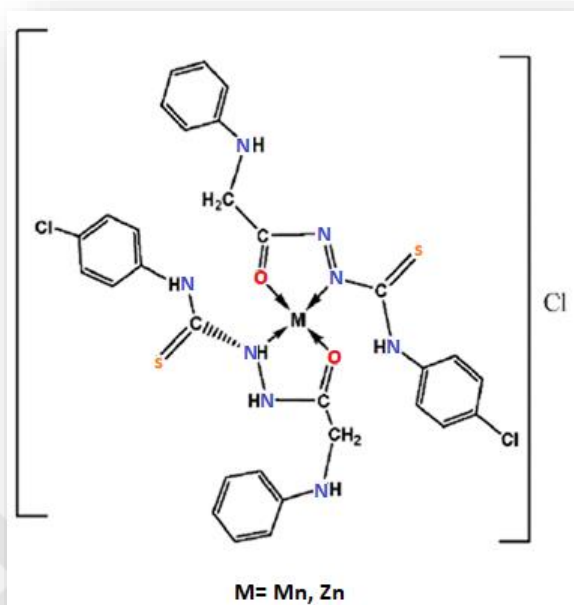


Figure 1.44 Chemical structures of the ligand and metal complexes

1.4.4 Palladium(II) Thiosemicarbazone Complexes

Palladium complexes show effective and wide-ranging biological activity against gram-negative and gram-positive pathogens, including antimicrobial, antimalarial and antiviral. The similar properties of the ligand and the complex and its lipophilic feature and simple transfer through cell membranes showed an increase in the cytotoxic and antimicrobial activities of such complexes. Looking at the results from this perspective, further research is ongoing to find out novel Pd(II) compounds that may be used as antitumors and antimicrobials (Badea et al., 2013).

Four new palladium thiosemicarbazone complexes were synthesized by Prabhakaran and his group in 2013 (Figure 1.45). The CT-DNA and BSA DNA/protein binding properties of these complexes, of which characterizations were performed, were also examined and their biological activities were observed. In addition, in cytotoxic studies, experiments with these newly synthesized complexes in lung cancer

(A549) and liver cancer (HepG2) cells were found to have better activity than thiosemicarbazone analogs (Kalaivani et al., 2013).

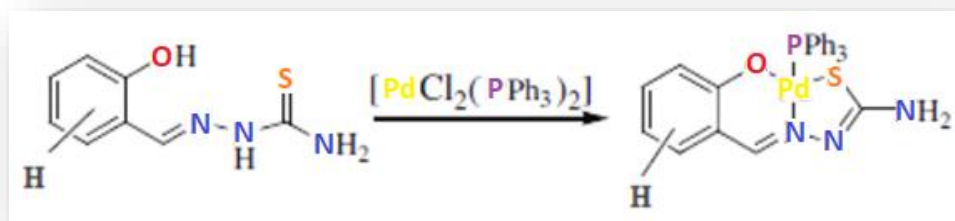


Figure 1.45 Synthesis reaction of ONS coordinated Pd(II) complex

In a study by Demetzi et al. in 2006, two new stable Pd(II) complexes (Figure 1.46) were synthesized from 3-hydroxypyridine-2-carbaldehyde thiosemicarbazone and Li_2PdCl_4 was used as starting material. The structure of the complex has been elucidated by spectroscopic techniques. (Demetzi, Yadav, & Kovalá-Demertzi, 2006).

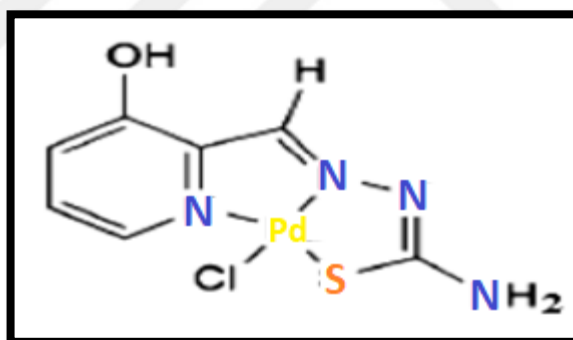


Figure 1.46 NNS donor Pd(II) complex

Pd(II) complexes of S-methyl/ethyl-4-H/phenyl thiosemicarbazones (Figure 1.47) were synthesized by Kızılcıklı and his working group in 2004. The characterization of the complexes was performed by spectroscopic techniques. Multidentate thiosemicarbazones are coordinated as mono-, bi-, or tridentate ligands, depending on their alkyl moiety and type of metal ion. (Kızılcıklı, Ülküseven, Daşdemir, & Akkurt, 2004).

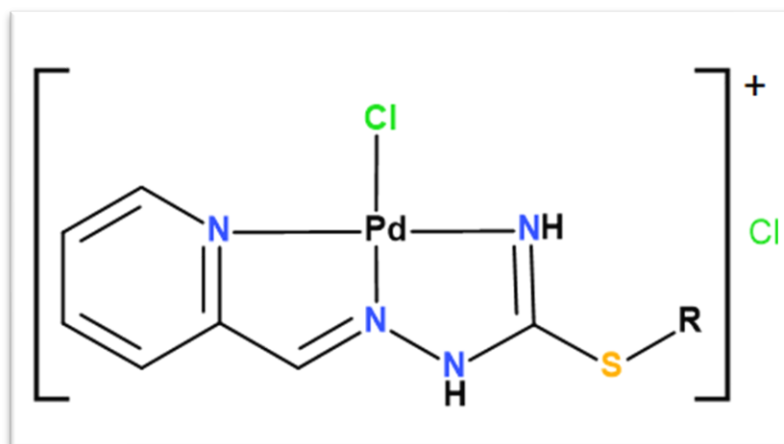


Figure 1.47 NNN donor Pd(II) complex

In the study conducted by Asiri and Khan in 2010, the antibacterial activity of the new Pd (II) metal complexes (Figure 1.48) and the mentioned thiosemicarbazones, which were synthesized by reacting $[Pd(DMSO)_2Cl_2]$ and thiosemicarbazones of various structures, were investigated. The structures of the obtained complexes were explained by spectroscopic techniques (Asiri, & Khan, 2010).

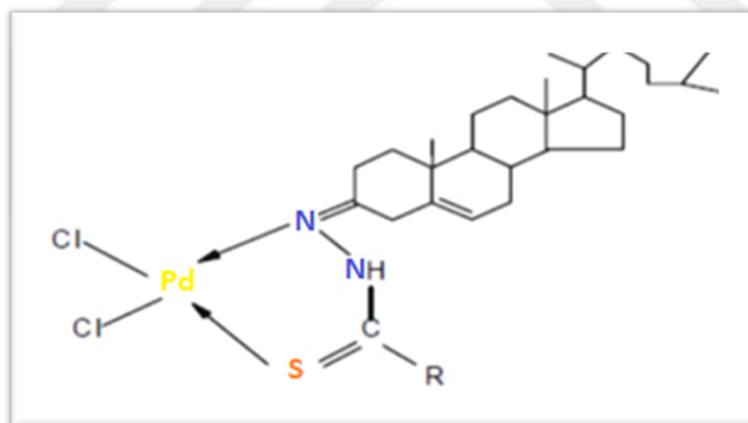


Figure 1.48 NS donor Pd(II) complex

Pd(II) complexes (Figure 1.50) of indole-based thiosemicarbazone ligands (Figure 1.49) containing N-benzyl were synthesized and characterized. It has been observed that the structure of the complexes is square plane (Balakrishnan et al., 2022).

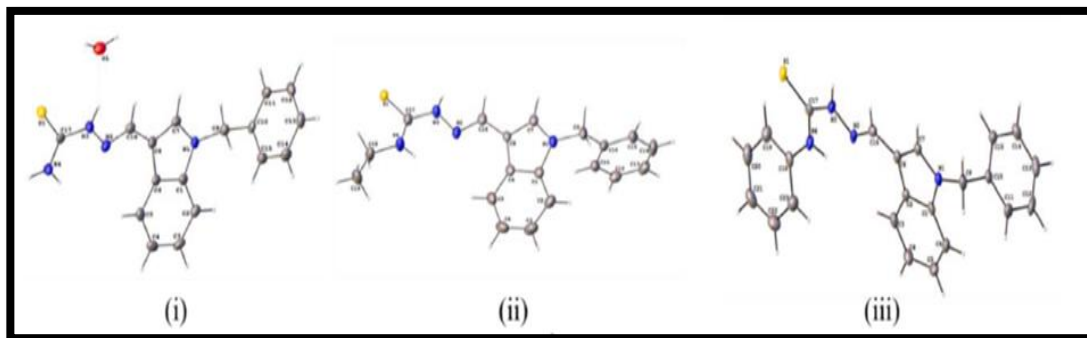


Figure 1.49 Molecular structures of ligands

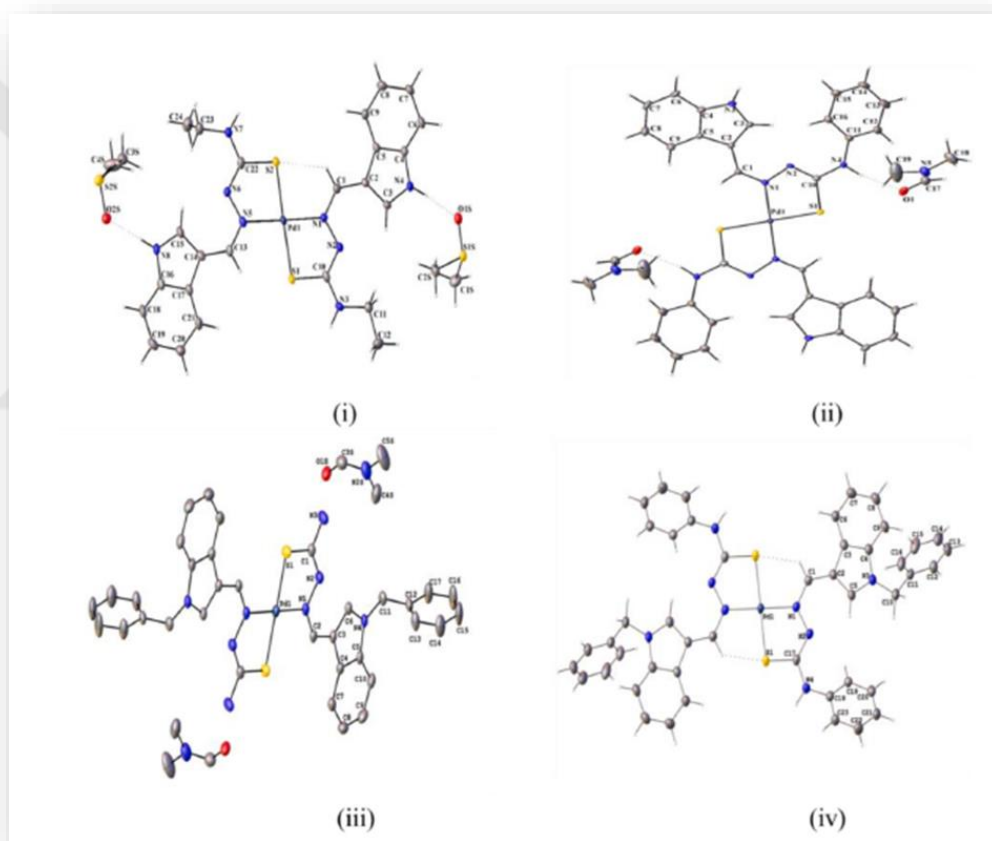


Figure 1.50 Molecular structures of Pd(II) complexes

CHAPTER TWO

MATERIAL AND METHOD

2.1 Instruments

Infrared Spectroscopy: Varian 1000 FT spectrophotometer (Dokuz Eylül University, Faculty of Science and Arts, Chemistry Department)

¹H NMR Spectroscopy: 400 MHz High Performance Digital FT-NMR instrument (Ege University, Science Faculty, Chemistry Department)

Single Crystal X-Ray Diffraction: Bruker / D8 Quest instrument (Sinop University, Scientific And Technological Researches Center)

2.2 Chemicals

All reactants and solvents are HPLC pure. 2-Acetyl 5-Bromo Thiophen-N-Methyl-Thiosemicarbazone ligand was synthesized according to the article (Guler, Kayalı, Sadan, Sen, & Subasi, 2022). Anhydrous CoCl₂ and NiCl₂, ZnCl₂ were purchased from Sigma-Aldrich. The starting metal complex Pd(COD)Cl₂ was prepared according to the literature (Drew, Doyle, & Shaver, 1972). DMSO, ethanol, diethyl ether, dichloromethane and dimethylformamide were obtained from Merck.

2.2.1 Purification of Solvents

All solvents have been dried using standardised techniques and stored under nitrogen until use (Perrin, Armarego, & Perrin, 1980).

2.3 Synthesis of the HL ligand

The synthesis of ligand HL (Figure 2.1) was performed using the following literature (Guler et al., 2022).



Figure 2.1 Synthesis of HL ligand

2.4 Preparation of the Starting Complex, $[\text{Pd}(\text{COD})\text{Cl}_2]$

The synthesis of starting complex (Figure 2.2) was performed using the following literature procedure (Drew et al., 1972).

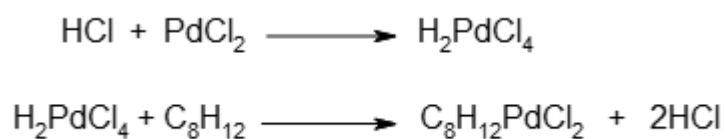


Figure 2.2 Synthesis of $\text{Pd}(\text{COD})\text{Cl}_2$

2.5 Synthesis of the Complexes

The synthesis of complexes (Figure 2.3) was performed using the following literature procedure (Sen et al., 2019).

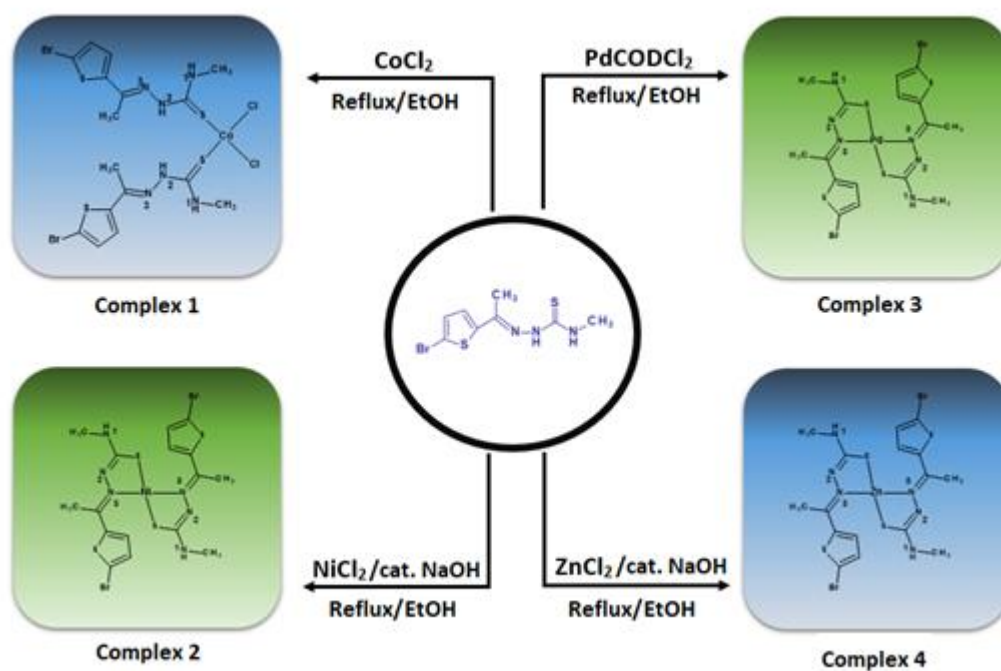


Figure 2.3 Synthesis of complexes

2.5.1 *Bis[chloro(2-Acetyl-5-Bromo-Thiophen-N-Methyl-Thiosemicarbazone)] cobalt(II), [CoCl₂(S-HL)₂]*

The ligand and $\text{CoCl}_2 \cdot 6\text{H}_2\text{O}$ salt (20 ml) were dissolved in EtOH at a ratio of [1;1] and refluxed for 3 hours. As a result of the reaction, the formation of a blue colored microcrystalline was observed. Afterwards, filtration was performed, and the resulting product was washed with EtOH.

2.5.2 *Bis[2-Acetyl-5-Bromo-Thiophen-N-Methyl-Thiosemicarbazone] nickel(II), [Ni(N,S-L)₂]*

The ligand and anhydrous NiCl_2 salt (20 ml) were dissolved in EtOH at a ratio of [1;1], and 2.3 drops of the prepared dilute NaOH solution were added to the medium to keep the pH between 6-7. The reaction was refluxed for 4 hours. As a result, black solid formation was observed. The resulting solid was dried by washing with EtOH. The compound was then dissolved in DMF/Diethyl ether to obtain a black crystalline product.

2.5.3 *Bis[2-Acetyl-5-Bromo-Thiophen-N-Methyl-Thiosemicarbazone]palladium (II)*, [Pd(N,S-L)₂]

The ligand and Pd(COD)Cl₂ (20 ml) were dissolved in EtOH at a ratio of [1;1] and refluxed for 3 hours. As a result of the reaction, the formation of a red solid was observed. The resulting solid was dried by washing with EtOH and DCM. The compound was then dissolved in DMF/Diethyl ether to obtain a red crystalline product.

2.5.4 *Bis[2-Acetyl-5-Bromo-Thiophen-N-Methyl-Thiosemicarbazone]zinc(II)*, [Zn(N,S-L)₂]

The ligand and anhydrous ZnCl₂ salt (20 ml) were dissolved in EtOH at a ratio of [1;1], and 2.3 drops of the prepared dilute a solution of NaOH was added in the medium to keep the pH between 6-7. Reaction has been refluxed for 4 hours. As a result, yellow solid formation was observed. The resulting solid dried by washing with EtOH. The compound was then dissolved in DMF/Diethyl ether to obtain a yellow crystalline product.

2.6 Determination and Refinement of The Crystal Structure

The molecular and crystal structures of complexes Co(II), Pd(II), Ni(II), and Zn(II) were elucidated by the single-crystal X-ray diffraction method. Bruker APEX II Quazar three-circle diffractometer has been used to collect the single-crystal data of all compounds. Indexing was performed using APEX2 (Madison, 2014). The structure was solved by the SHELXD (Sheldrick, 2008) structure solution program using Dual Space and refined with the help of the SHELXL (Sheldrick, 2015) refinement package using Least Squares minimisation. These calculations are carried out under the OLEX2 system (Dolomanov, Bourhis, Gildea, Howard, & Puschmann, 2009). To handle the geometric calculations, we have utilized the PLATON package (Spek, 2003). Table 2-1 contains details of the crystallographic data and some parameters of refinement for all complexes.

Table 2-1 Crystal data and structure refinement parameters for complexes Co(II), Pd(II), Ni(II), and Zn(II)

	Complex Co(II)	Complex Pd(II)	Complex Ni(II)	Complex Zn(II)
Chemical formula	C ₁₆ H ₂₀ Br ₂ Cl ₂ CoN ₆ S ₄	C ₁₆ H ₁₈ Br ₂ N ₆ PdS ₄	C ₁₆ H ₁₈ Br ₂ N ₆ NiS ₄	C ₃₅ H ₄₃ Br ₄ N ₁₃ OS ₈ Zn ₂
Formula weight	714.27	688.82	641.13	1368.68
Temperature (K)	273	273.15	293(2)	296(2)
Space group	P2 ₁ /c	Cc	P2 ₁ /c	Pc
Crystal system	Monoclinic	Monoclinic	Monoclinic	Monoclinic
a(Å)	14.731 (3)	4.898 (3)	12.8955 (7)	7.5959 (14)
b(Å)	7.6904 (13)	30.787 (19)	15.0548 (8)	22.746 (4)
c (Å)	23.576 (4)	15.277 (9)	12.4550 (6)	14.841 (3)
β (°)	99.313 (3)	90.09 (1)	111.3550 (10)	95.228 (5)
Cell volume (Å ³)	2635.6 (8)	2304 (2)	2252.0 (2)	2553.5 (8)
Formula unit cell Z	4	4	4	2
F(000)	1412.0	1344.0	1272.0	1360.0
ρ (g/cm ³)	1.800	1.986	1.891	1.780
μ (mm ⁻¹)	4.220	4.653	4.798	4.440
Crystal size (mm ³)	0.14 4 × 0.113 × 0.103	0.42 × 0.14 × 0.07	0.11 × 0.09 × 0.08	0.19 × 0.11 × 0.1
Reflections measured	26110	16519	67049	11317
	-19 ≤ h ≤ 19	-6 ≤ h ≤ 6	-17 ≤ h ≤ 17	-10 ≤ h ≤ 9
Range of h,k,l	-9 ≤ k ≤ 9	-39 ≤ k ≤ 39	-20 ≤ k ≤ 20	-30 ≤ k ≤ 30
	-29 ≤ l ≤ 30	-19 ≤ l ≤ 19	-16 ≤ l ≤ 16	-19 ≤ l ≤ 19
Data/restraints/parameters	6033/0/284	5150/2/266	5607/2/272	11317/2/579
Final R indexes [I ≥ 2σ(I)]	R1=0.0475; wR2=0.0720	R1 = 0.0555; wR2 = 0.1114	R1 = 0.0389; wR2 = 0.0835	R1 = 0.0562; wR2 = 0.0729
Final R indexes [all data]	R1 = 0.1432; wR2 = 0.0929	R1 = 0.1056; wR2 = 0.1274	R1 = 0.0817; wR2 = 0.1084	R1 = 0.1335; wR2 = 0.0885
GOOF on F ²	0.954	1.001	1.106	1.008
Largest diff. peak/hole (e Å ⁻³)	0.49-0.59	0.94-0.92	0.42 -0.48	0.65 -0.64

2.7 Antimicrobial activity

To determine the antimicrobial efficacy of compounds, *Gram-positive and Gram-negative* bacteria, and one yeast species (*Candida albicans* ATCC 10231) were tested. In order to maintain a final concentration of up to 5 mg mL⁻¹, the synthesized compounds were dissolved in dimethyl sulfoxide (DMSO). Gentamicin (10 µg/mL) or ampicillin (10 µg/mL) solutions for bacteria and fluconazole (25 µg/mL) solution for yeast were used as positive controls on the other hand, DMSO was utilized as a negative control. Test bacteria were subcultured using Tryptic Soy Agar (TSA, Merck

Millipore, Germany) and was incubated at 37°C for 18-24 h while yeast was cultured Sabouraud Dextrose Agar (SDA, Merck Millipore, Germany) and incubated at 30°C for 44-48 h. A densitometer (Grant Inst., Cambridge, UK) was used to adjust the turbidity of the microbial suspension to 0.5 McFarland prior to the antimicrobial activity testing.

2.8 Agar Well Diffusion Method

The antibacterial effectiveness of the compounds against test organisms was evaluated using the agar well diffusion assay. For this experiment, the final concentration of the microorganisms was adjusted to 10⁵ CFU ml⁻¹. 100 µl of cell suspension was inoculated sterile Mueller Hinton Agar (MHA, Merck Millipore, Germany) and this medium was poured into petri dishes. 30 µL of sample solution was adsorbed on blank discs and transferred onto MHA plate. After incubation period, the formation of the inhibition zones was observed, and the zone diameters were measured in millimeters. The tests were carried out three times.

2.9 Determination of MIC and MBC

Clinical and Laboratory Standards Institute (CLSI) 2015 guidelines were used to establish the MIC and MBC values of the samples. 80 µl of the compound's aqueous solution (at 5 mg ml⁻¹ concentration) was filled into the first well of a 96 wells plate each containing 80 µl of Mueller Hinton Broth. The samples were tested according to the twofold dilution principle. To achieve a final inoculum concentration of 10⁶ CFU ml⁻¹, 20 µl of the microbial solution was added to the wells. For every sample and control, experiments were run twice. Turbidity was used to quantify bacterial growth following incubation, and the MIC value was calculated as the lowest concentration at which there was no visible growth.

CHAPTER THREE

RESULTS AND DISCUSSIONS

3.1 Synthesis and Characterization of the Complexes

The Schiff base, HL (HL, where the dissociable proton is symbolized by H) was synthesized by the condensation of 4-methyl-3-thiosemicarbazide with 2-acetyl-5-bromo-thiophen (Figure 3.1).

Metal(II) complexes were readily synthesized by reaction of HL with metal(II) chlorides refluxing in ethanol (Figure 3.2). All the complexes are slightly soluble in EtOH, CHCl_3 , CH_2Cl_2 and are easily soluble in DMF, DMSO. The results of the elemental analyzes show that the complexes are of the $[\text{Co}(S\text{-HL})_2\text{Cl}_2]$, and $[\text{M}(N,S\text{-L})_2]$, (M: Ni, Pd, Zn) are within the calculated values.

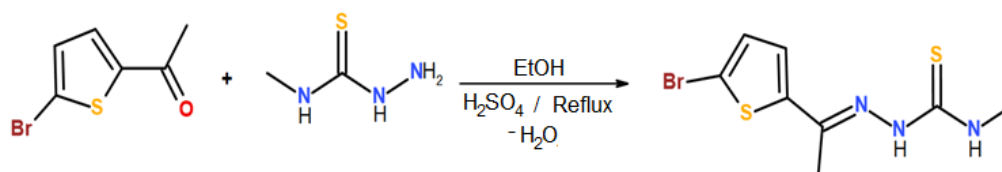


Figure 3.1 HL ligand

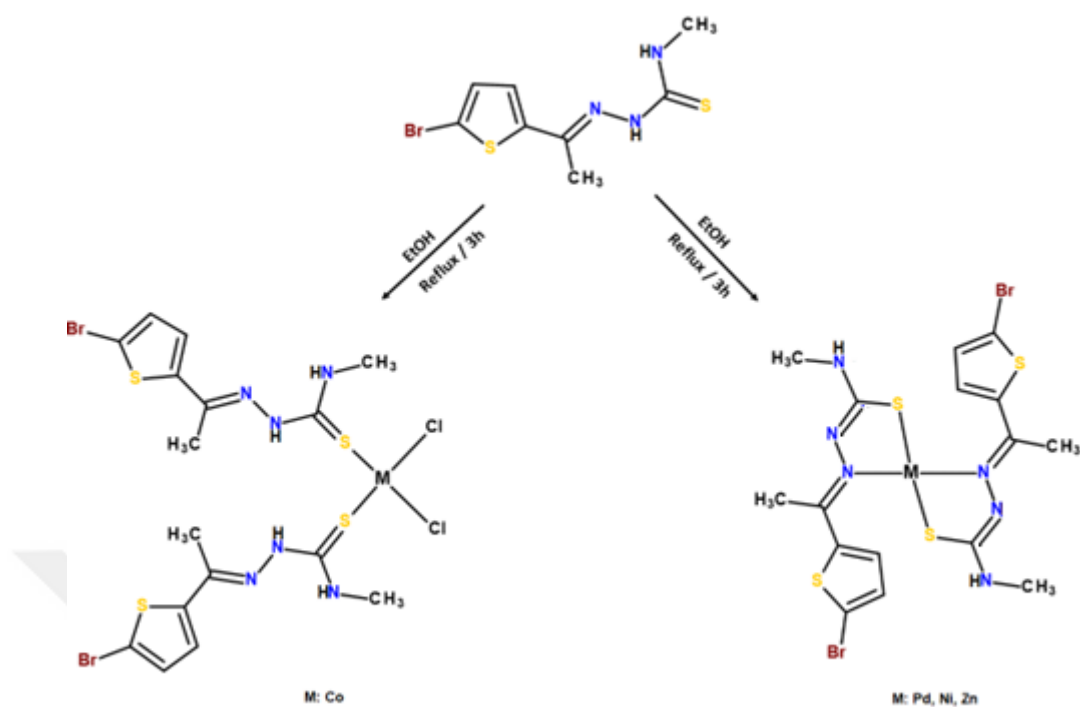


Figure 3.2 HL ligand and their metal complexes

3.2 Physical Properties

Each synthesized compound was purified in extremely high yields. The compounds are stable to air and light and soluble in DMSO and DMF.

Data from elemental analysis [$\text{Co}(S\text{-HL})_2\text{Cl}_2$] and [$\text{M}(N,S\text{-L})_2$], (M: Ni, 2; Pd, 3; Zn, 4). highly supports the formula of the compounds.

The analytical data for the novel compounds are shown in Table 3.1. The stoichiometry of the ligand (HL) and compounds were confirmed by elemental analysis.

Table 3-1 Physical properties and elemental analysis data for the thiosemicarbazone ligand and the complexes

Complex	Yield (%)	Colour	M.P.	Found / (Calcd.) (%)			
				C	H	N	S
HL	85	Yellow	208	32.88	3.45	14.38	21.95
				32.23	3.12	14.22	21.44
[Co(S-HL) ₂ Cl ₂]	65	Blue	240	26.23	3.12	11.22	20.04
				26.90	2.80	11.80	18.00
[Ni(N,S-L) ₂]	67	Black	230	27.32	3.12	12.24	18.35
				27.90	2.60	12.20	18.60
[Pd(N,S-L) ₂]	78	Red	247	27.23	3.02	11.82	19.23
				27.90	2.60	12.20	18.60
[Zn(N,S-L) ₂]	72	Yellow	223	28.13	2.85	12.82	17.23
				27.90	2.60	12.20	18.60

3.3 Infrared Spectra

The FT-IR bands selected for the compounds are presented in the Table 3-2.

Table 3-2 Characteristic FT-IR bands (cm^{-1}) of compounds

Compounds	$\nu\text{N(1)H} + \text{N(2)H}_{\text{sym}}$	$\nu(\text{C}=\text{N})$	$\nu(\text{N}-\text{N})$	$\nu(\text{C}=\text{S})$	$\nu(\text{thiophen ring stretchings})$
HL	3370(s) 3175(m)	1547(s) 1496(s)	1045(s)	974(s)	798(s) 694(s)
[CoCl₂(S-HL)₂]	3351(s) 3195(s)	1577(s)	1034(m)	995(s)	799(s) 674(m)
[Ni(N,S-L)₂]	3336(s)	1636(s) 1563(s)	1022(m)	-	789(s) 729(m)
[Pd(N,S-L)₂]	3395(s)	1556(s) 1503(s)	1029(m)	-	798(s) 729(m)
[Zn(N,S-L)₂]	3388(s)	1658(s) 1562(s)	1035(m)	-	790(s) 730(m)

Thiosemicarbazone ligands, which can bind in neutral or anionic forms, exist as thion-thiol tautomers. The loss of hydrogen in the $-\text{N}_2\text{H}$ or $-\text{SH}$ structures creates the anionic form. Differentiation of the stretching frequencies of the $\nu(\text{C}=\text{N})$ complexes versus the free ligand supports the formation of the complex (Figure 3.3). In the spectrum of the ligand, the $\text{C}=\text{N}$ stretching vibration shows strong bands at 1547 and 1496 cm^{-1} . It was observed that in the Co(II) complex, the $\nu(\text{C}=\text{N})$ vibrational band shifted slightly to higher wavenumbers (1577 cm^{-1}), while the same band shifted more sharply to higher wavenumbers ($1658\text{-}1503 \text{ cm}^{-1}$) in all other complexes. It is observed that complexing has no significant effect on this sharp band corresponding to $\nu(\text{C}=\text{N})$ in complex Co(II) complex. In addition, the presence of a second band corresponding to $\nu(\text{C}=\text{N})$ in the Pd(II) , Ni(II) and Zn(II) complexes shows that these complexes are bound in the form of anionic thiol (Prabhu, & Ramesh, 2016).

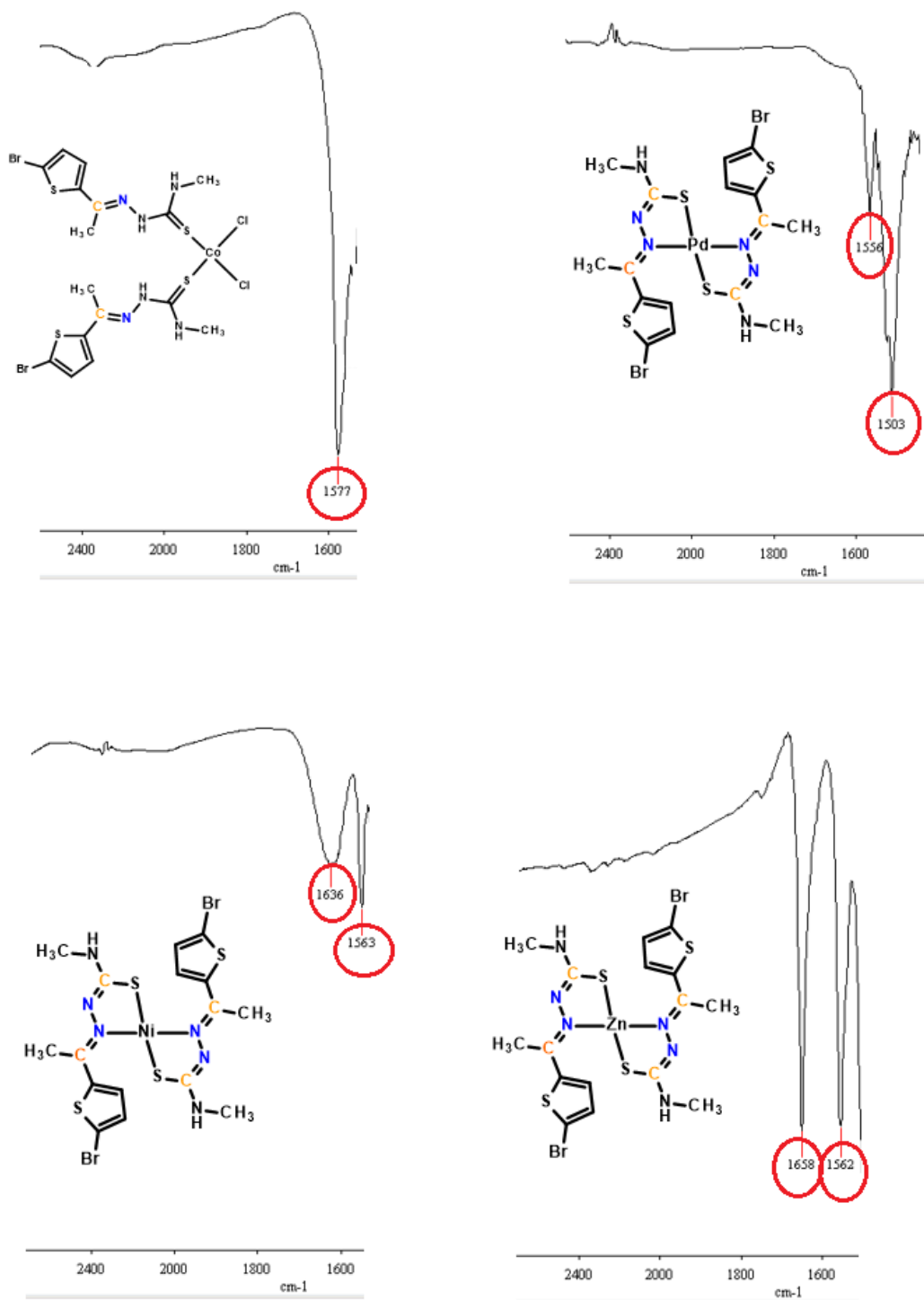


Figure 3.3 C=N bonds of complexes

Furthermore, the disappearance of bands $\nu(\text{N}(2)\text{H})$ in Pd(II), Ni(II) and Zn(II) complexes shows that ligands coordinate with metal centres in their anionic form.

Moreover, the presence of $\nu(\text{N(2)H})$ bands in the Co(II) complex proves that this complex is bound in neutral thiol form (Balakrishnan et al., 2019; Martinez et al., 2018). The presence of new $\nu(\text{M-S})$ and $\nu(\text{M-N})$ bands in complexes Ni(II), Pd(II) and Zn(II) in the range of $500\text{-}575\text{ cm}^{-1}$ and $425\text{-}475\text{ cm}^{-1}$, respectively, ensures the coordination of the ligand with the metal via bidentate N,S atoms. Moreover, the presence of only the $\nu(\text{M-S})$ band in Co(II) indicates that the complexation occurs as a monodentate over the S atom of the ligand (Sen et al., 2019).

In contrast, the $\nu(\text{C=S})$ vibration bands do not occur in the Ni(II) (Figure 3.6), Pd(II) (Figure 3.7) and Zn(II) (Figure 3.8) complexes. Based on these results, the Co(II) complexes are achieved with the neutral tautomer thione ligand. According to these results, it is observed that the ligand in Co(II) complexes has a neutral thion tautomer structure. A strong band ($\nu(\text{C=S})$) of Co(II) at 995 cm^{-1} in the spectrum shows the binding of the metal via the donor sulfur atom of the ligand. Thus, while coordination in $[\text{Co}(\text{S-HL})_2\text{Cl}_2]$ (Figure 3.5) takes place only through the S atom of the TSC ligand (Figure 3.4), coordination in $[\text{M}(\text{N,S-L})_2]$, (M: Ni, Pd, Zn) complexes occurs through thiolate S and N (imino) complexes.) atoms, as in all cases, are shifted their vibrational bands relative to these atoms in the same way. It was concluded that through the N and S donor atoms in the structure of the ligand, it forms coordination bonds with the metal ions in the complexes as N,S bidentate in $[\text{M}(\text{N,S-L})_2]$, (M: Ni, Pd, Zn). This is supported by the fact that the N-N band is at a lower frequency (Saghatforoush et al., 2021).

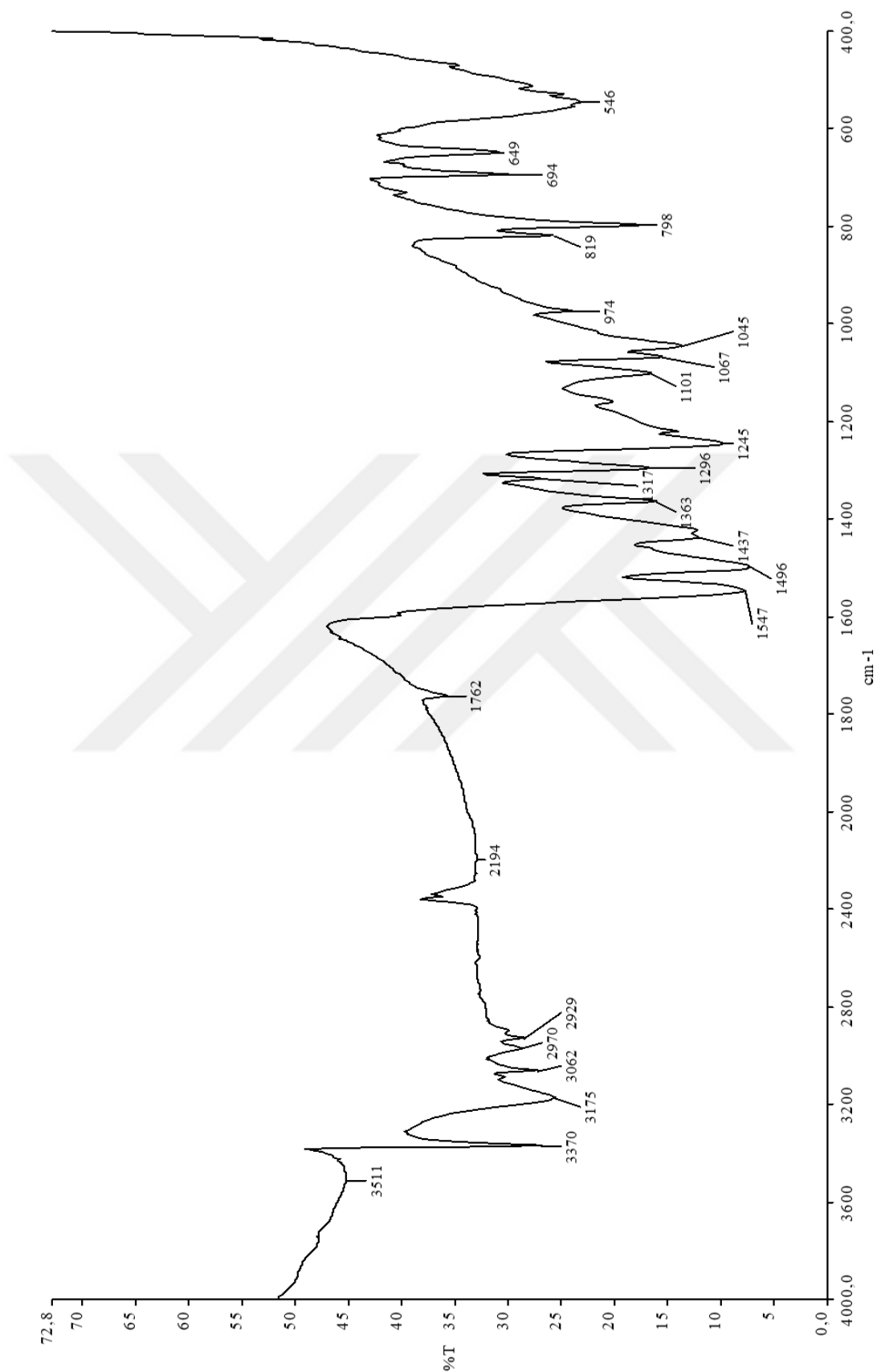


Figure 3.4 The FT-IR spectrum of HL

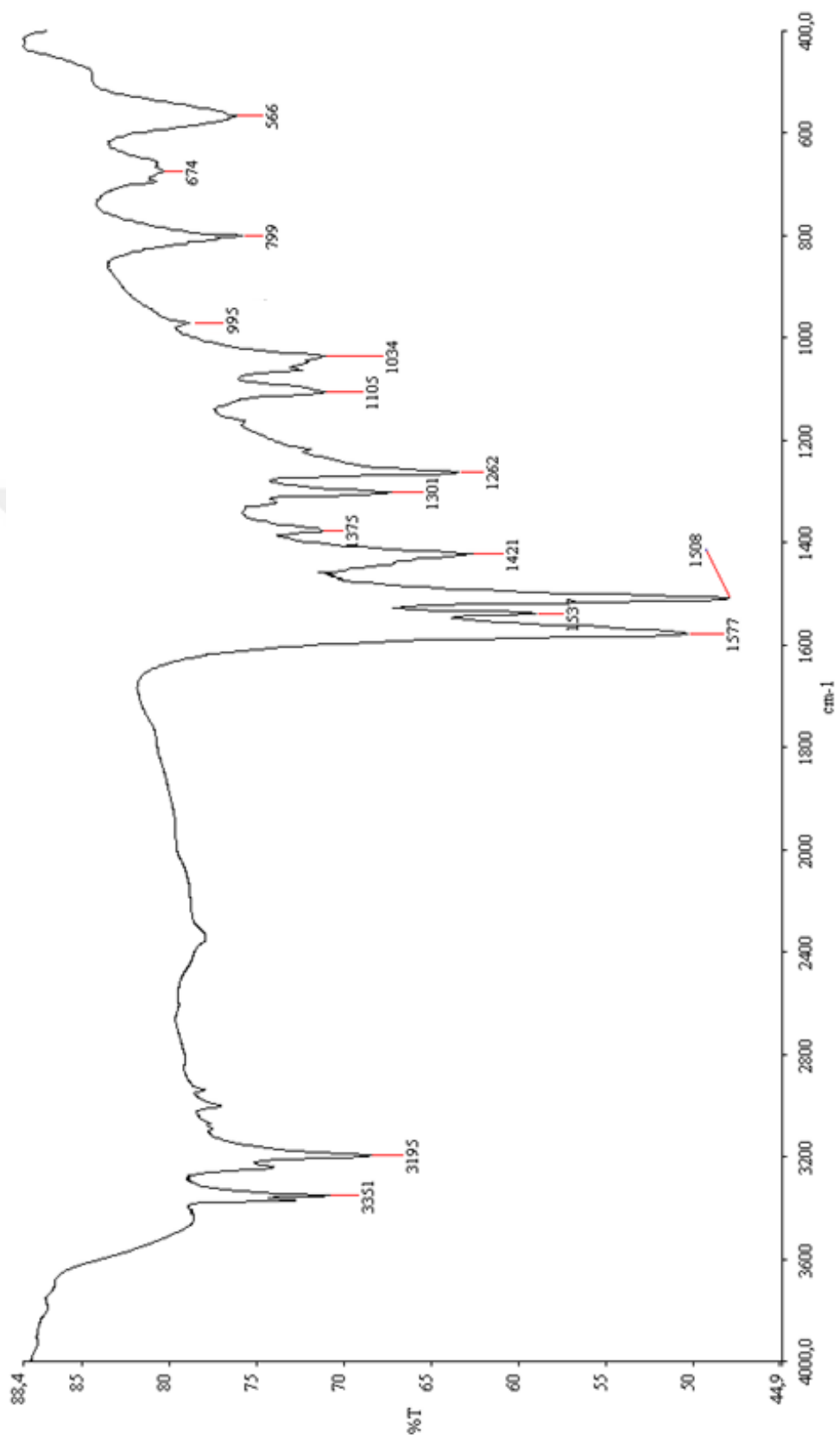


Figure 3.5 The FT-IR spectrum $[\text{CoCl}_2(\text{S-HL})_2]$

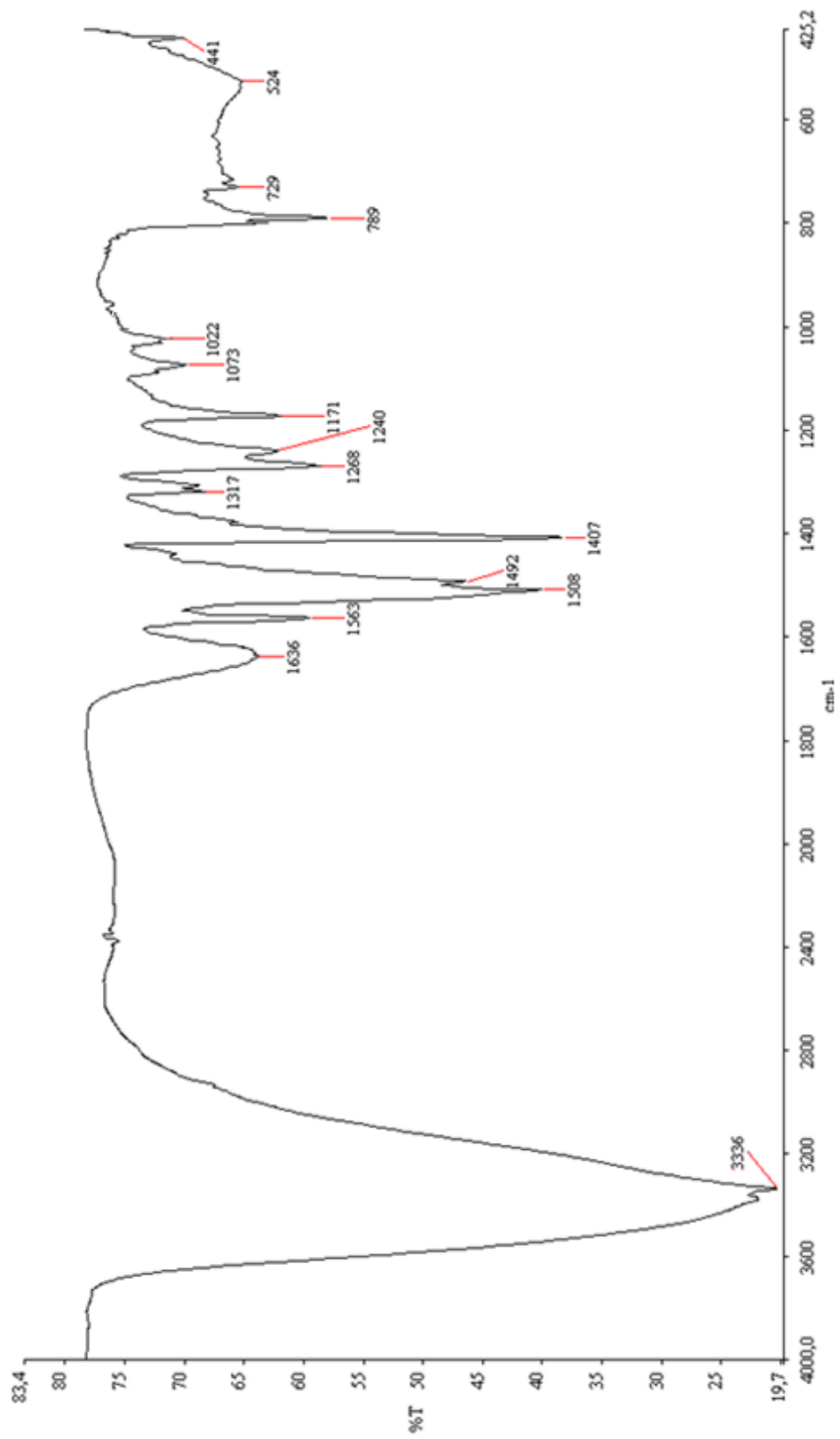


Figure 3.6 The FT-IR spectrum of [Ni(N,S-L)₂]

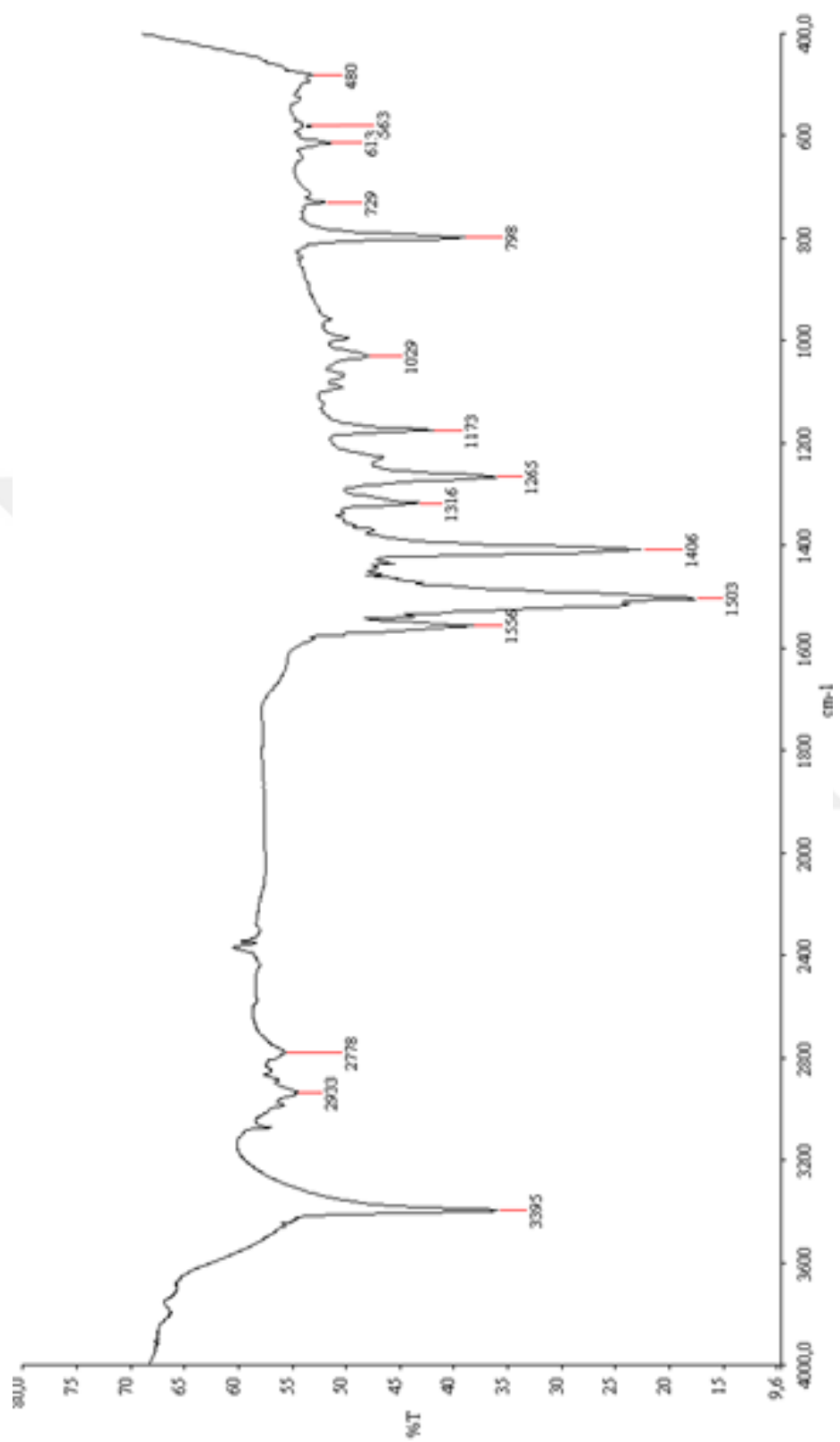


Figure 3.7 The FT-IR spectrum of [Pd(N,S-L)₂]

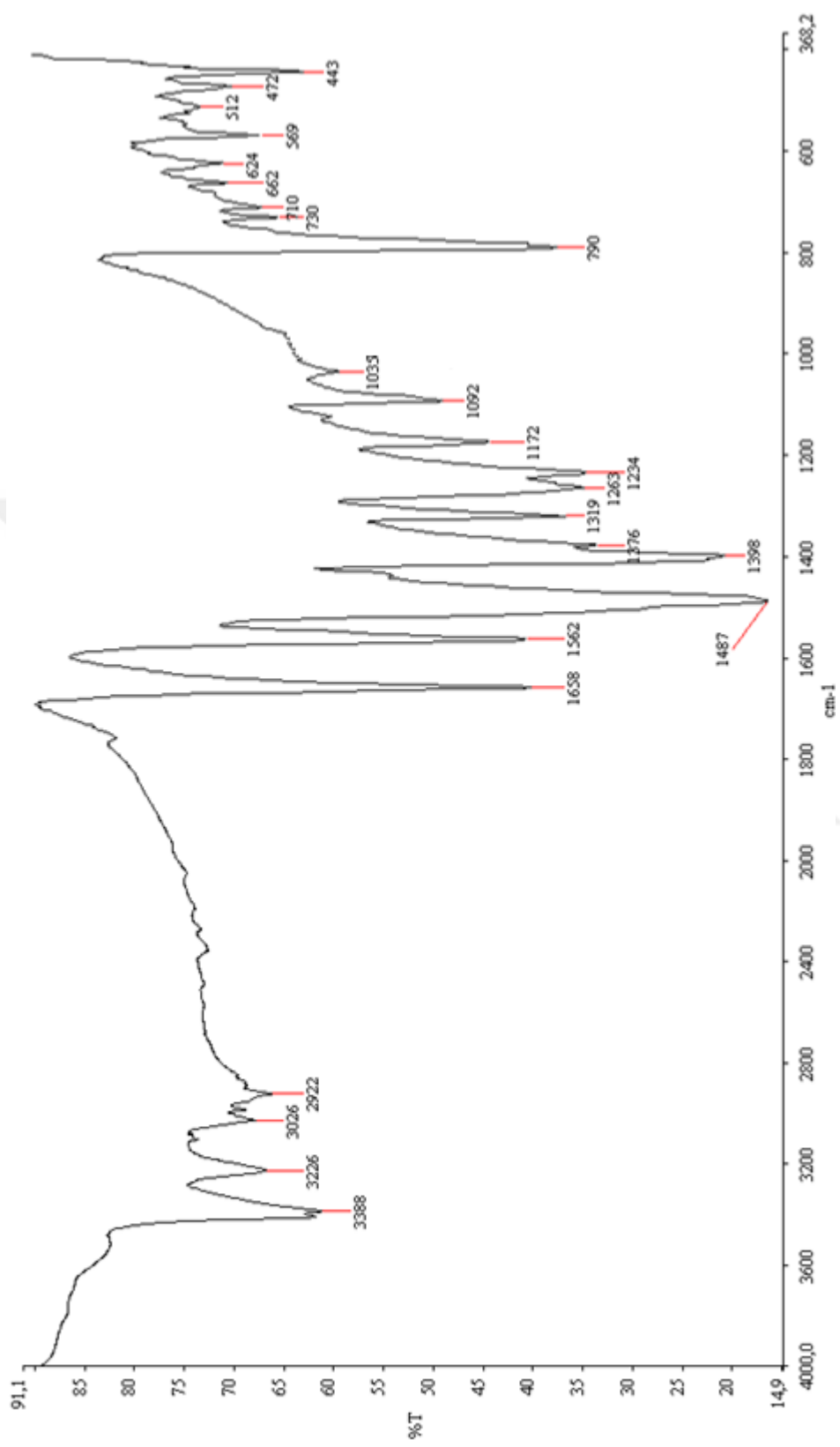


Figure 3.8 The FT-IR spectrum of [Zn(N,S-L)2]

3.4 ¹H-NMR Spectra

The ¹H-NMR for the compounds are presented in the Table 3-3.

Table 3-3 ¹H-NMR data for compounds

Compounds					
Shift(ppm), class, H's, J's(Hz)	HL	[CoCl ₂ (S-HL) ₂]	[Ni(N,S-L) ₂]	[Pd(N,S-L) ₂]	[Zn(N,S-L) ₂]
N(2)H	10.30, s, 1H	10.25, s, 1H	-	-	-
N(1)H	8.06, s, 1H	8.07, s, 1H	5.69, s, 1H	7.74, s, 1H	7.93, s, 1H
Thiophen ring protons	7.29, d, J=4.00, 1H; 7.18, d, J=3.96, 1H	7.24, d, J=3.9, 1H; 7.13, d, J=3.9, 1H	7.63, d, J=4.2, 1H; 7.36, d, J=4.2, 1H	7.57, d, J=4.3, 1H; 7.48, d, J=4.3, 1H	7.52, d, J=4.3, 1H; 7.33, d, J=4.3, 1H
NHCH ₃	3.01, d, 3H	2.95, d, J=3.9, 3H	4.59, d, J=4.5, 3H	2.93, d, J=4.4, 3H	2.98, d, J=4.8, 3H
N=CCH ₃	2.26, s, 3H	2.23, s, 3H	3.68, s, 3H	2.58, s, 3H	2.41, s, 3H

Ligand-Metal coordination for all complexes was supported by ¹H NMR spectral data under the guidance of the relevant literature (Sen et al., 2019). Ligand (Figure 3.12) and complex ¹H NMR spectra were assessed in DMSO with reference to TMS.

For the Co(II) complex (Figure 3.13), the free ligand and the presence of resonances of N(2)H protons in the complex spectrum prove that the compounds are neutrally bound (Figure 3.9). In the ¹H NMR spectrum of the free ligand, it was observed that the signal of the hydrazine N(2)H proton (at 10.30 ppm for HL) shifted towards the higher area (10.25 ppm (1H)) in the complex spectrum. Signals of protons belonging to N(2)H and N(1)H groups observed at 10.30 ppm (1H) and 8.06 ppm (1H) in the free

ligand are observed as 10.25 ppm (1H) and 8.07 ppm (1H), respectively. This proves that the ligand is bound in the thione form.

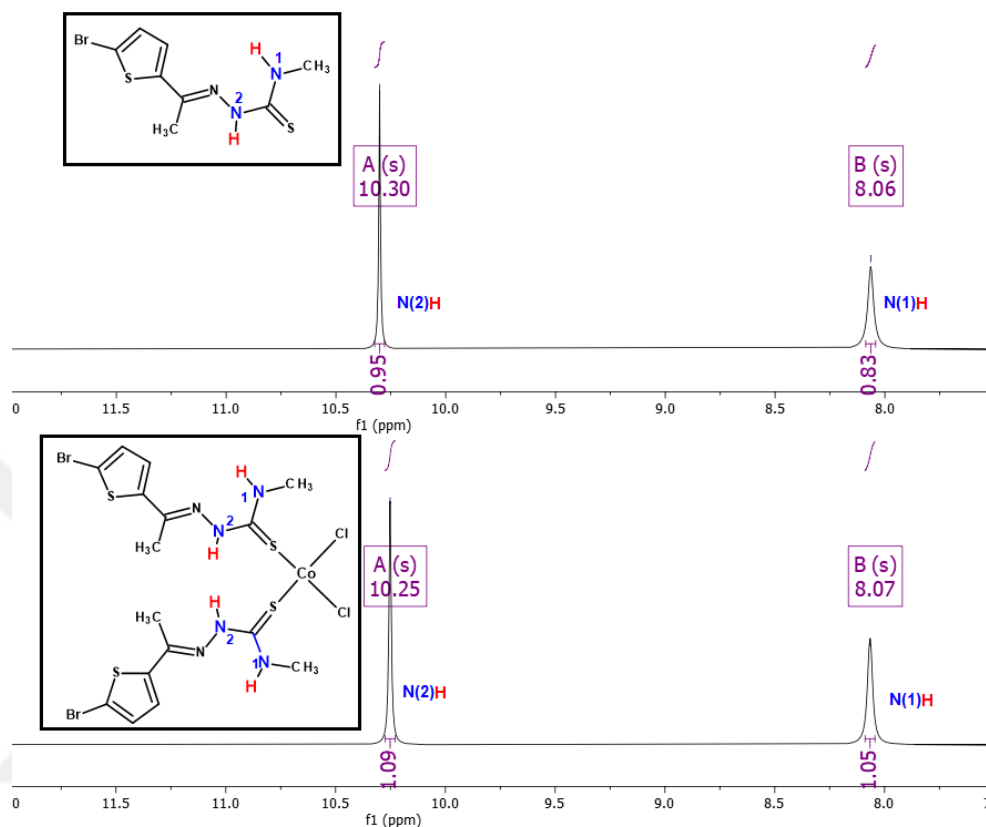


Figure 3.9 N(1)H and N(2)H protons of HL and Co complex

In the ^1H NMR spectra of Ni(II) (Figure 3.14), Pd(II) (Figure 3.15) and Zn(II) (Figure 3.16) complexes, it was observed that the signal of the N(1)H proton (8.06 ppm for HL) shifted towards the higher area (5.69 ppm (1H) for Ni(II), 7.74 ppm (1H) for Pd(II) and 7.93 ppm (1H) for Zn(II)) in the complex spectra (Figure 3.10). The fact that the signals of the protons belonging to the N(2)H group, which are observed as 10.30 ppm (1H) singlet in ligand not observed in the spectra of the complexes, proves that the ligand binds to the metal in the form of anionic thiol during the complexation.

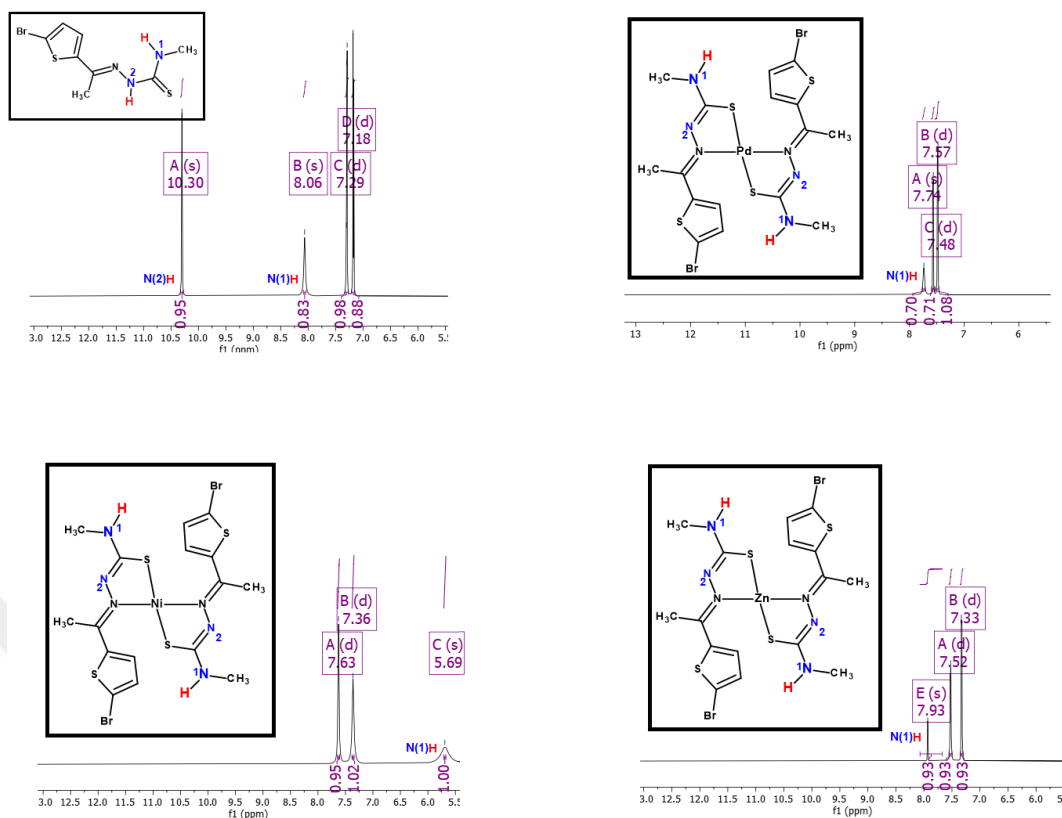


Figure 3.10 $\text{N}(1)\text{H}$ protons of HL and complexes

Protons of the thiophene ring were observed in all complexes as doublets (Co(II) = 7.24(1H) and 7.13(1H); Ni(II) = 7.63(1H) and 7.36(1H) ppm; Zn(II) = 7.52(1H) and 7.33(1H); Pd(II) = 7.57(1H) and 7.48(1H) ppm).

The doublet and a singlet due to the methyl moieties of (NHMe) and (N=CMe) in free ligand were detected at around 3.01 and 2.26 ppm respectively. (NHMe) the absorptions (Figure 3.11) have shifted lightly toward the upper field 2.95 ppm in $[\text{Co}(\text{S-HL})_2\text{Cl}_2]$, 2.93 ppm in $[\text{Pd}(\text{N,S-L})_2]$, 2.98 ppm in in $[\text{Zn}(\text{N,S-L})_2]$, whereas moved gradually to down field at 4.59 ppm for the in $[\text{Ni}(\text{N,S-L})_2]$. (N=CMe) absorptions are observed as singlets at 2.58-2.23 ppm region in Co(II), Pd(II) and Zn(II) complexes as observed at 3.68 ppm in Ni(II) complex

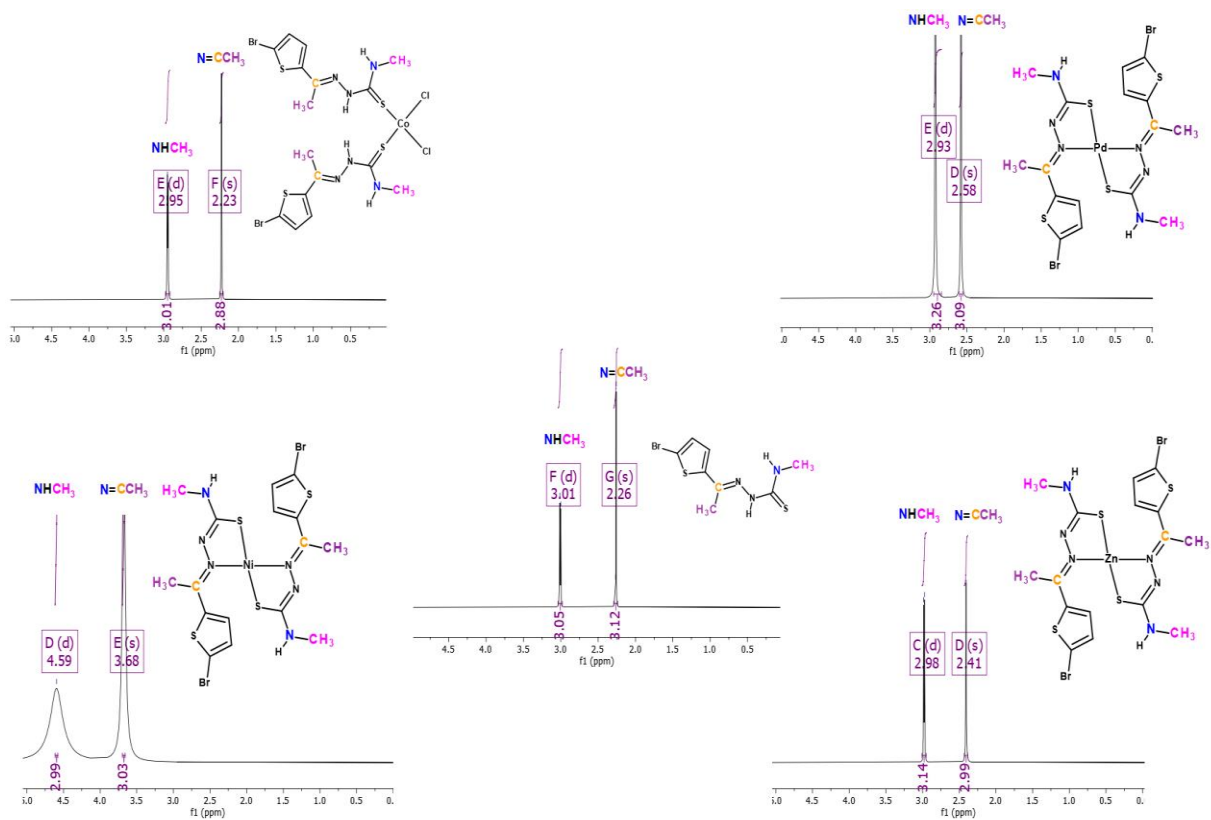


Figure 3.11 CH_3 protons of HL and complexes

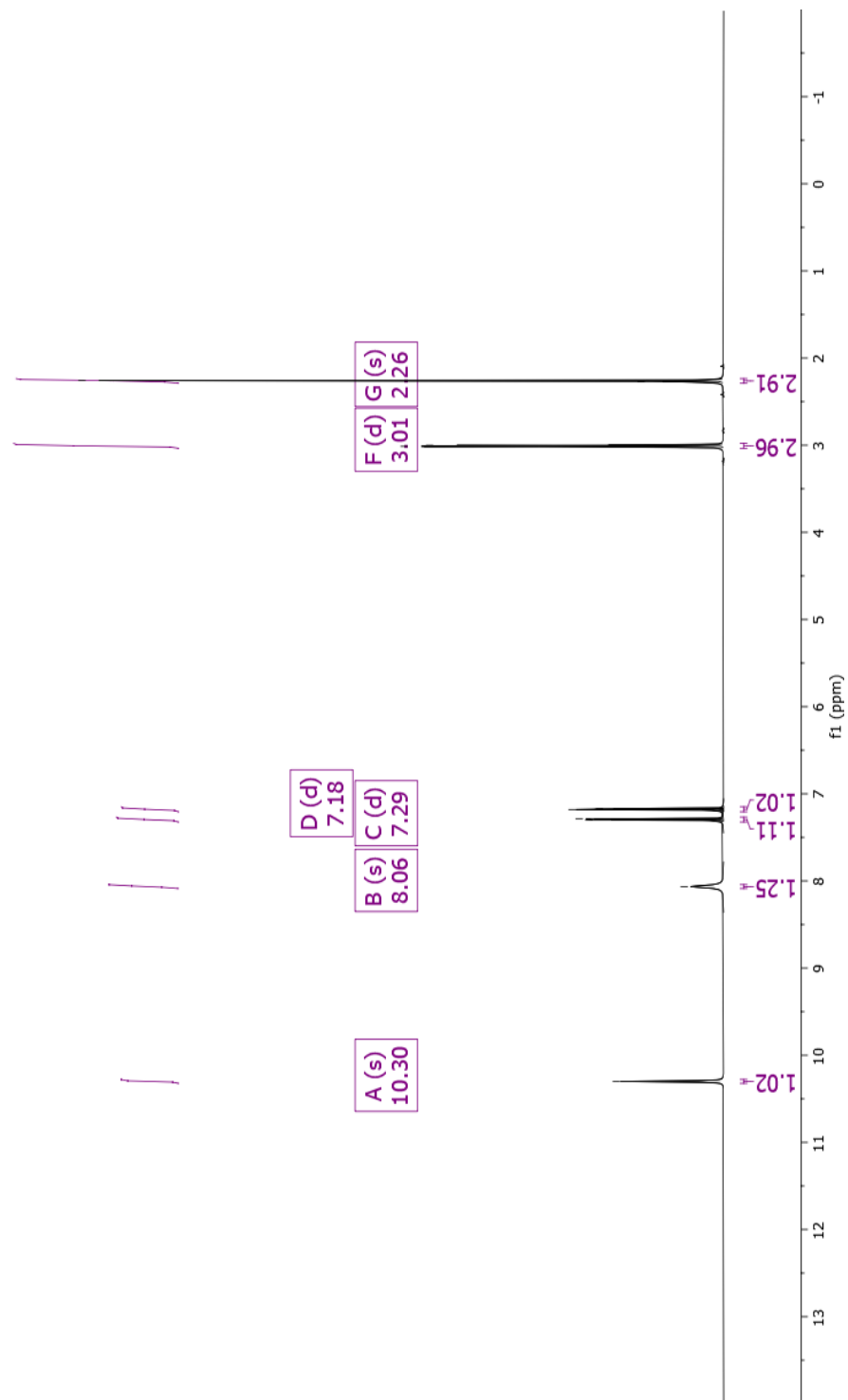


Figure 3.12 The ¹H-NMR spectrum of HL

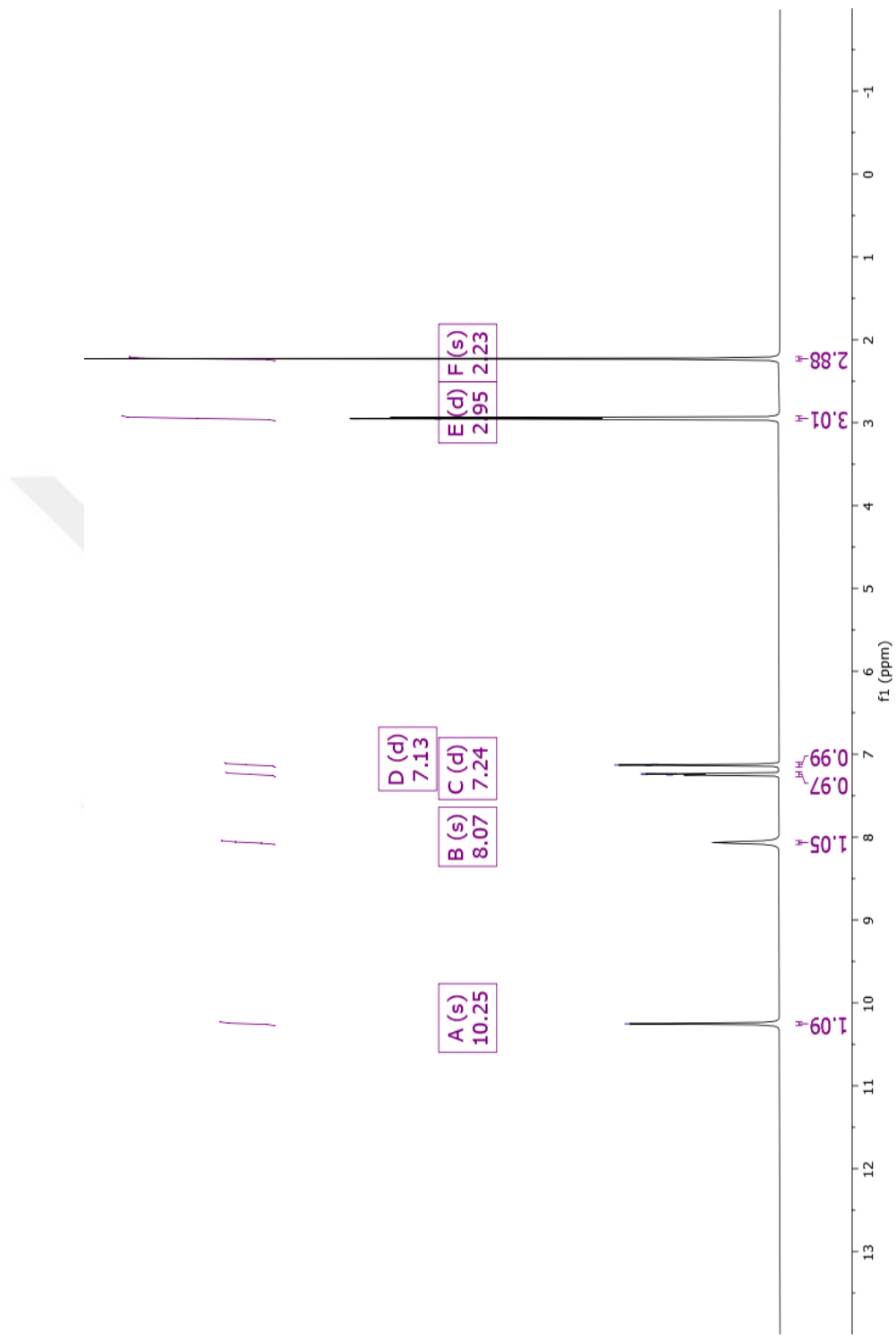


Figure 3.13 The ¹H-NMR spectrum of [CoCl₂(S-HL)₂]

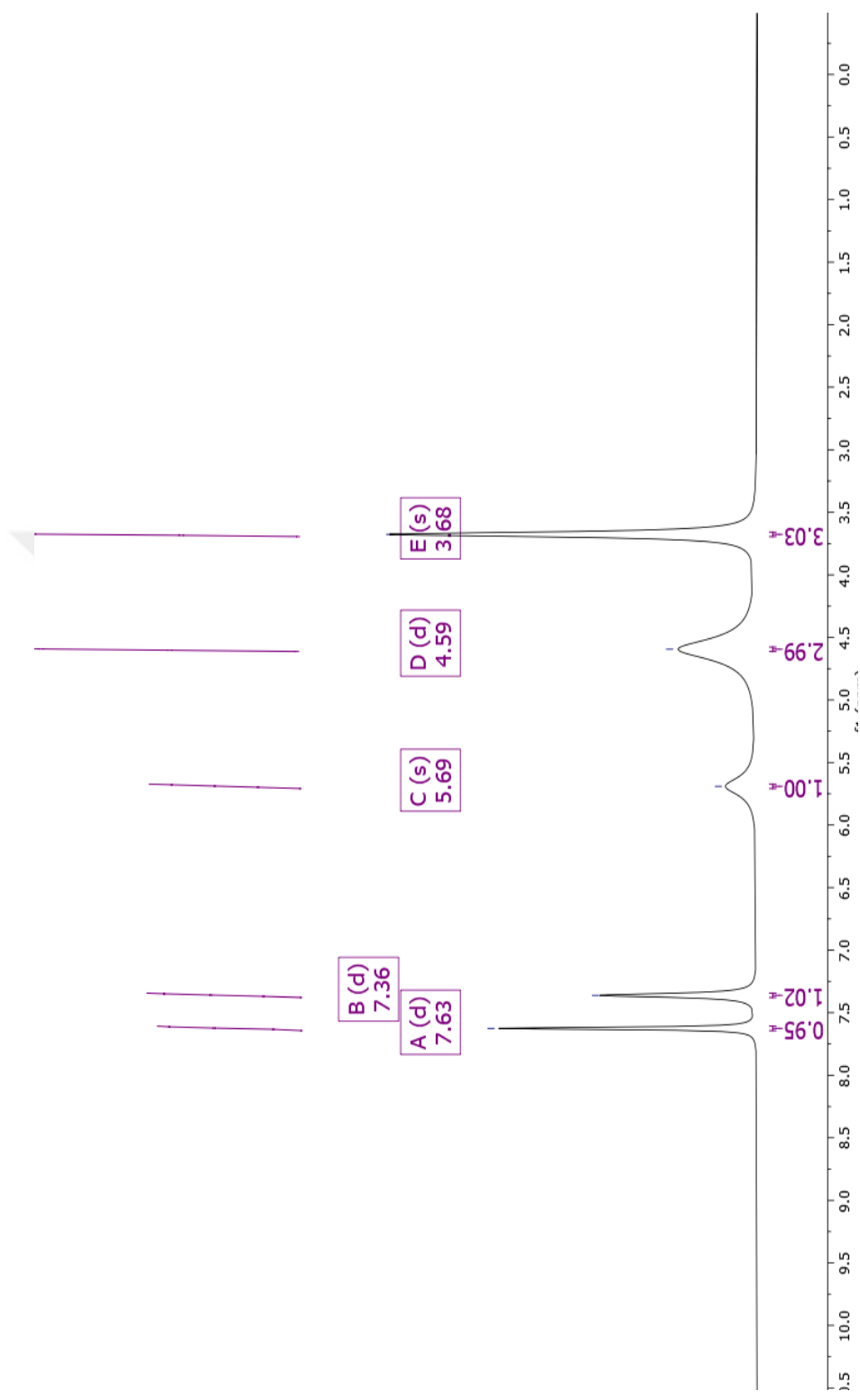


Figure 3.14 The ¹H-NMR spectrum of [Ni(N,S-L)₂]

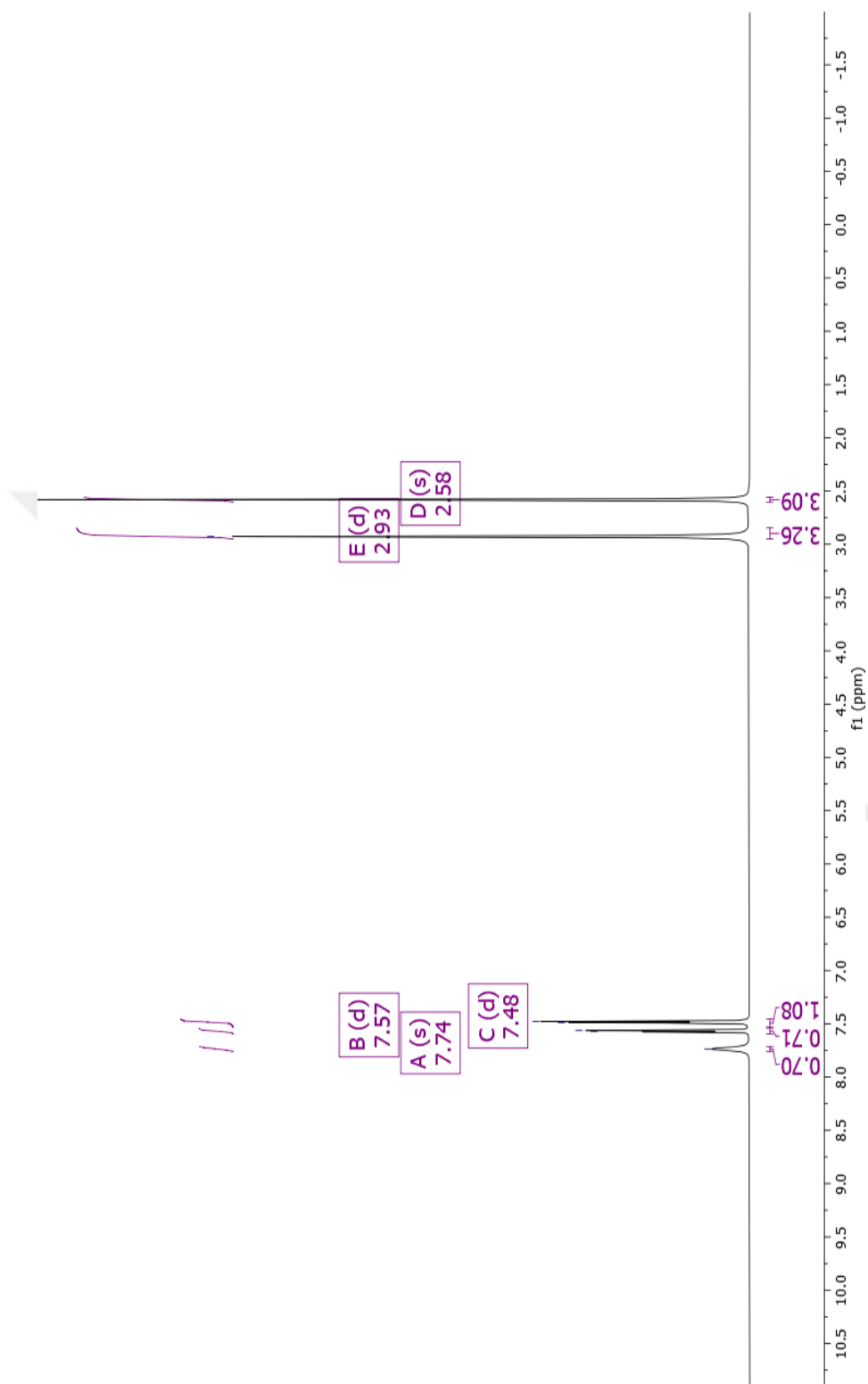


Figure 3.15 The ¹H-NMR spectrum of [Pd(N,S-L)₂]

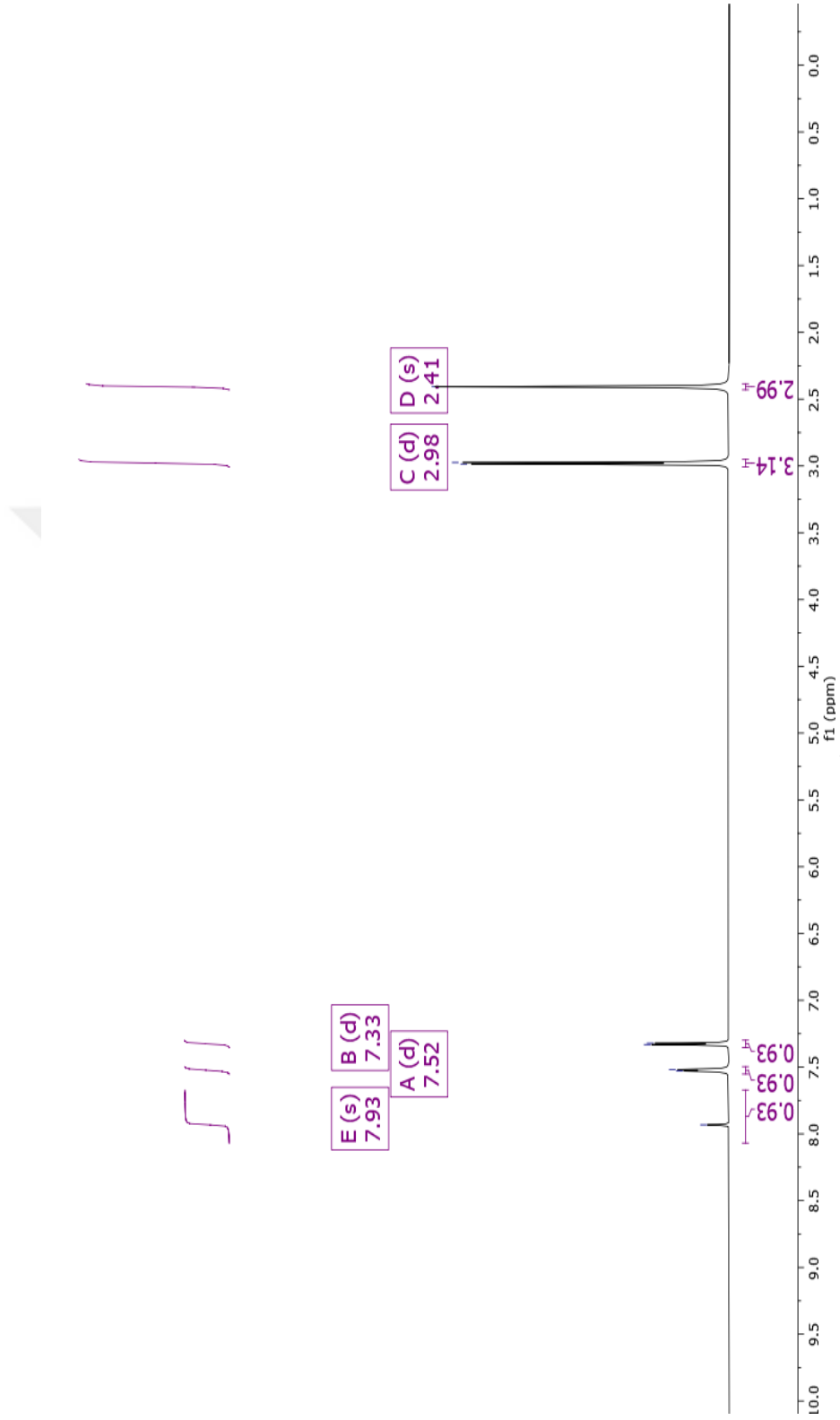


Figure 3.16 The ¹H-NMR spectrum of [Zn(N,S-L)₂]

3.5 Structural Description of Compounds

The molecular structures of complexes Co(II), Ni(II), Pd(II), and Zn(II) with atomic labelings are presented in Figure 3.17 and Figure 3.18. The complexes are crystallized in the same monoclinic unit cell with different space groups for Pd(II) and Zn(II) whereas with the same space group for Co(II) and Ni(II) as given in Table 2-1. Complexes Co(II), Pd(II), and Ni(II) possess one independent molecule per asymmetric unit while the asymmetric unit of Zn(II) is composed of two crystallographically independent molecules, as well as a dimethyl formamide solvent molecule. The coordination geometry around the metal atom of complexes Pd(II), Ni(II), and Zn(II) is four-coordinate geometry by two thiosemicarbazone ligands, each acting as monoanionic bidentate *N, S* donors. The structure of complex Co(II) shows that Co atom has a four-coordinate geometry with two neutral monodentate *S*-thiosemicarbazone ligands coordinated through two thiolate sulfur atoms and two Cl anions. Yang and co-workers (Yang, Powell, & Houser, 2007) proposed the τ_4 geometry index parameter to describe whether the coordination geometry of four-coordinate complexes is square planar or tetrahedral. The perfect tetrahedral geometry has the τ_4 value of 1 while if τ_4 is close to 0 then the geometry is similar to the perfect square-planar geometry. In the complexes Ni(II) and Pd(II), the four-coordinate geometry around the central metal atom is close to square planar with the τ_4 values of 0.246 and 0.170, respectively. Complex Co(II) has an expected tetrahedral conformation with the τ_4 value of 0.904. Two central Zn atoms of complex Zn(II) have the τ_4 values of 0.751 and 0.773 suggesting a highly distorted tetrahedral geometry. The C=S and C-N_{hydrazine} bond lengths of (1.701(5) Å, 1.694(5) Å) and (1.350(5) Å, 1.352(5) Å) in the coordinated ligand of complex Co(II) resemble the values 1.682(4) and 1.358(4) Å of the free ligand, respectively. This observation clearly attests to the coordination of the ligand to the Co atom in the form of a neutral thion. Unlike complex Co(II), in the remaining three complexes, while the C-S distance becomes significantly longer than that of the free ligand, it is the reverse for the C-N_{hydrazine} lengths (Table 3-4). These C-S and C-N distances are close to the expected C-S single bond distance (1.81 Å) and C=N double-bond distance (1.28 Å), respectively (Huheey,

Keiter, 1993) This behavior indicates that the thiosemicarbazone ligand binds to the metal atoms in those complexes in an anionic thiol form, during the complexation.

In all complexes, no extraordinary values are found for the bond angles and lengths in the thiophene ring, and these distances coincide with the values found in the literature (Sultan, Taha, Shah, Yamin, & Zaki, 2014; Fun, Jebas, Patil, & Dharmaprakash, 2008; Prasath, Bahvana, Ng, & Tiekink, 2010; Jing, Yu, & Chen, 2007; Kazak et al., 2000).

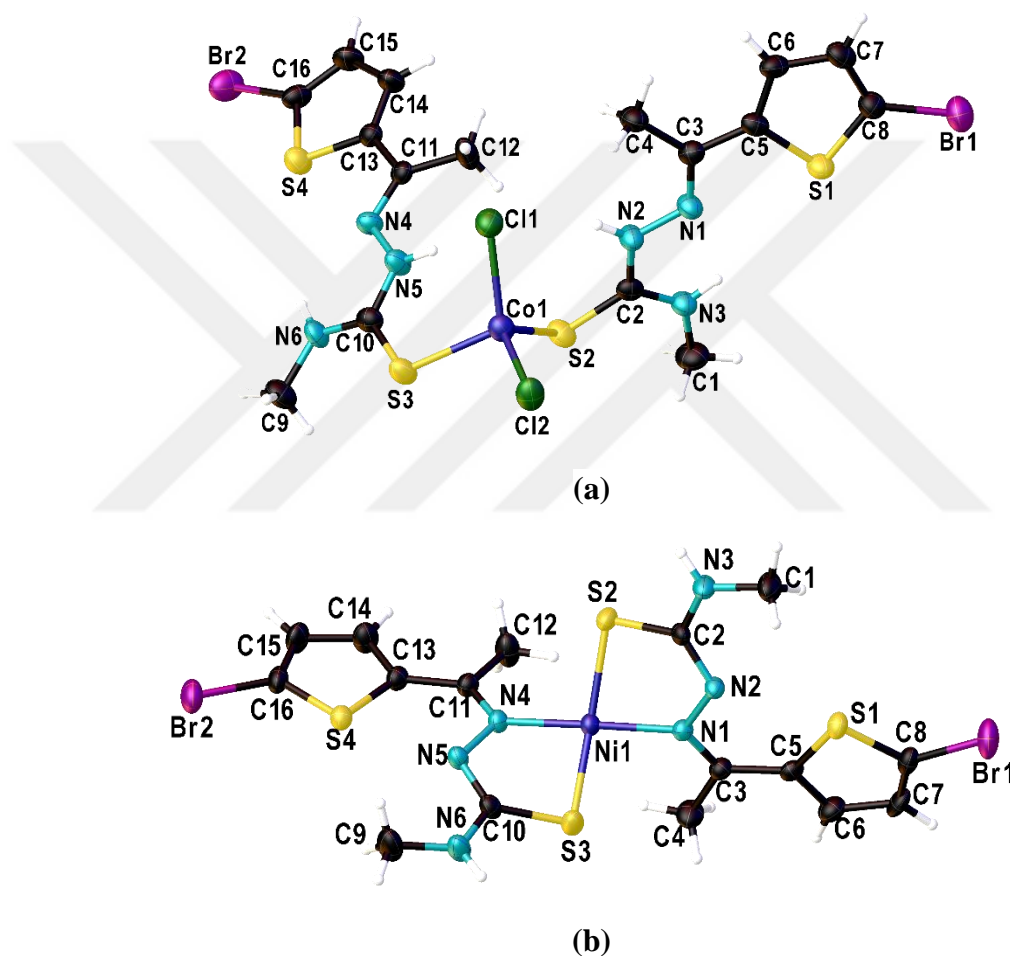
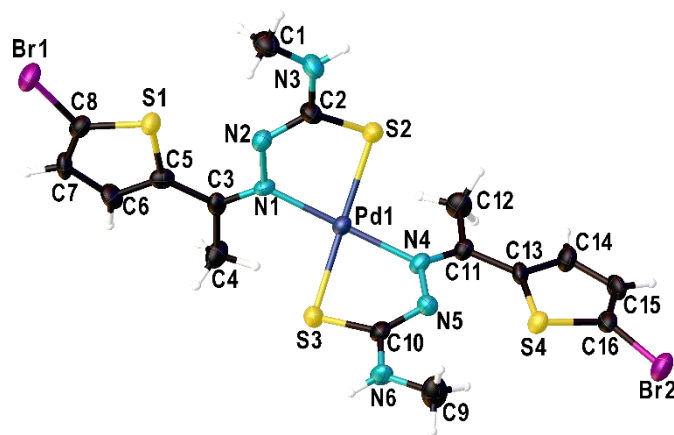
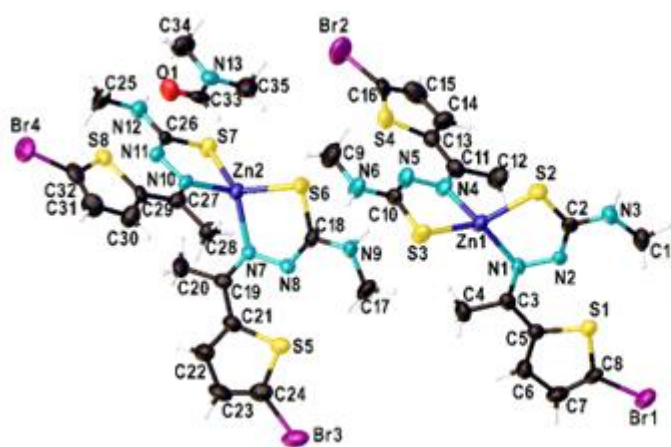


Figure 3.17 The molecular structures of the complexes (a) Co(II), (b) Ni(II)



(c)



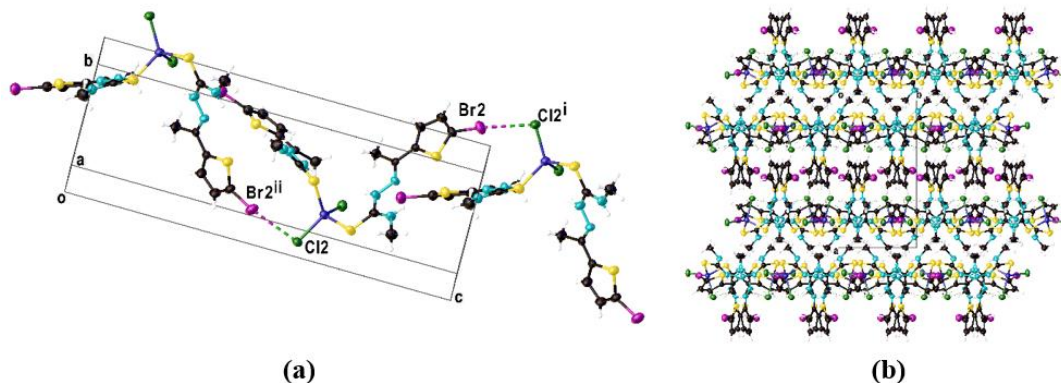
Thermal ellipsoids enclose 50% of the electron density for all complexes.

(d)

Figure 3.18 The molecular structures of the complexes (c) Pd(II) and (d) Zn(II)

In the crystal structure of complex Co(II), there are two different kinds of N–H···N and two different kinds of N–H···Cl intra-molecular interactions including the N and Cl atoms as acceptor, and they help stabilization of crystal packing. Intramolecular N3–H3···N1 and N6–H6···N4 interactions both generate S(5) ring motifs while N2–H2···Cl1 and N5–H5···Cl1 interactions both cause S(6) rings (Bernstein, Davis, Shimoni, & Chang, 1995). The crystal structure of the complex is devoid of any intermolecular hydrogen bond interactions. The Br2···Cl2ⁱ (Cl2···Br2ⁱⁱ) (symmetry code: (i) $x, 3/2-y, 1/2+z$, (ii) $x, 3/2-y, -1/2+z$) distances are 3.303 Å which are much shorter than the sum of van der Waals radii of 3.60 Å (Bondi, 1964). Hence, this distance value clearly indicates the presence of intermolecular interaction with the nonbonding character. Molecules are arranged by these nonbonding interactions along

the *c*-axis of the unit cell. Finally, the supramolecular aggregation is completed by C–H··· π interactions (Table 3.5) (Figure 3.19). There are no significant π ··· π interactions present in the crystal structure.

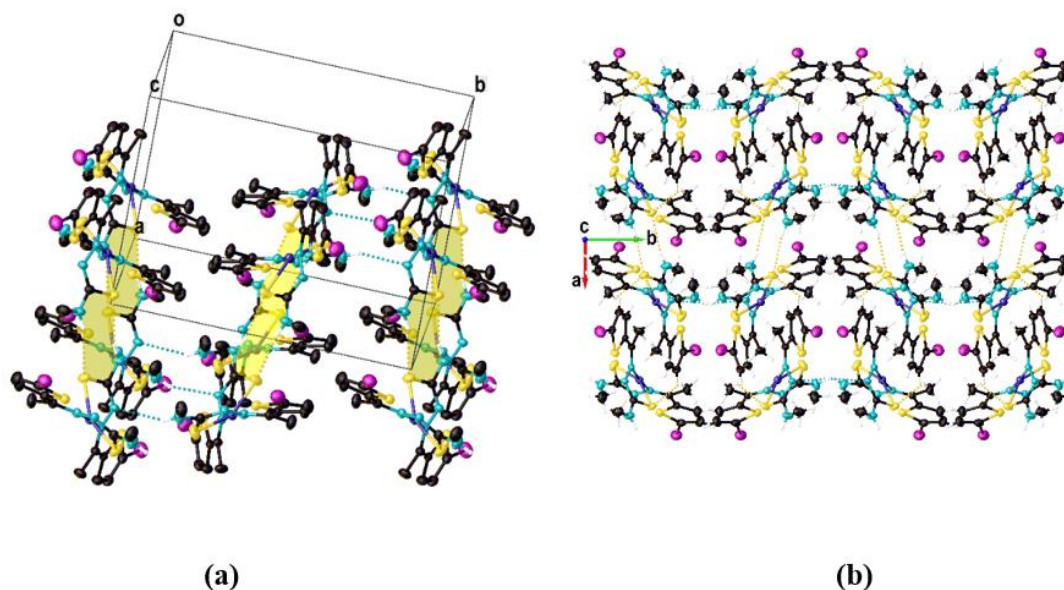


a) A partial view along the *a*-axis of the crystal packing of the compound, showing the nonbonding intermolecular Br···Cl interactions, leading to the formation of the arrangement of the molecules along the *c*-axis of the unit cell.

b) A view of the three-dimensional network along the *c* axis.

Figure 3.19 C–H··· π interactions of Co(II) complex

The crystal packing view of complex Ni(II) is shown in Figure 3.20. The neighboring molecules are connected to one another by a pair of intermolecular N–H···S hydrogen bonds which give rise to inversion dimers with an $R_2^2(8)$ ring motif. Besides, these dimer linkages are bonded by intermolecular N6–H6A···N2 hydrogen bonds to create a three-dimensional network. Additionally, two pseudo-six membered S(6) graph set motifs (Bernstein et al., 1995) are generated through intramolecular C4–H4A···S3 and C12–H12A···S2 hydrogen bonds, respectively which the molecular conformation of the compound is supported by this fact. The centroid-centroid separation is 3.780(2) Å for Cg1···Cg1ⁱⁱⁱ (symmetry code *iii*: 1-*x*, 1-*y*, 2-*z*) in which Cg1 is the centroid of the aromatic ring (S1/C–C8). It can be deduced that there is an intermolecular π – π interaction in the crystal structure since this value is smaller than the maximum separation for π – π interactions of 3.8 Å (Janiak, 200).

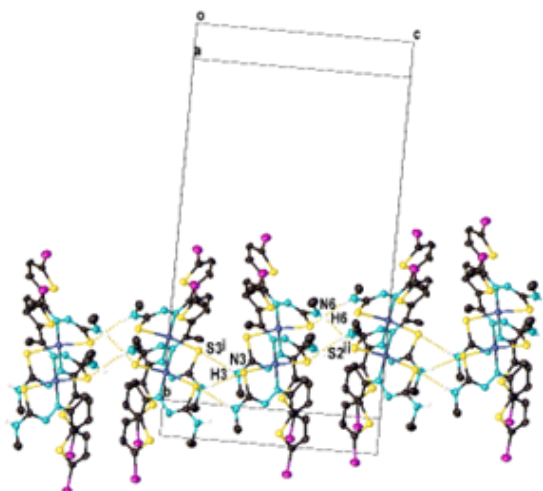


a) Representation of the packing diagram for the complex Ni(II). Molecules are connected by intermolecular N–H...S hydrogen bonds forming an $R_2^2(8)$ (painted in yellow) dimeric arrangement. Dimer linkages are also linked by N–H...N hydrogen bonds (dotted turquoise lines). For clarity, hydrogen atoms not playing role in bonding are omitted.

b) A view of the three-dimensional network along the *c* axis.

Figure 3.20 The crystal packing view of complex Ni(II)

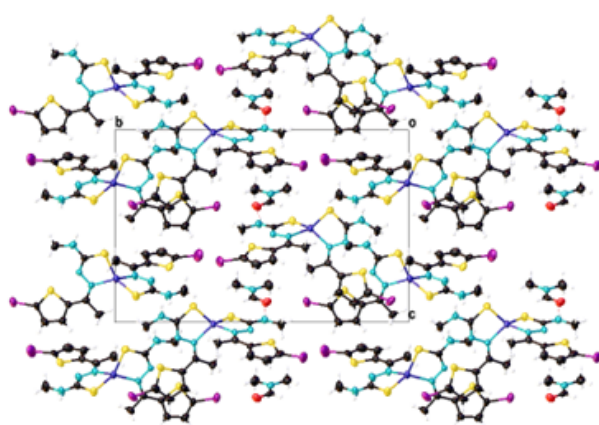
In the crystal packing of complex Pd(II), molecules are interlinked by intermolecular N3–H3...S3 and N6–H6...S2 hydrogen bonds as shown in Figure 3.21. These hydrogen bonds exhibit a two-dimensional supramolecular network lying along the *c*-axis of the unit cell. The molecules are also involved in three cyclic intramolecular C–H...S interactions forming two pseudo-six and a pseudo-nine membered graph set motifs (Janiak, 2000). Considerable $\pi\cdots\pi$ interactions have not been observed in the crystal structure.



A partial view along the a-axis of the crystal packing of complex Pd(II), showing the intermolecular N–H...S hydrogen bonds interactions which result in the formation of a two-dimensional supramolecular network lying along the c-axis of the unit cell. For clarity, hydrogen atoms not playing role in bonding are omitted.

Figure 3.21 Intermolecular N3–H3...S3 and N6–H6...S2 hydrogen bonds of Pd(II) complex

There are an intermolecular C–H...S hydrogen bond and C–O... π interaction in the crystal structure of complex Zn(II) which contribute to the stability of the crystal structure. Further, as seen from Figure 3.22, the dimethyl formamide solvent is linked to one of the molecules through the intermolecular N12–H12...O1 hydrogen bonds and contains an intramolecular C–H...O interaction. Besides, the complex contains an intramolecular C–H...N interaction, as well as four intramolecular C–H... π interactions that consolidates the molecular conformation. The crystal structure exists a ring...ring interaction [Cg1...Cg6^{iv}=3.738(4) Å, inter-planar distance=3.626(3) Å, α =4.5(3)°, symmetry code: (iv) -1+x,-y,-1/2+z. Cg1 and Cg6 are the centroids of the aromatic rings (S1/C5–C8) and (S5/C21–C24), respectively.] Detailed parameters of all the hydrogen bonds and intermolecular interactions for all complexes are enlisted in Table 3-5.



A partial view along the *a*-axis of the crystal packing of complex Zn(II), showing the intra- and intermolecular interactions. The intermolecular N–H···O interactions connecting the dimethyl formamide solvent to the molecule are also shown.

Figure 3.22 The intermolecular N12–H12···O1 hydrogen bonds

Table 3-4 Selected bond lengths (Å) and angles (°) for the complexes Ni(II), Pd(II), Zn(II) and Co(II)

	Ni(II)	Pd(II)	Zn(II)		Co(II)
M–S2	2.2117(10)	2.317(3)	2.284(2)	Co1–Cl1	2.2645(15)
M–S3	2.1680(11)	2.322(3)	2.2794(19)	Co1–Cl2	2.2202(15)
M–N1	1.903(3)	2.041(9)	2.058(5)	Co1–S2	2.3067(15)
M–N4	1.903(3)	2.039(9)	2.091(6)	Co1–S3	2.3376(14)
S1–C5	1.729(4)	1.719(10)	1.730(7)	S1–C5	1.721(5)
S1–C8	1.718(4)	1.699(10)	1.712(7)	S1–C8	1.710(5)
S4–C13	1.735(4)	1.731(10)	1.720(7)	S4–C13	1.730(4)
S4–C16	1.710(4)	1.723(10)	1.682(8)	S4–C16	1.710(5)
N2–C2	1.309(4)	1.332(12)	1.313(7)	N2–C2	1.350(5)
N2–N1	1.401(4)	1.391(11)	1.381(6)	N2–N1	1.381(5)
N4–C11	1.303(4)	1.286(12)	1.309(8)	N4–C11	1.297(5)
N4–N5	1.388(4)	1.375(11)	1.366(7)	N4–N5	1.383(5)
N1–M–S2	84.05(9)	81.8(2)	86.47(15)	Cl1–Co1–S2	108.35(5)
N4–M–S3	85.32(9)	81.7(2)	85.67(16)	Cl1–Co1–S3	110.24(6)
N1–M–N4	174.52(12)	175.9(4)	119.2(2)	Cl2–Co1–Cl1	115.90(6)
N4–M–S2	97.98(9)	97.5(2)	114.69(16)	Cl2–Co1–S2	116.64(6)
N1–M–S3	95.40(9)	97.6(2)	127.73(15)	Cl2–Co1–S3	102.93(5)
S2–M–S3	150.82(5)	160.14(10)	126.38(8)	S2–Co1–S3	101.53(5)

Table 3-5 Hydrogen bonds and other weak interactions for complexes Co(II), Ni(II), Pd(II), and Zn(II). (Å, °)

$D-H \cdots A$	$D-H$	$H \cdots A$	$D \cdots A$	$D-H \cdots A$
Complex Co(II)				
N2-H2...C11	0.86	2.48	3.303(4)	162
N3-H3...N1	0.86	2.17	2.574(6)	109
N5-H5...C11	0.86	2.59	3.358(4)	149
N6-H6...N4	0.86	2.21	3.604(5)	108
C4-H4C...Cg1 ⁱⁱⁱ	0.96	2.82	3.595	139
Complex Ni(II)				
N3-H3...S2 ⁱ	0.86	2.61(3)	3.443(4)	167(3)
N6-H6A...S2 ⁱⁱ	0.84	2.50(3)	3.202(4)	142(4)
C4-H4A...S3	0.96	2.83	3.355(4)	116
C12-H12A...S2	0.96	2.73	3.325(5)	121
Complex Pd(II)				
N3-H3...S3 ⁱ	0.86	2.84	3.678(9)	166
N6-H6...S2 ⁱⁱ	0.86	2.84	3.672(9)	165
C4-H4A...S3	0.96	2.75	3.313(10)	118
C9-H9A...S4	0.96	2.72	3.614(13)	154
C12-H12C...S2	0.96	2.85	3.342(12)	113
Complex Zn(II)				
C28-H28C...S7 ⁱ	0.96	2.88	3.787(6)	158.1
N12-H12...O1 ⁱⁱ	0.86	2.04	2.898(8)	172.0
C28-H28A...N7	0.96	2.63	3.434(7)	141.9
C34-H34A...O1				
C33-O-1...Cg2 ⁱⁱⁱ				
C12-H12C...Cg3	0.96	2.85	3.418(8)	119
C20-H20C...Cg4	0.96	2.77	3.576(8)	143
C28-H28A...Cg5	0.96	2.50	3.439(7)	165
C35-H35C...Cg4	0.96	2.74	3.448(8)	131

Symmetry transformations used to generate equivalent atoms: *i*: 2-x,1-y,2-z Ni(II); 1/2+x,3/2-y,1/2+z Pd(II); 1+x,y,z Zn(II) *ii*: x,3/2-y,-1/2+z Ni(II); 1/2+x,3/2-y,-1/2+z Pd(II); -1+x,y,z Zn(II) *iii*: 1-x,1-y,1-z Co(II); x,1-y,-1/2+z Zn(II). Cg1, Cg2, Cg3, Cg4 and Cg5 are the centroids of aromatic rings (S1/C5-C8), (S8/C29-C32), (Zn1/S2/C2/N2/N1), (Zn2/S7/C26/N11/N10), and (Zn2/S6/C18/N8/N7), respectively.

3.6 Antibacterial Studies

Reference organisms Gram-positive *E. faecalis*, *S. aureus* and Gram-negative *P. aeruginosa*, *E. coli*, *S. marcescens*, bacteria and *C. albicans* containing pathogenic species were tested in order to propagate the in vitro antimicrobial behaviour of the metal complexes and synthesized Schiff base ligand. For this purpose, agar diffusion (Table 3-6) method and MIC test were performed (Table 3-7).

Table 3-6 Comparison of antimicrobial activities of different metal ligands with agar diffusion method

Organisms	Inhibition zone diameter (mm±SD)							
	HL	Co(S-HL) ₂ Cl ₂	Ni(N,S-L) ₂	Pd(N,S-L) ₂	Zn(N,S-L) ₂	Amp	Gen	Flu
<i>S. aureus</i>	1,2±0,12	8,2±0,09	7,1±0,19	7,5±0,08	4,1±0,09	28±0,00	-	-
<i>E. faecalis</i>	7,1±0,19	7,4±0,14	8,1±0,09	12,1±0,08	12,0±0,05	26±0,50	-	-
<i>E. coli</i>	0,0±0,00	1,3±0,05	0,0±0,00	2,2±0,24	0,0±0,00	-	23±0,50	-
<i>S. marcescens</i>	0,0±0,00	0,8±0,05	0,0±0,00	0,0±0,00	1,0±0,08	-	24±0,00	-
<i>P. aeruginosa</i>	0,0±0,00	2,2±0,21	1,1±0,09	0,0±0,00	1,0±0,05	-	18±0,50	-
<i>C. albicans</i>	1,1±0,12	2,2±0,08	0,0±0,00	1,3±0,05	1,9±0,05	-	-	26±0,00
Negative control (6% DMSO): 0.0 mm								

Table 3-7 Minimum inhibition concentrations of different metal ligands

Organisms	MIC (µg/ml)				
	HL	Co(S-HL) ₂ Cl ₂	Ni(N,S-L) ₂	Pd(N,S-L) ₂	Zn(N,S-L) ₂
<i>S. aureus</i>	2500	312	625	1250	625
<i>E. faecalis</i>	312	78	78	156	39
<i>E. coli</i>	1250	625	1250	312	1250
<i>S. marcescens</i>	>2500	2500	>2500	1250	>2500
<i>P. aeruginosa</i>	1250	625	1250	1250	1250
<i>C. albicans</i>	>2500	1250	>2500	2500	1250

When these results were examined, it was found that ligand-metal complexes had antimicrobial activity at varying rates. HL ligand formed a 0-7.1 mm zone of inhibition against test organisms and showed activity in the concentration range of 312-2500 µg/ml. It was observed that the ligand generally showed weaker activity than the metal complexes. During chelation, the ligand orbital overlaps and the positive charge of the metal ions is partially shared with the donor groups. As a result, the polarity of the metal ion decreases. This promotes electron delocalization along the chelating ring, facilitating the attachment of metal complexes to the cell membrane, and causing the active sites of microbial enzymes to be blocked and ultimately the organism to be inhibited Ahmed, & Yunus, 2014; El-Sawaf, El-Essawy, Nassar, & El-Samanody, 2018).

The complexes have been shown to be more effective against Gram-positive bacteria especially inhibiting enteric bacteria, *E. faecalis*, at very low concentrations (39 µg/ml) (Figure 3.23). The Zn(N,S-L)₂ complex had the best antibacterial activity against *E. faecalis*, while the Co(S-HL)₂Cl₂ complex showed the best activity against *S. aureus* bacteria. Co(S-HL)₂Cl₂ and Pd(N,S-L)₂ were relatively more effective against Gram-negative bacteria. Ligand-metal complexes were found to be more effective on Gram positive bacteria. Gram negative bacteria have developed some resistance mechanisms against metal ions. Some enzymes and protein complexes in the outer membrane layers and in the periplasmic region reduce and precipitate metal ions. The outer membrane vesicles are thought to function in the removal of these precipitated minerals. In addition, flow pumps in the outer membrane and cytoplasmic membrane of gram-negative bacteria ensure that metal ions are pumped out of the cell (Gillan, 2016).

Although a little antifungal activity was observed in the ligand-metal complexes Zn(N,S-L)₂ and Co(S-HL)₂Cl₂ complexes, it was determined that other complexes did not have a lethal effect against *C.albicans*. These results are similar to another study showing that fungal strains are resistant to metal complexes (Uçar et al., 2021).

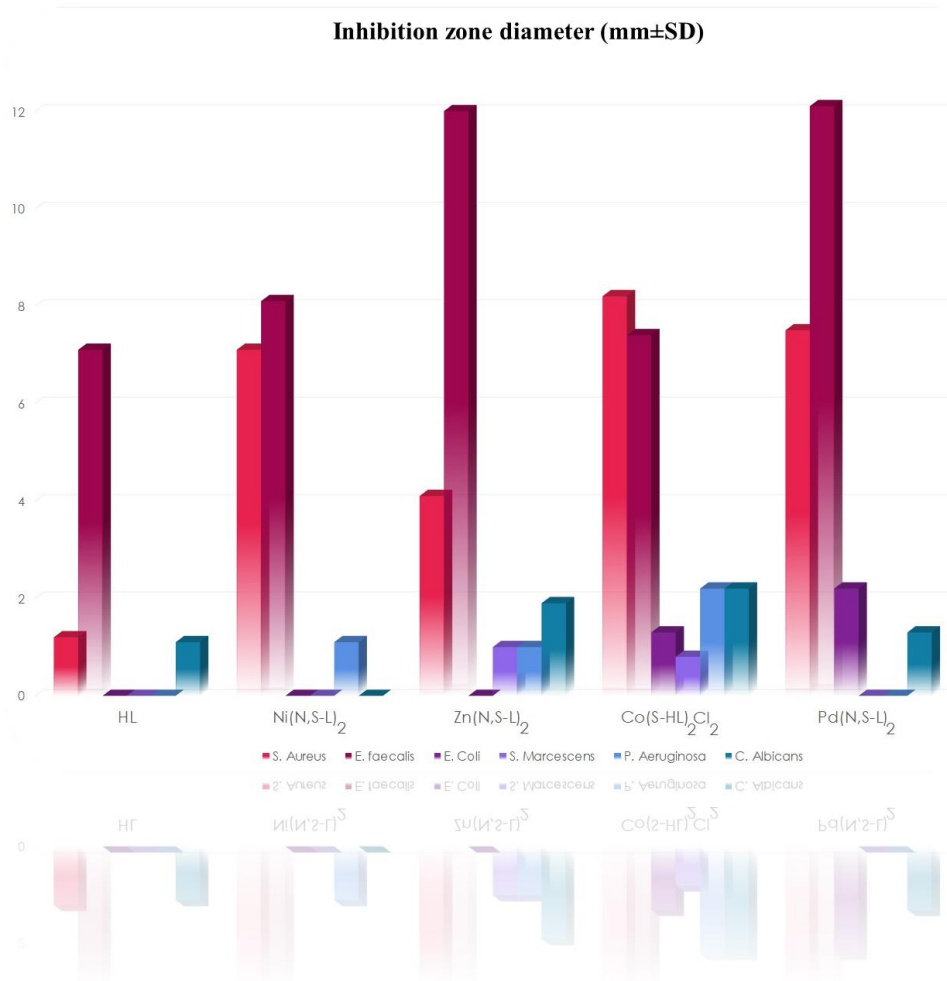


Figure 3.23 Inhibition zone diameter

CHAPTER FOUR

CONCLUSIONS

Co(II), Ni(II), Pd(II) and Zn(II) transition metal complexes of HL synthesized with a 1:1 M ratio of ligand and metal(II) salts were successfully synthesized, and all compounds were characterized using spectroscopic analysis methods. The molecular structures of $[\text{Co}(\text{S-HL})_2\text{Cl}_2]$, $[\text{Ni}(\text{N,S-L})_2]$, $[\text{Pd}(\text{N,S-L})_2]$ and $[\text{Zn}(\text{N,S-L})_2]$, were X-ray crystallographically confirmed. In the Co(II) complex, coordination is achieved through the S atom of the two neutral TSC ligands and the two Cl anions. The center of the metallic ions in the compound is four-coordinate in a distorted tetrahedral configuration. In Ni(II) and Pd(II) complexes, the ligand is coordinated over N and S atoms to the metal in the anionic form bidentate NS and generally adopts a distorted square pyramidal geometry. It was found that the Zn(II) complex had a distorted tetrahedral geometry. Moreover, similar to the Pd(II) and Ni(II) complexes, Zn(II) complex, has two donor atoms (NS) coordinated to the Zn(II) ion as the bidentate ligands. The synthesised compounds and their free TSC ligand were examined for their antimicrobial activities. Our conclusion is that metal complexes are more active than their free ligands. The Zn(II) complex had the best antibacterial activity against *E. faecalis*, while the Co(II) complex showed the best activity against *S. aureus* bacteria. Co(II) and Pd(II) complexes were relatively more effective against Gram-negative bacteria. A little antifungal activity was observed in Zn(II) and Co(II) complexes.

REFERENCES

- Abdalla, E. M., Hassan, S. S., Elganzory, H. H., Aly, S. A., & Alshater, H. (2021). Molecular Docking, DFT Calculations, Effect of High Energetic Ionizing Radiation, and Biological Evaluation of Some Novel Metal (II) Heteroleptic Complexes Bearing the Thiosemicarbazone Ligand. *Molecules*, 26(19), 5851. <https://doi.org/10.3390/molecules26195851>
- Aguirre, A. R., Parrilha, G. L., Louro, S. R., Alves, O. C., Diniz, R., Durval, F., & Beraldo, H. (2022). Structural and theoretical studies on copper (II) and zinc (II) complexes with a 9-anthraldehyde-derived thiosemicarbazone. *Polyhedron*, 217, 115724. <https://doi.org/10.1016/j.poly.2022.115724>
- Al iAhmed, M. F., & Yunus, V. M. (2014). Microwave Synthesis & Antimicrobial Activity of Some Cu (II), Co (II), Ni (II) & Cr (III) complexes with Schiff base 2, 6-pyridinedicarboxaldehyde Thiosemicabazone. *Oriental Journal Of Chemistry (An International Open Free Access, Peer Reviewed Research Journal)*, 30(1), 111-117. <http://doi.org/10.13005/ojc/300114>
- Ali, M. A., Mirza, A. H., Monsur, A., Hossain, S., & Nazimuddin, M. (2001). Synthesis, characterization, antifungal properties and X-ray crystal structures of five-and six-coordinate copper (II) complexes of the 6-methyl-2-formylpyridine4N-dimethylthiosemicarbazone. *Polyhedron*, 20(9-10), 1045-1052. [https://doi.org/10.1016/S0277-5387\(01\)00724-0](https://doi.org/10.1016/S0277-5387(01)00724-0)
- Alomar, K., Khan, M. A., Allain, M., & Bouet, G. (2009). Synthesis, crystal structure and characterization of 3-thiophene aldehyde thiosemicarbazone and its complexes with cobalt (II), nickel (II) and copper (II). *Polyhedron*, 28(7), 1273-1280. <https://doi.org/10.1016/j.poly.2009.02.042>

- Al-Riyahee, A. A., Horton, P. N., Coles, S. J., Amoroso, A. J., & Pope, S. J. (2022). Ni (II), Cu (II) and Zn (II) complexes of functionalised thiosemicarbazone ligands: Syntheses and reactivity, characterization and structural studies. *Polyhedron*, 225, 116079. <https://doi.org/10.1016/j.poly.2022.116079>
- Angelusiu, M. V., Almajan, G. L., Rosu, T., Negoiu, M., Almajan, E. R., & Roy, J. (2009). Copper (II) and uranyl (II) complexes with acylthiosemicarbazide: Synthesis, characterization, antibacterial activity and effects on the growth of promyelocytic leukemia cells HL-60. *European journal of medicinal chemistry*, 44(8), 3323-3329. <https://doi.org/10.1016/j.ejmech.2009.03.016>
- Asiri, A. M., & Khan, S. A. (2010). Palladium (II) complexes of NS donor ligands derived from steroidal thiosemicarbazones as antibacterial agents. *Molecules*, 15(7), 4784-4791. <https://doi.org/10.3390/molecules15074784>
- Badea, M., Iosub, E., Chifiriuc, C. M., Marutescu, L., Iorgulescu, E. E., Lazar, V., & Olar, R. (2013). Thermal, spectral, electrochemical and biologic characterization of new Pd (II) complexes with ligands bearing biguanide moieties. *Journal of thermal analysis and calorimetry*, 111(3), 1753-1761. <https://doi.org/10.1007/s10973-012-2288-4>
- Bailor Jr, J. C. (1953). *Inorganic syntheses*. McGraw- HillBook Company.
- Bakkar, M. S., Siddiqi, M. Y., & Monshi, M. S. (2003). Preparation and Investegation of the Bonding Mode in the Complexes of Pt (II) with Thiosemicarbazone Ligands. *Synthesis and reactivity in inorganic and metal-organic chemistry*, 33(7), 1157-1169. <https://doi.org/10.1081/SIM-120023484>

Balakrishnan, N., Haribabu, J., Krishnan, D. A., Swaminathan, S., Mahendiran, D., Bhuvanesh, N. S., & Karvembu, R. (2019). Zinc (II) complexes of indole thiosemicarbazones: DNA/protein binding, molecular docking and in vitro cytotoxicity studies. *Polyhedron*, *170*, 188-201. <https://doi.org/10.1016/j.poly.2019.05.039>

Balakrishnan, N., Haribabu, J., Malekshah, R. E., Swaminathan, S., Balachandran, C., Bhuvanesh, N., & Karvembu, R. (2022). Effect of N-benzyl group in indole scaffold of thiosemicarbazones on the biological activity of their Pd (II) complexes: DFT, biomolecular interactions, in silico docking, ADME and cytotoxicity studies. *Inorganica Chimica Acta*, *534*, 120805. <https://doi.org/10.1016/j.ica.2022.120805>

Bel'skii, V. K., Prisyazhnyuk, A. I., Kolchinskii, E. V., & Koksharova, T. V. (1987). X-ray structural investigation of crystals of dichlorobis (4-phenylthiosemicarbazone acetone) zinc. *Journal of Structural Chemistry*, *27*(5), 808-811. <https://doi.org/10.1007/bf00748530>

Bermejo, E., Carballo, R., Castiñeiras, A., Domínguez, R., Maichle-Mössmer, C., Strähle, J., et. al, (1999). Synthesis, characterization and antifungal activity of group 12 metal complexes of 2-acetylpyridine-⁴N-ethylthiosemicarbazone (H4EL) and 2-acetylpyridine-N-oxide-⁴N-ethylthiosemicarbazone (H4ELO) *Polyhedron*, *18*(27), 3695-3702. [https://doi.org/10.1016/S0277-5387\(99\)00309-5](https://doi.org/10.1016/S0277-5387(99)00309-5)

Bermejo, M. R., Pedrido, R., Fernández, M. I., González-Noya, A. M., Maneiro, M., Rodríguez, M. J., & Vázquez, M. (2004). The first neutral Sn (II) complex derived from a pentadentate thiosemicarbazone ligand. *Inorganic Chemistry Communications*, *7*(1), 4-8. <https://doi.org/10.1016/j.inoche.2003.09.013>

Bernstein, J., Davis, R. E., Shimoni, L., & Chang, N. L. (1995). Patterns in hydrogen bonding: functionality and graph set analysis in crystals. *Angewandte Chemie International Edition in English*, 34(15), 1555-1573.
<https://doi.org/10.1002/anie.199515551>

Bondi, A. V. (1964). van der Waals volumes and radii. *The Journal of physical chemistry*, 68(3), 441-451. <https://doi.org/10.1021/j100785a001>

Campbell, M. J. (1975). Transition metal complexes of thiosemicarbazide and thiosemicarbazones. *Coordination Chemistry Reviews*, 15(2-3), 279-319.
[https://doi.org/10.1016/S0010-8545\(00\)80276-3](https://doi.org/10.1016/S0010-8545(00)80276-3)

Cardia, M. C., Begala, M., Delogu, A., Maccioni, E., & Plumitallo, A. (2000). Synthesis and antimicrobial activity of novel arylideneisothiosemicarbazones. *II Farmaco*, 55(2), 93-98. [https://doi.org/10.1016/S0014-827X\(99\)00124-X](https://doi.org/10.1016/S0014-827X(99)00124-X)

Casas, J. S., Castellano, E. E., Ellena, J., García-Tasende, M. S., Sánchez, A., Sordo, J., & Vidarte, M. J. (2003). Synthesis, Spectroscopic and Structural Aspects of Mono- and Diorganothallium (III) Complexes of 2, 6-Diacetylpyridine Bis (thiosemicarbazone)(H₂DAPTSC)—A New Coordination Mode of the HDAPTSC—Anion. *Zeitschrift für anorganische und allgemeine Chemie*, 629(2), 261-267. <https://doi.org/10.1002/zaac.200390042>

Casas, J. S., García-Tasende, M. S., & Sordo, J. (2000). Main group metal complexes of semicarbazones and thiosemicarbazones. A structural review. *Coordination Chemistry Reviews*, 209(1), 197-261.

Chandra, S., Raizada, S., Tyagi, M., & Gautam, A. (2007). Synthesis, spectroscopic, and antimicrobial studies on bivalent nickel and copper complexes of bis (thiosemicarbazone). *Bioinorganic Chemistry and Applications*, 2007.

<https://doi.org/10.1155/2007/51483>

Coghi, L., Lanfredi, A. M. M., & Tiripicchio, A. (1976). Crystal and molecular structure of thiosemicarbazide hydrochloride. *Journal of the Chemical Society, Perkin Transactions 2*(15), 1808-1810. <https://doi.org/10.1039/P29760001808>

Demertzis, M. A., Yadav, P. N., & Kovala-Demertzi, D. (2006). Palladium (II) Complexes of the Thiosemicarbazone and N-Ethylthiosemicarbazone of 3-Hydroxypyridine-2-carbaldehyde: Synthesis, Properties, and X-Ray Crystal Structure. *Helvetica Chimica Acta*, 89(9), 1959-1970.

<https://doi.org/10.1002/hlca.200690187>

Dolomanov, O. V., Bourhis, L. J., Gildea, R. J., Howard, J. A., & Puschmann, H. (2009). OLEX2: a complete structure solution, refinement and analysis program. *Journal of applied crystallography*, 42(2), 339-341.

<https://doi.org/10.1107/S0021889808042726>

Drew, D., Doyle, J. R., & Shaver, A. G. (1972). Cyclic diolefin complexes of platinum and palladium. *Inorganic Syntheses*, 13, 47-55.

<https://doi.org/10.1002/9780470132449.ch11>

El-Sawaf, A. K., El-Essawy, F., Nassar, A. A., & El-Samanody, E. S. A. (2018). Synthesis, spectral, thermal and antimicrobial studies on cobalt (II), nickel (II), copper (II), zinc (II) and palladium (II) complexes containing thiosemicarbazone

ligand. *Journal of Molecular Structure*, 1157, 381-394.
<https://doi.org/10.1016/j.molstruc.2017.12.075>

Emara, A. A., Seleem, H. S., & Madyan, A. M. (2009). Synthesis, spectroscopic investigations, and biological activity of metal complexes of N-benzoylthiosemicarbazide. *Journal of Coordination Chemistry*, 62(15), 2569-2582. <https://doi.org/10.1080/00958970902866538>

Fun, H. K., Jebas, S. R., Patil, P. S., & Dharmaprakash, S. M. (2008). (E)-1-(2-Thienyl)-3-(2, 4, 5-trimethoxyphenyl) prop-2-en-1-one. *Acta Crystallographica Section E: Structure Reports Online*, 64(8), o1510-o1511.
<https://doi.org/10.1107/S1600536808021375>

Gatterman, L., & Wieland, H. (1932). *Laboratory methods of organic chemistry*. The Macmillan Company.

Gil, M., Bermejo, E., Castiñeiras, A., Beraldo, H., & West, D. X. (2000). Structural and spectral study of nickel (II) complexes of pyridyl bis {3-piperidyl-, bis {hexamethyleneiminyl-, bis {N (4)-diethyl-, and bis {N (4)-dipropylthiosemicarbazones}. *Zeitschrift für Anorganische und Allgemeine Chemie*, 626(11), 2353-2360. [https://doi.org/10.1002/1521-3749\(200011\)626:11%3c2353::aid-zaac2353%3e3.0.co;2-h](https://doi.org/10.1002/1521-3749(200011)626:11%3c2353::aid-zaac2353%3e3.0.co;2-h)

Gillan, D. C. (2016). Metal resistance systems in cultivated bacteria: are they found in complex communities. *Current opinion in biotechnology*, 38, 123-130.
<https://doi.org/10.1016/j.copbio.2016.01.012>

- Gokulnath, G., Manikandan, R., Anitha, P., & Umarani, C. (2021). Synthesis, characterization, in vitro antimicrobial and anticancer activity of metal (II) complexes of Schiff base-derived from 3-formyl-2-mercaptoquinoline and thiosemicarbazide. *Phosphorus, Sulfur, and Silicon and the Related Elements*, 196(12), 1078-1083. <https://doi.org/10.1080/10426507.2021.1966630>
- Gómez-Saiz, P., García-Tojal, J., Maestro, M. A., Mahía, J., Arnaiz, F. J., Lezama, L., et. al, (2003). New 1, 3, 4-Oxadiazolecopper (II) derivatives obtained from thiosemicarbazone complexes. *European Journal of Inorganic Chemistry*, 2003(14), 2639-2650. <https://doi.org/10.1002/ejic.200200689>
- Gospodinov, N., Stanev, S., & Dorev, K. (1962). Preparation of thiosemicarbazides. *Farmatsia, Sofia*, 12(6), 39-42.
- Guler, S., Kayali, H. A., Sadan, E. O., Sen, B., & Subasi, E. (2022). Half-Sandwich Arene Ruthenium (II) Thiosemicarbazone Complexes: Evaluation of Anticancer Effect on Primary and Metastatic Ovarian Cancer Cell Lines. *Frontiers in pharmacology*, 13, 882756-882756. <https://doi.org/10.3389/fphar.2022.882756>
- Güveli, Ş., & Ülküseven, B. (2011). Nickel (II)–triphenylphosphine complexes of ONS and ONN chelating 2-hydroxyacetophenone thiosemicarbazones. *Polyhedron*, 30(8), 1385-1388. <https://doi.org/10.1016/j.poly.2011.02.041>

Güveli, Ş., Özdemir, N., Bal-Demirci, T., Ülküseven, B., Dinçer, M., & Andaç, Ö. (2010). Quantum-chemical, spectroscopic and X-ray diffraction studies on nickel complex of 2-hydroxyacetophenone thiosemicarbazone with triphenylphosphine. *Polyhedron*, 29(12), 2393-2403. <https://doi.org/10.1016/j.poly.2010.05.004>

Haribabu, J., Jeyalakshmi, K., Arun, Y., Bhuvanesh, N. S., Perumal, P. T., & Karvembu, R. (2017). Synthesis of Ni (II) complexes bearing indole-based thiosemicarbazone ligands for interaction with biomolecules and some biological applications. *JBIC Journal of Biological Inorganic Chemistry*, 22(4), 461-480. <https://doi.org/10.1007/s00775-016-1424-1>

Hassanien, M. M., Gabr, I. M., Abdel-Rhman, M. H., & El-Asmy, A. A. (2008). Synthesis and structural investigation of mono-and polynuclear copper complexes of 4-ethyl-1-(pyridin-2-yl) thiosemicarbazide. *spectrochimica acta part a: molecular and biomolecular spectroscopy*, 71(1), 73-79. <https://doi.org/10.1016/j.saa.2007.11.009>

Huheey, J. E., Keiter, E. A., & Keiter, R. L. (1993). Principles and applications of inorganic chemistry.

Husain, K., Abid, M., & Azam, A. (2007). Synthesis, characterization and antiamoebic activity of new indole-3-carboxaldehyde thiosemicarbazones and their Pd (II) complexes. *European journal of medicinal chemistry*, 42(10), 1300-1308. <https://doi.org/10.1016/j.ejmech.2007.02.012>

- Hussein, M. A., Guan, T. S., Haque, R. A., Ahamed, M. B. K., & Majid, A. M. A. (2015). Synthesis and characterization of thiosemicarbazonato molybdenum (VI) complexes: In vitro DNA binding, cleavage, and antitumor activities. *Polyhedron*, 85, 93-103. <https://doi.org/10.1016/j.poly.2014.02.048>
- Janiak, C. (2000). A critical account on π - π stacking in metal complexes with aromatic nitrogen-containing ligands. *Journal of the Chemical Society, Dalton Transactions*, (21), 3885-3896. <https://doi.org/10.1039/B003010O>
- Jing, Z. L., Yu, M., & Chen, X. (2007). 2-(2-Thienylmethyleneamino) isoindoline-1, 3-dione. *Acta Crystallographica Section E: Structure Reports Online*, 63(9), o3714-o3714. <https://doi.org/10.1107/S160053680703752X>
- Jouad, E. M., Larcher, G., Allain, M., Riou, A., Bouet, G. M., Khan, M. A., & Do Thanh, X. (2001). Synthesis, structure and biological activity of nickel (II) complexes of 5-methyl 2-furfural thiosemicarbazone. *Journal of Inorganic Biochemistry*, 86(2-3), 565-571. [https://doi.org/10.1016/S0162-0134\(01\)00220-3](https://doi.org/10.1016/S0162-0134(01)00220-3)
- Jouad, E. M., Riou, A., Allain, M., Khan, M. A., & Bouet, G. M. (2001). Synthesis, structural and spectral studies of 5-methyl 2-furaldehyde thiosemicarbazone and its Co, Ni, Cu and Cd complexes. *Polyhedron*, 20(1), 67-74. [https://doi.org/10.1016/S0277-5387\(00\)00598-2](https://doi.org/10.1016/S0277-5387(00)00598-2)
- Kalaivani, P., Prabhakaran, R., Kaveri, M. V., Huang, R., Staples, R. J., & Natarajan, K. (2013). Synthesis, spectral, X-ray crystallography, electrochemistry, DNA/protein binding and radical scavenging activity of new palladium (II) complexes containing triphenylarsine. *Inorganica Chimica Acta*, 405, 415-426. <https://doi.org/10.1016/j.ica.2013.06.038>

Kannan, S., Sivagamasundari, M., Ramesh, R., & Liu, Y. (2008). Ruthenium (II) carbonyl complexes of dehydroacetic acid thiosemicarbazone: synthesis, structure, light emission and biological activity. *Journal of Organometallic Chemistry*, 693(13), 2251-2257. <https://doi.org/10.1016/j.jorganchem.2008.03.023>

Kasuga, N. C., Sekino, K., Ishikawa, M., Honda, A., Yokoyama, M., Nakano, S., & Nomiya, K. (2003). Synthesis, structural characterization and antimicrobial activities of 12 zinc (II) complexes with four thiosemicarbazone and two semicarbazone ligands. *Journal of inorganic biochemistry*, 96(2-3), 298-310. [https://doi.org/10.1016/S0162-0134\(03\)00156-9](https://doi.org/10.1016/S0162-0134(03)00156-9)

Kasuga, N. C., Sekino, K., Koumo, C., Shimada, N., Ishikawa, M., & Nomiya, K. (2001). Synthesis, structural characterization and antimicrobial activities of 4- and 6-coordinate nickel (II) complexes with three thiosemicarbazones and semicarbazone ligands. *Journal of inorganic biochemistry*, 84(1-2), 55-65. [https://doi.org/10.1016/S0162-0134\(00\)00221-X](https://doi.org/10.1016/S0162-0134(00)00221-X)

Kazak, C., Aygün, M., Turgut, G., Odabaşoğlu, M., Özbey, S., & Büyükgüngör, O. (2000). 2-[(4-Hydroxyphenyl) iminomethyl] thiophene. *Acta Crystallographica Section C: Crystal Structure Communications*, 56(8), 1044-1045. <https://doi.org/10.1107/S0108270100007770>

Keshk, E. M., El-Desoky, S. I., Hammouda, M. A. A., Abdel-Rahman, A. H., & Hegazi, A. G. (2008). Synthesis and reactions of some new quinoline thiosemicarbazide derivatives of potential biological activity. *Phosphorus, Sulfur, and Silicon and the Related Elements*, 183(6), 1323-1343. <https://doi.org/10.1080/10426500701641304>

Khalilian, M. H., Mirzaei, S., & Taherpour, A. A. (2015). Comprehensive insights into the structure and coordination behavior of thiosemicarbazone ligands: a computational assessment of the E–Z interconversion mechanism during coordination. *New Journal of Chemistry*, 39(12), 9313-9324. <https://doi.org/10.1039/C5NJ02041G>

Kızılcıklı, İ., Ülküseven, B., Daşdemir, Y., & Akkurt, B. (2004). Zn (II) and Pd (II) Complexes of Thiosemicarbazone-S-alkyl Esters Derived from 2/3-Formylpyridine. *Synthesis and reactivity in inorganic and metal-organic chemistry*, 34(4), 653-665. <https://doi.org/10.1081/SIM-120035948>

Kovala-Demertzi, D., Yadav, P. N., Wiecek, J., Skoulika, S., Varadinova, T., & Demertzis, M. A. (2006). Zinc (II) complexes derived from pyridine-2-carbaldehyde thiosemicarbazone and (1E)-1-pyridin-2-ylethan-1-one thiosemicarbazone. Synthesis, crystal structures and antiproliferative activity of zinc (II) complexes. *Journal of Inorganic Biochemistry*, 100(9), 1558-1567. <https://doi.org/10.1016/j.jinorgbio.2006.05.006>

Kovala-Demertzi, D., Yadav, P.N., Demertzis, M. A., Jasiski, J.P., Andreadaki, F.J. & Kostas, I. D. (2004). First use of a palladium complex with a thiosemicarbazone ligand as catalyst precursor for the Heck reaction. *Tetrahedron*, 45, 2923-2926. <https://doi.org/10.1016/j.tetlet.2004.02.062>

Labisbal, E., Haslow, K. D., Sousa-Pedrares, A., Valdés-Martínez, J., Hernández Ortega, S., & West, D. X. (2003). Copper(II) and nickel(II) complexes of 5-methyl-2-hydroxyacetophenone N(4)-substituted thiosemicarbazones. *Polyhedron*, 22(20), 2831-2837. [https://doi.org/10.1016/S0277-5387\(03\)00405-4](https://doi.org/10.1016/S0277-5387(03)00405-4)

Lhuachan, S., Siripaisarnpipat, S., & Chaichit, N. (2003). Synthesis, spectra and crystal structure of two copper (I) complexes of acetone-thiosemicarbazone. *European Journal of Inorganic Chemistry*, (2), 263-267.
<https://doi.org/10.1002/ejic.200390035>

Lobana T.S., Bawa G., Castineiras A., & Butcher R.J. (2007). First example of pyrrole-2-carbaldehyde thiosemicarbazone as tridentate dianion in [Pd(η^3 -N⁴,N³,S-ptsc)(PPh₃)] complex. *Inorganic Chemistry Communications*, 10, 505-509. <https://doi.org/10.1016/j.inoche.2006.12.024>

Lobana, T. S., & Butcher, R. J. (2004). Metal–thiosemicarbazone interactions. Synthesis of an iodo-bridged dinuclear [diiodobis (pyrrole-2-carbaldehydethiosemicarbazone) dicopper (I)] complex. *Transition Metal Chemistry*, 29(3), 291-295.
<https://doi.org/10.1023/B:TMCH.0000020371.72284.4d>

Lobana, T. S., Bawa, G., Butcher, R. J., Liaw, B. J., & Liu, C. W. (2006). Thiosemicarbazones of ruthenium (II): crystal structures of [bis (diphenylphosphino) butane][bis (pyridine-2-carbaldehydethiosemicarbazonato)] ruthenium (II) and [bis (triphenylphosphine)][bis (benzaldehydethiosemicarbazonato)] ruthenium (II). *Polyhedron*, 25(15), 2897-2903. <https://doi.org/10.1016/j.poly.2006.04.018>

Lobana, T. S., Kaushal, M., Bhatia, R., Bala, R., Butcher, R. J., & Jasinski, J. P. (2022). Crystal structures of 3/4-pyridyl-based thiosemicarbazones and related Cu and Ni coordination compounds. *Acta Crystallographica Section C: Structural Chemistry*, 78(1). <https://doi.org/10.1107/S205322962101319X>

Lobana, T. S., Kumari, P., Zeller, M., & Butcher, R. J. (2008). The influence of the substituents at N¹ nitrogen on geometry of nickel(II) complexes with heterocyclic thiosemicarbazones. *Inorganic Chemistry Communications*, 11(9), 972-974. <https://doi.org/10.1016/j.inoche.2008.04.032>

Lobana, T. S., Sharma, R., Bawa, G., & Khanna, S. (2009). Bonding and structure trends of thiosemicarbazone derivatives of metals—an overview. *Coordination Chemistry Reviews*, 253(7-8), 977-1055. <https://doi.org/10.1016/j.ccr.2008.07.004>

Madison, W. I. (2014). c) APEX2, version 2014.11-0, Bruker AXS.

Martínez, V. R., Aguirre, M. V., Todaro, J. S., Piro, O. E., Echeverría, G. A., Ferrer, E. G., & Williams, P. A. (2018). Azilsartan and its Zn (II) complex. Synthesis, anticancer mechanisms of action and binding to bovine serum albumin. *Toxicology in Vitro*, 48, 205-220. <https://doi.org/10.1016/j.tiv.2018.01.009>

Mostafa, S. I., Bekheit, M. M., El-Agez, M. M., Thompson, L. K., & Efvenson, E. M. (2000). Synthesis, spectral, magnetic and thermal studies of 1-phenylacetyl-4-phenyl-3-thiosemicarbazide complexes. *Synthesis and Reactivity in Inorganic and Metal-Organic Chemistry*, 30(10), 2029-2049. <https://doi.org/10.1080/00945710009351886>

Novaković, S. B., Bogdanović, G. A., & Leovac, V. M. (2006). Transition metal complexes with thiosemicarbazide-based ligands. Part L. Synthesis, physicochemical properties and crystal structures of Co (II) complexes with acetone S-methylisothiosemicarbazone. *Polyhedron*, 25(5), 1096-1104. <https://doi.org/10.1016/j.poly.2005.08.051>

- Padhye, S., & Kauffman, G. B. (1985). Transition metal complexes of semicarbazones and thiosemicarbazones. *Coordination Chemistry Reviews*, 63, 127-160. [https://doi.org/10.1016/0010-8545\(85\)80022-9](https://doi.org/10.1016/0010-8545(85)80022-9)
- Pal, I., Basuli, F., & Bhattacharya, S. (2002). Thiosemicarbazone complexes of the platinum metals. A story of variable coordination modes. *Journal of Chemical Sciences*, 114(4), 255-268. <https://doi.org/10.1007/BF02703818>
- Pedrido, R., Bermejo, M. R., Romero, M. J., Vázquez, M., González-Noya, A. M., Maneiro, M., et. al, (2005). Syntheses and X-ray characterization of metal complexes with the pentadentate thiosemicarbazone ligand bis (4-N-methylthiosemicarbazone)-2, 6-diacetylpyridine. The first pentacoordinate lead (II) complex with a pentagonal geometry. *Dalton Transactions*, (3), 572-579. <https://doi.org/10.1039/b416296j>
- Perrin, D. D., Armarego, W. L. F., & Perrin, D. R. (1980). Purification of Laboratory Chemicals. *Pergamon*, New York.
- Prabhu, R. N., & Ramesh, R. (2013). Synthesis and structural characterization of palladium (II) thiosemicarbazone complex: application to the Buchwald–Hartwig amination reaction. *Tetrahedron Letters*, 54(9), 1120-1124. <https://doi.org/10.1016/j.tetlet.2012.12.070>
- Prabhu, R. N., & Ramesh, R. (2016). Square-planar Ni (II) thiosemicarbazonato complex as an easily accessible and convenient catalyst for Sonogashira cross-coupling reaction. *Tetrahedron Letters*, 57(44), 4893-4897. <http://doi.org/10.1016/j.tetlet.2016.09.049>

Prasath, R., Bhavana, P., Ng, S. W., & Tiekink, E. R. (2010). N, N'-Bis [(E)-(5-chloro-2-thienyl) methylidene] ethane-1, 2-diamine. *Acta Crystallographica Section E: Structure Reports Online*, 66(11), o2883-o2883.

<https://doi.org/10.1107/S160053681004167X>

Prathapachandra Kurup, M. R., & Joseph, M. (2003). Transition Metal Complexes of Furan-2-aldehyde Thiosemicarbazone. *Synthesis and reactivity in inorganic and metal-organic chemistry*, 33(7), 1275-1287. <https://doi.org/10.1081/SIM-120023500>

Rai, A., Sengupta, S. K., & Pandey, O. P. (2005). Lanthanum (III) and praseodymium (III) complexes with isatin thiosemicarbazones. *Spectrochimica Acta Part A: Molecular and Biomolecular Spectroscopy*, 61(11-12), 2761-2765. <https://doi.org/10.1016/j.saa.2004.09.031>

Rapheal, P. F., Manoj, E., Kurup, M. P., & Fun, H. K. (2021). Nickel (II) complexes of N (4)-substituted thiosemicarbazones derived from pyridine-2-carbaldehyde: Crystal structures, spectral aspects and Hirshfeld surface analysis. *Journal of Molecular Structure*, 1237, 130362. <https://doi.org/10.1016/j.molstruc.2021.130362>

Refat, M. S., El-Deen, I. M., Anwer, Z. M., & El-Ghol, S. (2009). Bivalent transition metal complexes of coumarin-3-yl thiosemicarbazone derivatives: Spectroscopic, antibacterial activity and thermogravimetric studies. *Journal of Molecular Structure*, 920(1-3), 149-162. <https://doi.org/10.1016/j.molstruc.2008.10.059>

Saghatforoush, L., Hosseinpour, S., Moeini, K., Mardani, Z., Bezpalko, M. W., & Scott Kassel, W. (2021). Investigation of the binding ability of a new thiosemicarbazone-based ligand and its zn (ii) complex toward proteins and dna: spectral, structural, theoretical, and docking studies. *Journal of Structural Chemistry*, 62(5), 748-761. <https://doi.org/10.1134/S0022476621050115>.

Scovill, J. P., Klayman, D. L., & Franchino, C. F. (1982). 2-Acetylpyridine thiosemicarbazones. 4. Complexes with transition metals as antimalarial and antileukemic agents. *Journal of Medicinal Chemistry*, 25(10), 1261-1264. <https://doi.org/10.1021/jm00352a036>

Şen, B., Kalhan, H. K., Demir, V., Güler, E. E., Kayalı, H. A., & Subaşı, E. (2019). Crystal structures, spectroscopic properties of new cobalt (II), nickel (II), zinc (II) and palladium (II) complexes derived from 2-acetyl-5-chloro thiophene thiosemicarbazone: Anticancer evaluation. *Materials Science and Engineering: C*, 98, 550-559. <https://doi.org/10.1016/j.msec.2018.12.080>

Sen, S., Shit, S., Mitra, S., & Batten, S. R. (2008). Structural and spectral studies of a new copper (II) complex with a tridentate thiosemicarbazone ligand. *Structural Chemistry*, 19(1), 137-142. <https://doi.org/10.1007/s11224-007-9263-x>

Sharma, S., Athar, F., Maurya, M. R., & Azam, A. (2005). Copper (II) complexes with substituted thiosemicarbazones of thiophene-2-carboxaldehyde: synthesis, characterization and antiamoebic activity against *E. histolytica*. *European journal of medicinal chemistry*, 40(12), 1414-1419. <https://doi.org/10.1016/j.ejmech.2005.05.013>

Shashidhar, Shivakumar, K., & Halli, M. B. (2006). Synthesis, characterization and antimicrobial studies on metal complexes with a naphthofuran thiosemicarbazide derivatives. *Journal of Coordination Chemistry*, 59(16), 1847-1856.

<https://doi.org/10.1080/00958970600655548>

Sheldrick, G. M. (2008). A short history of SHELX. *Acta Crystallographica Section A: Foundations of Crystallography*, 64(1), 112-122.

<https://doi.org/10.1107/S0108767307043930>

Sheldrick, G. M. (2015). Crystal structure refinement with SHELXL. *Acta Crystallographica Section C: Structural Chemistry*, 71(1), 3-8.

<https://doi.org/10.1107/S2053229614024218>

Spek, A. L. J. (2003). Single-crystal structure validation with the program PLATON. *Journal of applied crystallography*, 36(1), 7-13.

<https://doi.org/10.1107/S0021889802022112>

Spingarn, N. E., & Sartorelli, A. C. (1979). Synthesis and evaluation of the thiosemicarbazone, dithiocarbazone, and 2'-pyrazinylhydrazone of pyrazinecarboxaldehyde as agents for the treatment of iron overload. *Journal of Medicinal Chemistry*, 22(11), 1314-1316. <https://doi.org/10.1021/jm00197a007>

Sultan, S., Taha, M., Shah, S. A. A., Yamin, B. M., & Zaki, H. M. (2014). (E)-3-Chloro-N'-(2-fluorobenzylidene) thiophene-2-carbohydrazide. *Acta Crystallographica Section E: Structure Reports Online*, 70(7), o751-o751.

<https://doi.org/10.1107/S1600536814011568>

Ucar, A., Findik, M., Kuzu, M., Pehlivanoglu, S., Sayin, U., Sayin, Z., & Akgemci, E. G. (2021). Cytotoxic effects, microbiological analysis and inhibitory properties

on carbonic anhydrase isozyme activities of 2-hydroxy-5-methoxyacetophenone thiosemicarbazone and its Cu (II), Co (II), Zn (II) and Mn (II) complexes. *Research on Chemical Intermediates*, 47(2), 533-550.
<https://doi.org/10.1007/s11164-020-04284-8>

Wang, B. D., Yang, Z. Y., Lü, M. H., Hai, J., Wang, Q., & Chen, Z. N. (2009). Synthesis, characterization, cytotoxic activity and DNA binding Ni (II) complex with the 6-hydroxy chromone-3-carbaldehyde thiosemicarbazone. *Journal of Organometallic Chemistry*, 694(25), 4069-4075.
<https://doi.org/10.1016/j.jorganchem.2009.08.024>

Wilson, B. A., Venkatraman, R., Whitaker, C., & Tillison, Q. (2005). Synthesis and Structure-Activity Correlation Studies of Metal Complexes of α -N-heterocyclic Carboxaldehyde Thiosemicarbazones in *Shewanella oneidensis*. *International Journal of Environmental Research and Public Health*, 2(1), 170-174.
<https://doi.org/10.3390/ijerph2005010170>

Yamazaki, C. (1975). The structure of isothiosemicarbazones. *Canadian Journal of Chemistry*, 53(4), 610-615. <https://doi.org/10.1139/v75-085>

Yang, L., Powell, D. R., & Houser, R. P. (2007). Structural variation in copper (I) complexes with pyridylmethylamide ligands: structural analysis with a new four-coordinate geometry index, τ 4. *Dalton Transactions*, (9), 955-964.
<https://doi.org/10.1039/B617136B>

Youssef, N. S., El-Zahany, E., El-Seidy, A. M., Caselli, A., & Cenini, S. (2009). Synthesis and characterization of some transition metal complexes with a novel Schiff base ligand and their use as catalysts for olefin cyclopropanation. *Journal*

of Molecular Catalysis A: Chemical, 308(1-2), 159-168.

<https://doi.org/10.1016/j.molcata.2009.04.004>

Zidan, A. S., & El-Said, A. I. (2004). Studies of mixed ligand complexes from dialkyldithiophosphate and thiosemicarbazide or thiosemicarbazones with nickel (II). *Phosphorus, Sulfur, and Silicon*, 179(7), 1293-1305.

<https://doi.org/10.1080/10426500490468100>

